

## INFORMATION TO USERS

This manuscript has been reproduced from the microfilm master. UMI films the text directly from the original or copy submitted. Thus, some thesis and dissertation copies are in typewriter face, while others may be from any type of computer printer.

**The quality of this reproduction is dependent upon the quality of the copy submitted.** Broken or indistinct print, colored or poor quality illustrations and photographs, print bleedthrough, substandard margins, and improper alignment can adversely affect reproduction.

In the unlikely event that the author did not send UMI a complete manuscript and there are missing pages, these will be noted. Also, if unauthorized copyright material had to be removed, a note will indicate the deletion.

Oversize materials (e.g., maps, drawings, charts) are reproduced by sectioning the original, beginning at the upper left-hand corner and continuing from left to right in equal sections with small overlaps.

ProQuest Information and Learning  
300 North Zeeb Road, Ann Arbor, MI 48106-1346 USA  
800-521-0600

UMI<sup>®</sup>



**BIOACCUMULATION AND AIR-WATER EXCHANGE OF THE PAH  
PHENANTHRENE IN PHYTOPLANKTON AND  
RARITAN BAY, NEW JERSEY**

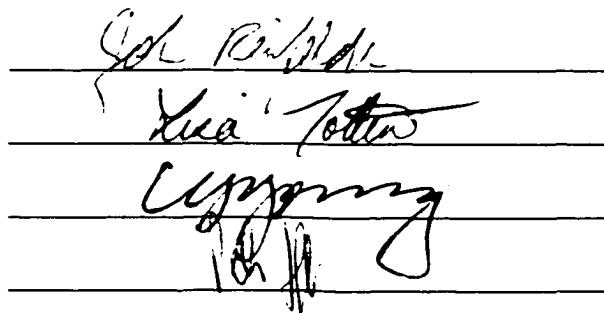
by

**CHENG-WEI FAN**

A Dissertation submitted to the  
Graduate School-New Brunswick  
Rutgers, The State University of New Jersey  
in partial fulfillment of the requirements  
for the degree of  
Doctor of Philosophy  
Graduate Program in Environmental Sciences

written under the direction of  
Professor John R. Reinfelder

and approved by



New Brunswick, New Jersey

October, 2002

UMI Number: 3066702

UMI<sup>®</sup>

---

UMI Microform 3066702

Copyright 2003 by ProQuest Information and Learning Company.

All rights reserved. This microform edition is protected against  
unauthorized copying under Title 17, United States Code.

---

ProQuest Information and Learning Company  
300 North Zeeb Road  
P.O. Box 1346  
Ann Arbor, MI 48106-1346

# **ABSTRACT OF THE DISSERTATION**

## **BIOACCUMULATION AND AIR-WATER EXCHANGE OF THE PAH PHENANTHRENE IN PHYTOPLANKTON AND RARITAN BAY, NEW JERSEY**

By CHENG-WEI FAN

Dissertation Director:

Professor John R. Reinfelder

In order to improve the understanding of the interactions between bioaccumulation in phytoplankton and air-water exchange of polycyclic aromatic hydrocarbons (PAHs) in the NY/NJ Hudson River Harbor Estuary, the accumulation kinetics of the common PAH phenanthrene was studied in two species of coastal diatoms, *Thalassiosira weissflogii* and *T. pseudonana*, using a two-compartment kinetics bioaccumulation model. This model coupled with air-water exchange and sedimentation processes was then applied to field data from Raritan Bay, collected during four cruises from April 2000 to April 2001.

The bioaccumulation kinetics parameters of phenanthrene in the two species of coastal diatoms were measured in laboratory experiments using  $^{14}\text{C}$ -labeled phenanthrene. The accumulation of phenanthrene in these diatoms follows a two-compartment mechanism, which includes fast surface sorption and subsequent accumulation into the cell's interior.

Field measurements of dissolved and particulate phenanthrene concentrations in Raritan Bay suggest the presence of a particulate phase (possible soot particles) to which PAHs sorbed more strongly compared to organic carbon. Using an extended soot carbon-partitioning equation, a small fraction (5–10%) of particulate phenanthrene was estimated to be associated with organic carbon in the suspended particle phase, suggesting the predominance of the soot-like phase for PAHs, such as phenanthrene, methylphenanthrenes, and pyrene, in Raritan Bay.

A dynamic model that coupled air-water exchange and phytoplankton accumulation of phenanthrene was applied to field data from Raritan Bay, New Jersey, to investigate the mutual interactions of the two processes. Annual dynamic simulations show that using a monthly collected database from a nearby shore site (Sandy Hook, New Jersey) for gas phase concentrations of phenanthrene as input provides a better prediction of dissolved phase concentrations than seasonal over-water measurements. This modeling results suggest that processes such as horizontal air and water movements may maintain disequilibria between air, water, and suspended particles phases for hydrophobic organic pollutants.

## **ACKNOWLEDGEMENTS**

I appreciate the helps many people gave me during the years I stayed at Rutgers as a graduate student.

Firstly, I would like to thank my advisor, Dr. John R. Reinfelder for helping me in many ways. Without him, I would not be able to finish this thesis.

I want to thank my thesis committee, Dr. Peter Jaffe, Dr. Lisa Totten, and Dr. Lily Y. Young, who spent their valuable time on reading my thesis and gave me valuable suggestions. I also want to thank Dr. Steve Eisenreich for his support.

I want to thank Dr. Jordi Dachs, Dr. Wen-Hsin Liang, Andrea Polidori, and Dr. Ho-Jin Lim for their helps.

I want to thank Capt. J. Hughs of R/V Walford, Eric. Nelson, Cari Gigliotti, ShuYan, Tom Glenn IV, Daryl VanRy for the assistance in field and laboratory work.

The helps from my labmates, Yan, Melanie, Sandy, Kristine, and Tamara, are greatly appreciated. A special "thank you" to Dr. Sung Il Chang, for all the helps and those coffee breaks we spent together.

I would like to thank my parents, my siblings and their families in Taiwan for their fully support. Finally, I want to present this thesis to my wife, Dr. Yunn-Shin Shiue (also known as Jessie), who is the most important reason this thesis can be completed.

## TABLE OF CONTENTS

<b>Abstract</b>	ii
<b>Acknowledgements</b>	iv
<b>Table of contents</b>	v
<b>List of tables</b>	viii
<b>List of figures</b>	x
<b>Chapter 1. Introduction</b>	1
1.1 Background	2
1.1.1 Accumulation kinetics of HOCs in phytoplankton	2
1.1.2 Dissolved phase-suspended particle partitioning of HOCs	3
1.1.3 Modeling air-water-phytoplankton exchange of HOCs	4
1.2 Research objectives	4
<b>Chapter 2. Kinetics of Phenanthrene Accumulation in Coastal Marine Diatoms</b>	9
Abstract	9
2.1 Introduction	10
2.2 Materials and methods	12
2.3 Results	17
2.4 Discussion	21
2.5 Conclusions	30
References	31
<b>Chapter 3. Polycyclic Aromatic Hydrocarbons (PAHs) in the Air, Water, and Suspended particle of the NY/NJ Hudson River Harbor Estuary</b>	48



Abstract	48
3.1 Introduction	49
3.2 Materials and methods	51
3.3 Results	55
3.4 Discussion	61
3.5 Conclusions	66
References	67
<b>Chapter 4. Modeling air-water exchange and phytoplankton bioaccumulation of phenanthrene: a field test in Raritan Bay, New Jersey, USA</b>	<b>90</b>
Abstract	90
4.1 Introduction	91
4.1.1 Model description	92
4.2 Materials and methods	94
4.3 Results	95
4.4 Discussion	100
4.5 Conclusions	103
References	104
<b>Chapter 5. Conclusions and future work</b>	<b>121</b>
5.1 Conclusions	121
5.2 Future work	122
References	124
<b>Appendix I Subcellular fractionation of phenanthrene radiotracer in <i>T. weissflogii</i></b>	<b>126</b>

<b>Appendix II Zooplankton bioaccumulation of phenanthrene</b>	130
<b>Appendix III Organic carbon and elemental carbon measurements</b>	133
<b>Curriculum Vita</b>	136

## LIST OF TABLES

Table 2.1	Characteristic of tested algal cultures	34
Table 2.2	Rate constants and dry weight-normalized partition coefficients. Short-term phenanthrene accumulation experiments were conducted in SOW at 18-22°C and 4-6°C.	35
Table 2.3	Uptake rate constants, depuration rate constants, dry weight-normalized partition coefficients in cell interior, and the overall dry weight-normalized bioconcentration factors. Long-term phenanthrene accumulation experiments were conducted in the continuous light at 18°C.	36
Table 2.4	Phenanthrene loss rate constants, partition coefficients, fraction of surface accumulation( $x_1$ ), and overall bioconcentration factors in <i>T. pseudonana</i> , <i>T. weissflogii</i> , and <i>D. tertiolecta</i> . $K_s$ , $K_i$ , and $BCF$ are dry weight-normalized partition coefficients. $BCF_{oc}$ and $BCF_{lipid}$ are normalized to cellular organic carbon or lipid content, respectively.	37
Table 2.5	Rate constants and dry weight-normalized partition coefficients of phenanthrene <i>T. weissflogii</i> in the presence of DOC. Short-term phenanthrene accumulation experiments were conducted at 18–22°C.	38
Table 2.6	Phenanthrene dry weight normalized $BCFs$ in various phytoplankton species.	39
Table 3.1	Air temperature, wind direction, and wind speeds measured in Raritan Bay.	70
Table 3.2	Water temperature, dissolved oxygen (DO), salinity, pH, and water column stratification status in Raritan Bay.	71
Table 3.3	Tide chart in Raritan bay presented at local time.	72
Table 3.4	Total suspended matter (TSM), chlorophyll a (Chl a), total particulate lipid (TPL), particulate organic carbon (POC), organic carbon fraction ( $f_{oc}$ ), particulate organic nitrogen (PON), C/N ratio, and bacteria abundance measured in Raritan Bay surface water. Values are mean $\pm$ SD of triplicate samples for suspended matter measurements, mean $\pm$ SD of 10 countings for bacteria abundance.	73
Table 3.5	Dissolved nutrients, including phosphate, nitrate, nitrite, and ammonium concentrations measured in Raritan Bay surface water. Values are presented as mean $\pm$ SD of duplicate measurements or a single measurement.	74

Table 3.6 Chlorophyll a (Chl a) and phaeopigment measured and growth rate ( $\mu$ , $d^{-1}$ ) estimated in the short-term incubation experiments. Values are mean $\pm$ SD of triplicate samples.	75
Table 3.7 Particulate organic carbon (POC) and particulate organic nitrogen (PON) measured and growth rate ( $\mu$ , $d^{-1}$ ) and C/N ratio estimated in the short-term incubation experiments. Values are mean $\pm$ SD of triplicate samples.	76
Table 3.8 PAHs measured in Raritan Bay.	77
Table 4.1 Physical-chemical properties of phenanthrene.	108
Table 4.2 Kinetic parameters for bioaccumulation of phenanthrene by phytoplankton.	109
Table 4.3 Gas and dissolved concentrations of phenanthrene, environmental parameters used for instantaneous and dynamic simulations.	110
Table 4.4 Average surface water parameters and instantaneous water-phytoplankton fluxes in Raritan Bay.	111
Table 4.5 Equations used in the coupled model.	112
Table 4.6 Variables used in dynamic simulations.	113
Table 4.7 Parameters used in dynamic simulations for phenanthrene in Raritan Bay. Simulation were conducted using cruises data.	114
Table 4.8 Parameters used in dynamic simulations for phenanthrene in Raritan Bay. Simulation were conducted using Sandy Hook database.	115
Table A.1.1 Subcellular fractionation of phenanthrene radiotracer in <i>T. weissflogii</i> . The fractions of membrane bound phenanthrene were calculated by dividing the radioactivity in the pellet fraction by the radioactivity of intact cells.	128
Table A.3.1 Elemental and organic carbon measurements of plankton net samples in Raritan Bay	134
Table A.3.2 Organic carbon-partitioning and soot carbon-partitioning models applied to plankton net samples in Raritan Bay.	135

## LIST OF FIGURES

- Figure 2.1 Short-term phenanthrene uptake in *T. weissflogii*. The total and algal  $^{14}\text{C}$ -phenanthrene radioactivities over the exposure time are shown. (A) Experiment was conducted at 18-22°C with a total phenanthrene concentration of  $3.46 \times 10^{-8}$  M. (B) Experiment was conducted at 4-6°C with a total phenanthrene concentration of  $4.53 \times 10^{-8}$  M. 40
- Figure 2.2 Short-term phenanthrene uptake in *T. pseudonana*. The total and algal  $^{14}\text{C}$ -phenanthrene radioactivities over the exposure time are shown. (A) Experiment was conducted at 18-22°C with a total phenanthrene concentration of  $3.90 \times 10^{-8}$  M. (B) Experiment was conducted at 4-6°C with a total phenanthrene concentration of  $4.18 \times 10^{-8}$  M. 41
- Figure 2.3 Long-term phenanthrene uptake in *T. weissflogii* at 18°C with  $2.49 \times 10^{-8}$  M phenanthrene. (A) The total and algal  $^{14}\text{C}$ -phenanthrene radioactivities, (B) cell density, and (C) cellular radioactivity over the exposure time are shown. 42
- Figure 2.4 Long-term phenanthrene uptake in *T. pseudonana* at 18°C with  $2.07 \times 10^{-8}$  M phenanthrene. (A) The total and algal  $^{14}\text{C}$ -phenanthrene radioactivities, (B) cell density, and (C) cellular radioactivity over the exposure time are shown. 43
- Figure 2.5 Cellular phenanthrene concentrations in *T. weissflogii* over (A) the first hour of exposure, and (B) 11 d of exposure in unit of  $10^{-15}$  g cell $^{-1}$ . The dots (●) are measured data, the lines are model results. Experiment was conducted at 18°C with a total phenanthrene concentration of  $9.08 \times 10^{-8}$  M. 44
- Figure 2.6 Cellular phenanthrene concentrations in *T. pseudonana* over (A) the first hour of exposure, and (B) 11 d of exposure in unit of  $10^{-15}$  g cell $^{-1}$ . The dots (●) are measured data, the lines are model results. Experiment was conducted at 18°C with a total phenanthrene concentration of  $80.8 \times 10^{-8}$  M. 45
- Figure 2.7 The relationship between surface sorption fraction of phenanthrene and cell surface area to volume ratio in the phenanthrene accumulation in *T. weissflogii* (●), *T. pseudonana* (■), and *T. tertiolecta* (▼). The line describes the regression result  $x_1 = 24.26 A/V + 8.419$  ( $r^2 = 0.99$ ). 46
- Figure 2.8 Dependence of phenanthrene dry weight-normalized BCF on the fraction of organic carbon in *T. weissflogii* (●), *T. pseudonana* (■), and *T. tertiolecta* (▼). 47
- Figure 3.1 The sampling site in the Raritan bay, New Jersey. 78
- Figure 3.2 Average concentrations of (A) total suspended matter, (B) chlorophyll a 79

& phaeopigment, (C) total particulate lipid, and (D) particulate organic carbon of each sampling cruise in Raritan Bay.

Figure 3.3 Average concentrations of (A) nitrate, (B) nitrite, (C) phosphate, and (D) ammonium of each sampling cruise in Raritan Bay. 80

Figure 3.4 The relative abundance (%) of 5 dominant phytoplankton genera in the Raritan Bay with respect to the (A) total cells counted and (B) total bio-volume. 81

Figure 3.5 Average PAH concentrations in (A) atmospheric particles, (B) gas phase (C) suspended particles in water, and (D) dissolved phases measured in the cruise of Apr/2000 from Raritan bay. Error bars are standard deviation of 5 measurements. 82

Figure 3.6 Average PAH concentrations in (A) atmospheric particles, (B) gas phase (C) suspended particles in water, and (D) dissolved phases measured in the cruise of Aug/2000 from Raritan bay. Error bars are standard deviation of 6 measurements. 83

Figure 3.7 Average PAH concentrations in (A) atmospheric particles, (B) gas phase (C) suspended particles in water, and (D) dissolved phases measured in the cruise of Oct/2000 from Raritan bay. Error bars are standard deviation of 6 measurements. 84

Figure 3.8 Average PAH concentrations in (A) atmospheric particles, (B) gas phase (C) suspended particles in water, and (D) dissolved phases measured in the cruise of Apr/2001 from Raritan bay. Error bars are standard deviation of 6 measurements. 85

Figure 3.9 Average PAH concentrations in suspended particulate phase measured in the four cruises from Raritan Bay. (A) Apr/2000, (B) Aug/2000, (C) Oct/2000, and (D) Apr/2001. ■ present Infiltrax samples □ present plankton net samples 86

Figure 3.10 Average organic carbon normalized PAH concentrations in suspended particulate phase measured in the four cruises from Raritan Bay. (A) Apr/2000, (B) Aug/2000, (C) Oct/2000, and (D) Apr/2001. ■ present Infiltrax samples □ present plankton net samples. 87

Figure 3.11  $\log K_{oc}$  versus  $\log K_{ow}$  for PAHs measured in the four cruises from Raritan Bay. (A) Apr/2000, (B) Aug/2000, (C) Oct/2000, and (D) Apr/2001. Thin lines represent regressions of  $\log K_{oc}$  versus  $\log K_{ow}$  for each sampling time during seasonal field campaigns. Thick Solid lines represent 1:1 slope lines, and dotted lines represent equation 3-3. PAHs ( $\log K_{ow}$ ) include fluorene (4.18), anthracene(4.54), phenanthrene (4.57), 1methylfluorene(4.97), methylphenanthrenes(5.07), pyrene(5.18), fluoranthene(5.22), 4,5methylenephenanthrene(5.25), benzo[a]fluorene(5.69), benzo[b]fluorene(5.69), benz[a]anthracene(5.84), chrysene/Triphenylene(5.84), and benzo[e]pyrene(6.44); see Table 3.8 for refs. 88

Figure 3.12 The partition coefficients of (A) phenanthrene, (B) 89

methylphenanthrenes, (C) pyrene, and (D) benzo[e]pyrene as a function of organic carbon fractions measured in Apr/2000(●), Aug/2000(○), Oct/2000(▼), and Apr/2001(▽) from Raritan Bay.  $K_p$  values were calculated using equation 3-1. The solid lines were calculated from the equation  $K_p = f_{oc} K_{oc}$ , and the  $K_{oc}$  values were calculated using equation 3-3. Dotted line was calculated from the equation  $K_p = f_{oc} BCF_{oc}$ , where  $BCF_{oc}$  is the phenanthrene bioconcentration factor of 36,000 measured in laboratory experiments (Chapter 2). PAHs ( $\log K_{ow}$ ) include phenanthrene (4.57), methylphenanthrenes(5.07), pyrene(5.18), and benzo[e]pyrene(6.44).

Figure 4.1 Phenanthrene concentrations in gas and dissolved phases and instantaneous air-water exchange fluxes in the morning (■), and afternoon (□) in Raritan Bay. Negative fluxes denote gas absorption into surface water, and positive fluxes denote volatilization to atmosphere. 116

Figure 4.2 Schematic of the air-water-phytoplankton exchange of phenanthrene in Raritan Bay. 117

Figure 4.3 Predicted and measured dissolved phase concentrations of phenanthrene in Raritan Bay. Lines represent the predicted results and dots represent measured results. 118

Figure 4.4 Predicted and measured dissolved phase concentrations of phenanthrene in Raritan Bay. Simulations were based on gas phase concentrations of phenanthrene from (●) sampling cruises in Raritan Bay or (○) Sandy Hook, New Jersey. Solid squares (■) represent the measured data in Raritan Bay. 119

Figure 4.5 Predicted phenanthrene concentrations in particulate organic carbon (POC). Phenanthrene concentrations are presented in the unit of (A)  $\text{ng kgC}^{-1}$  and (B)  $\text{ng m}^{-3}$ . Simulations were based on gas phase concentrations of phenanthrene from (●) sampling cruises in Raritan Bay or (○) Sandy Hook database. Solid squares (■) represent the estimated phenanthrene concentrations in suspended particles corrected for soot fraction (Chapter 3). 120

Figure A.1.1 Evaporation results over (A) 5 d and (B) 7 d exposure time. 128

Figure A.2.1 Frequency of the body length in 97 copepod individuals. 129

Figure A.2.2 Accumulation of dissolved phenanthrene in copepods with concentrations ranged from  $1.36 \times 10^{-8}$  to  $8.26 \times 10^{-8}$  M over (○) 1h, (□) 2 h, and (▲) 3 h exposure time. 131

## Chapter 1. Introduction

Phytoplankton bioaccumulation and air-water exchange are two important physical-biological processes controlling the fate and transfer for hydrophobic organic compounds (HOCs) in aquatic environments<sup>1,2</sup>. The accumulation of HOCs by phytoplankton is an important removal mechanism for these compounds from surface waters. HOCs accumulated by phytoplankton may be carried to bottom sediments with settling cells, or ingested by higher organisms, such as zooplankton, in the first step of bioconcentration up the food web<sup>3,4,5</sup>. Air-water exchange (gas sorption or volatilization) controls chemical loading as well as the fate and transport of HOCs in aquatic environments<sup>6,7,8,9,10</sup>. The mutual interactions of air-water and water-phytoplankton exchange processes have only been studied for a limited numbers of HOCs, but could be important in controlling HOC levels in aquatic food webs. For example, using a dynamic model, which couples air-water exchange and phytoplankton uptake, it has been shown that air-water exchange in two lakes (northwestern Ontario, Canada) supports the concentrations of a polychlorinated biphenyl (PCB 52) in phytoplankton<sup>1</sup>.

The Lower Hudson River Estuary has been reported to be impacted greatly by anthropogenic inputs of polycyclic aromatic hydrocarbons (PAHs) from nearby urban and industrial regions<sup>10,11</sup>. The overall goal of this dissertation is to understand the effects of air-water exchange on both dissolved and phytoplankton concentrations of PAHs in the Lower Hudson River Estuary. To achieve this goal, a dynamic model that couples of air-water exchange, phytoplankton accumulation, and particle sedimentation was parameterized and run for the PAH phenanthrene in Raritan Bay, New Jersey. The



model was supported by laboratory determined phenanthrene accumulation kinetics in phytoplankton and simultaneous gas, dissolved, and suspended particle phase PAH concentrations measured during four cruises in Raritan Bay.

## **1.1 Background**

### **1.1.1 Accumulation kinetics of HOCs in phytoplankton**

Phytoplankton plays an important role in the fate and transport of hydrophobic organic contaminants (HOCs), which have a strong affinity for algal cells in aquatic environments<sup>1,2,3,4,5</sup>. The partitioning of HOCs between phytoplankton and the dissolved aqueous phase has often been modeled as a rapid, equilibrium based, thermodynamic process which is driven by the concentration or fugacity gradients between phases. Recent studies on HOC bioaccumulation in phytoplankton have addressed the questions of equilibrium versus kinetics, single-compartment versus multi-compartment, and the biochemical composition of the sorbing matrix. From these recent bioaccumulation studies of various HOCs (PCBs and chlorobenzene) in various algal species (diatoms, green algae, marine prymnesiophyte, and cyanobacteria), it can be concluded that the bioaccumulation of HOCs in phytoplankton is best described as a two-compartment kinetics model in which the compound first rapidly partitions in the cell surface and subsequently diffuses into the cell's interior. These studies also indicated that organic carbon is the likely sorbing matrix<sup>1,13,14,15,16</sup>. The bioaccumulation of PAHs in phytoplankton has been examined in previous studies<sup>5,17,18,19,20,21</sup>, but the kinetics of PAH accumulation have received little attention and previous work involved only two genera of chlorophycean microalgae and

one species of cyanobacteria. Quantification of the kinetics of PAH accumulation in phytoplankton is needed for understanding the accumulation mechanism of PAHs in phytoplankton.

### **1.1.2 Dissolved phase-suspended particle partitioning of HOCs**

In aquatic environments, the partitioning of HOCs between the dissolved and suspended particulate phases can be quantified with a partition coefficient, a ratio of the concentration of HOC in suspended particulate matter phase to that in dissolved phase. Laboratory studies have shown that sorption coefficients normalized to organic carbon ( $K_{oc}$ ) are relatively invariant for natural sediments and soil, and the  $K_{oc}$  values for a range of compounds are correlated to their octanol-water partition coefficients ( $K_{ow}$ ). Several organic carbon-partitioning models that provide reasonable estimates of  $K_{oc}$  from  $K_{ow}$  values have been reported<sup>22,23,24</sup>. However, several recent field observations of PAHs have shown that  $K_{oc}$  values for PAHs are much higher than the predictions based on the organic carbon-partitioning equations. These elevated observed  $K_{oc}$  values have led to the proposition that the presence of soot-like particles, which have a high affinity for PAHs<sup>25,26,27</sup>, could affect the PAH partitioning. The elevated  $K_{oc}$  values for phenanthrene and fluoranthene in a marine sediment<sup>25</sup> and for fluoranthene and pyrene in estuarine suspended particles<sup>27</sup> can be quantitatively explained with the extended soot carbon-partitioning model. It has been suggested that sorption of PAHs to organic matter dominates the water-particle partitioning in the New York-New Jersey Harbor Estuary<sup>10</sup>. However, the effect of the sorption of PAHs to soot may also be important. The relative importance of PAHs partitioning in particulate organic carbon,

which is related to phytoplankton biomass, and a possible soot particle phase require further study.

### **1.1.3 Modeling air-water-phytoplankton exchange of HOCs**

A two-layer resistance model<sup>28</sup> has been used to calculate the direction and magnitude of the gas transfer of HOCs across the air-water interface of aquatic environments. Most of the fluxes calculated were based on simultaneous samples of gas and dissolved phases concentrations of HOCs via intensive short-term field sampling campaigns<sup>6,7,8,9,10</sup>. These results reflected the temporal and spatial variations of HOC concentrations and environmental parameters such as temperature and wind speeds. This observation has raised the question of whether it is appropriate to extend these instantaneous gas exchange fluxes to an annual time scale. For example, Bamford et al (1999)<sup>8</sup> reported an annual fluxes (April 1997 to March 1998) of phenanthrene and fluorene in Chesapeake Bay using 35 pairs of air and water concentrations rather than using the database from 3 intensive sampling cruises, in which large daily and seasonal variations were observed. Achman et al (1993)<sup>6</sup> suggested that an annual fluxes must be calculated using sampling interval of no greater than one month. Therefore, evaluations of the environmental variability of measured PAH concentrations and environmental parameters are needed before performing a dynamic model simulation.

## **1.2 Research objectives**

The primary objectives for the work presented in this thesis are:

1. To determine the accumulation kinetics of phenanthrene in phytoplankton and then to evaluate empirically the two-compartment HOC accumulation mechanism (cell surface and cell interior).
2. To evaluate the importance of cell surface area to volume ratio ( $A/V$ ) to phenanthrene uptake kinetics and intracellular partitioning.
3. To determine the sorbing matrix for phenanthrene in phytoplankton.
4. To determine the water-phytoplankton partition coefficients of PAHs, and then to examine whether an organic carbon-partitioning model can be applied to PAHs measured in Raritan Bay.
5. To estimate phenanthrene fluxes among air, water, and suspended particle compartments in Raritan Bay.
6. To validate a dynamic model which couples air-water-phytoplankton exchange processes.

To address objectives 1 to 3, laboratory experiments were designed to determine the accumulation kinetics in two species of coastal diatoms. Objective 1 was achieved in short-term and long-term accumulation experiments. Objectives 2 and 3 were achieved by testing two study diatoms, which differ in cell surface area to cell volume ratio ( $A/V$ ) by a factor of 2, in dry weight by a factor of 10, in total lipid by a factor of 8.5, and in organic carbon content by a factor of 16.

To achieve objectives 4 to 6, seasonal intensive sampling campaigns were performed in Raritan Bay, New Jersey, to obtain simultaneous measurements of PAHs in atmospheric, dissolved, and suspended particle phases. Objective 4 was approached

by simultaneous measurements of dissolved and suspended particulate matter concentrations of PAHs. Objective 5 was approached by simultaneous collection of gas and dissolved phases PAH samples to determine the directions and magnitudes of fluxes. Objective 6 was achieved by comparing the simulation and measured results.

## References

- (1). Dachs, J.; Eisenreich, S.J.; Baker, J.E.; Ko, F.; Jeremiason, J.D. Coupling of phytoplankton uptake and air-water exchange of persistent organic pollutants. *Environ Sci Technol.* **1999**, 33, 3653 -3660.
- (2). Dachs, J.; Eisenreich, S.J.; Hoff, R.M. Influence of eutrophication on air-water exchange, vertical fluxes, and phytoplankton concentrations of persistent organic pollutants. *Environ Sci Technol.* **2000**, 34, 1095 -1102.
- (3). Koelmans, A.A.; van der Woude, H.; Hattink, J.; Niesten, D.J.M. Long-term bioconcentration kinetics of hydrophobic chemicals in *Selenastrum capricornutum* and *Microcystis aeruginosa*. *Environ Toxicol Chem.* **1999**, 18, 1164 -1172.
- (4). Swackhamer, D.L.; Skoglund, R.S. Bioaccumulation of PCBs by algae: kinetics versus equilibrium. *Environ Toxicol Chem.* **1993**, 12, 831 -838.
- (5). Halling-Sorenson, B.; Nyholm, N.; Kusk, K.O.; Jacobsson, E. Influence of Nitrogen Status on the Bioconcentration of Hydrophobic Organic Compounds to *Selenastrum carcornutum*. *Ecotoxicol Environ Saf.* **2000**, 45, 33 -42.
- (6). Achman, D.R.; Hombuckle, K.C.; Eisenreich, S.J. Volatilization of polychlorinated biphenyls from Green Bay, Lake Michigan. *Environ Sci Technol.* **1993**, 27, 75 -87.
- (7). Nelson, E.D.; Macconnell, L.L.; Baker, J.E. Diffusive exchange of gaseous polycyclic aromatic hydrocarbons and polychlorinated biphenyls across the air-water interface of the Chesapeake bay. *Environ Sci Technol.* **1998**, 32, 912 -919.
- (8). Bamford, H.A.; Offenber, J.H.; Larsen, R.K.; Ko, F.; Baker, J.E. Diffusive exchange of polycyclic aromatic hydrocarbons across the air-water interface of the Patapsco River, an urbanized subestuary of the Chesapeake Bay. *Environ Sci Technol.* **1999**, 33, 2138 -2144.
- (9). Swackhamer, D.L.; Schottler, S.; Pearson, R.F. Air-water exchange and mass balance of toxaphene in the Greak Lakes. *Environ Sci Technol.* **1999**, 33, 3864 -3872.

- (10). Gigliotti, C.L.; Brunciak, P.A.; Dachs, J.; Glenn IV, T.R.; Nelson, E.D.; Totten, L.A.; Eisenreich, S.J. Air-water exchange of polycyclic aromatic hydrocarbons in the NY-NJ harbor estuary. *Environ Toxicol Chem.* **2002**, 21, 235 -244.
- (11). Gigliotti, C.L.; Dachs, J.; Nelson, E.D.; Brunciak, P.A.; Eisenreich, S.J. Polycyclic aromatic hydrocarbons in the New Jersey coastal atmosphere. *Environ Sci Technol.* **2000**, 34, 3547 -3554.
- (12). Sijm, D.T.H.M.; Broersen, K.W.; de Roode, D.F.; Mayer, P. Bioconcentration kinetics of hydrophobic chemicals in different densities of *Chlorella pyrenoidosa*. *Environ Toxicol Chem.* **1998**, 17, 1695 -1704.
- (13). Wang, K.; Rott, B.; Korte, F. Uptake and bioaccumulation of three PCBs by *Chlorella fusca*. *Chemosphere.* **1982**, 11, 525 -530.
- (14). Koelmans, A.A.; Jimenez, C.S.; Lijklema, L. Sorption of chlorobenzenes to mineralizing phytoplankton. *Environ Toxicol Chem.* **1993**, 12, 1425 -1439.
- (15). Koelmans, A.A.; Anzion, S.F.; Lijklema, L. Dynamics of organic micropollutant biosorption to cyanobacteria and detritus. *Environ Sci Technol.* **1995**, 29, 933 -940.
- (16). Skoglund, R.S.; Stange, K.; Swackhamer, D.L. A kinetics model for predicting the accumulation of PCBs in phytoplankton. *Environ Sci Technol.* **1996**, 30, 2113 -2120.
- (17). Twiss, M.R.; Granier, L.; Lafrance, P.; Campbell, P.G.C. Bioaccumulation of 2,2',5,5'-tetrachlorobiphenyl and pyrene by picoplankton (*Synechococcus leopoliensis*, Cyanophyceae): influence of variable humic acid concentrations and pH. *Environ Toxicol Chem.* **1999**, 18, 2063 -2069.
- (18). Sijm, D.T.H.M.; Middelkoop, J.; Vrisekoop, K. Algal density dependent bioconcentration factors of hydrophobic chemicals. *Chemosphere.* **1995**, 31, 4001 - 4012.
- (19). Casserly, D.M.; Davis, E.M.; Downs, T.D.; Guthrie, R.K. Sorption of organics by *Selenastrum capricornutum*. *Water Res.* **1983**, 17, 1591 -1594.
- (20). Geyer, H.; Politzki, G.; Freitag, D. Prediction of ecotoxicological behavior of chemicals: relationship between n-octanol/Water partition coefficient and bioaccumulation of organic chemicals by alga *Chlorella*. *Chemosphere.* **1984**, 13, 269 - 284.
- (21). Mailhot, H. Prediction of algal bioaccumulation and uptake rate of nine organic compounds by ten physicochemical properties. *Environ Sci Technol.* **1987**, 21, 1009 - 1013.

- (22). Karickhoff, S.W.; Brown, D.S. Sorption of hydrophobic pollutants on natural sediments. *Wat Res.* **1979**, 13, 241 -248.
- (23). Karickhoff, S.W. Semi-empirical estimation of sorption of hydrophobic pollutants on natural sediments and soils. *Chemosphere.* **1981**, 10, 833 -846.
- (24). Karickhoff, S.W. Organic pollutants sorption in aquatic systems. *J Hydraulic Engineering.* **1984**, 110, 707 -735.
- (25). Gustafsson, O.; Haghseta, F.; Chan, C.; Macfarlane, J.; Gschwend, P.M. Quantification of the dilute sedimentary soot phase: implication for PAH speciation and bioavailability. *Environ Sci Technol.* **1997**, 31, 203 -209.
- (26). Buchell, T.D.; Gustafsson, O. Quantification of the soot-water distribution coefficient of PAHs provides mechanistic basis for enhanced sorption observations. *Environ Sci Technol.* **2000**, 34, 5144 -5151.
- (27). Zhou, J.L.; Fileman, T.W.; Evans, S.; Donkin, P.; Readman, J.W.; Mantoura, R.F.C.; Rowland, S. The partition of fluoranthrene and pyrene between suspended particles and dissolved phase in the Humber estuary: a study of the controlling factors. *The Science of the Total Environment.* **1999**, 243/244, 305 -321.
- (28). Schwarzenbach, R.P., Gschwend, P.M., Imboden, D.M. Environmental Organic Chemistry. Wiley-Interscience:New York, 1993.

## Chapter 2. Kinetics of Phenanthrene Accumulation in Coastal Marine Diatoms

### Abstract

The accumulation kinetics of the common polycyclic aromatic hydrocarbon phenanthrene were studied in two species of coastal diatoms, *Thalassiosira weissflogii* and *T. pseudonana*. Short-term and long-term accumulation kinetics were investigated in diatoms exposed to 9-<sup>14</sup>C-phenanthrene for 1 min to 11 d. Rate constants, partition coefficients, and overall bioconcentration factors were obtained from a first-order two-compartment model. The short-term desorption rate constant ( $k_{des}$ ) was 2.2 times greater in *T. pseudonana* (1273 d<sup>-1</sup>) than in *T. weissflogii* (575 d<sup>-1</sup>), reflecting a 2.8-fold greater surface area to volume ratio ( $A/V$ ) in *T. pseudonana* compared with *T. weissflogii*. However, long-term depuration rate constants ( $k_d$ ) were similar (0.55 – 0.62 d<sup>-1</sup>) in both diatom species. The short-term phenanthrene accumulation results showed that surface partition coefficients ( $K_s$ ) increased 1.25–1.50-fold and  $k_{des}$  decreased 3.0–3.5-fold while temperature decreased from 18 – 22°C to 4 – 6°C for the two diatoms tested. The presence of dissolved organic carbon (DOC) reduced phenanthrene accumulation in the cell surface compartments of the two diatoms. Dry weight-normalized phenanthrene bioconcentration factors ( $BCF$ ) were two times higher in *T. weissflogii* ( $38.3 \pm 5.9$  m<sup>3</sup>kg<sup>-1</sup>) than in *T. pseudonana* ( $17.0 \pm 0.9$  m<sup>3</sup>kg<sup>-1</sup>). However, organic carbon normalization yielded similar phenanthrene bioconcentration factors,  $BCF_{oc}$  for *T. weissflogii* and *T. pseudonana* ( $46.1 \pm 12$  m<sup>3</sup>kgC<sup>-1</sup> and  $32.7 \pm 7$  m<sup>3</sup>kgC<sup>-1</sup>, respectively). Growth dilution could be a significant factor in the bioaccumulation of



phenanthrene in marine phytoplankton since typical in situ phytoplankton growth rates ( $k_G$ ,  $0.3 - 1.0 \text{ d}^{-1}$ ) are similar to  $k_d$  ( $0.56 - 0.62 \text{ d}^{-1}$ ) for both species. The fraction of phenanthrene in the cell surface compartment at steady-state ( $x_1$ ) was greater for the smaller cell *T. pseudonana* ( $r \cong 1.5 \text{ }\mu\text{m}$ ;  $x_1 = 49\%$ ) than for *T. weissflogii* ( $r \cong 4.5 \text{ }\mu\text{m}$ ;  $x_1 = 23\%$ ). Thus intracellular partitioning, which may affect phenanthrene trophic transfer, depends on phytoplankton cell size.

## 2.1 Introduction

Phytoplankton plays an important role in the fate and transport of hydrophobic organic contaminants (HOCs), which have a strong affinity for algal cells in aquatic environments. Once accumulated in phytoplankton, HOCs can be carried to bottom sediments with settling cells or ingested by higher organisms, such as zooplankton, in the first step of bioconcentration up the food web. A significant portion of HOCs found in aquatic food webs may be accumulated through trophic transfer, rather than directly from water. Therefore, understanding the accumulation mechanisms of HOCs in phytoplankton is necessary for developing predictive model of HOC bioaccumulation<sup>1,2,3,4</sup>.

The partitioning of HOCs between phytoplankton and the dissolved aqueous phase has often been modeled as a thermodynamic process which is driven by the concentration or fugacity gradients between phases. Observations of slow accumulation, which contradict the assumption of rapid equilibrium, demonstrate the need for a kinetic evaluation and long term (days to weeks) accumulation experiments<sup>3,5</sup>. Long-term studies of HOC bioaccumulation in microalgae support a the two-compartment

accumulation model in which the compound first rapidly partitions in the cell surface and subsequently diffuses into the cell's interior<sup>6,7,8,9,10</sup>. The extent and rates of HOC accumulation in either compartment may be influenced by dissolved organic carbon<sup>1,5,11,12,13,14</sup>, temperature<sup>15</sup>, and phytoplankton growth rate<sup>8,9</sup>, cell size<sup>8,16</sup>, or biochemical composition<sup>4,5,17</sup>.

Studies of the bioaccumulation of polycyclic aromatic hydrocarbons (PAHs) in microalgae limited compared to those of other HOCs, such as polychlorinated biphenyls (PCBs) and chlorobenzene. PAHs are a class of organic chemicals consisting of two or more fused benzene rings in linear, angular or cluster arrangements and are of environmental interest due to health concerns related to their carcinogenicity and their ubiquity in aquatic environments. The bioaccumulation of PAHs in phytoplankton has been examined in previous studies<sup>4,12,13,18,19,20</sup>, but the kinetics of PAH accumulation have received little attention and previous work involved only two genera of chlorophycean microalgae and one species of cyanobacteria.

The objectives of this study were to determine the accumulation kinetics of phenanthrene in two coastal diatom species and thus evaluate empirically the two-compartment HOC accumulation mechanism (cell surface and cell interior). A secondary objective was to evaluate the importance of cell surface area to volume ratio ( $A/V$ ) on the phenanthrene uptake kinetics and intracellular partitioning. Thus the two study diatoms differed in  $A/V$  by a factor of 2. Phenanthrene is one of the most abundant PAHs found in coastal aquatic environments<sup>21</sup> and is on the EPA's Priority Pollutant list (USEPA water quality criteria). The impact of environmental factors such as water

temperature and DOC and biological factors such as growth rate and cell lipid content on phenanthrene accumulation were also examined.

## 2.2 Materials and methods

**Cultures.** Coastal diatoms *Thalassiosira weissflogii* (clone ACTIN) and *Thalassiosira pseudonana* (3H) were cultured in acid-cleaned polycarbonate bottles containing synthetic seawater medium (Aquil)<sup>22</sup> at 18°C, under constant illumination ( $200 \mu\text{mol m}^{-2} \text{s}^{-1}$ ). Growth was monitored by measurements of in vivo chlorophyll-a fluorescence. Diatom cells were harvested in late exponential growth stage by filtration on 3  $\mu\text{m}$  polycarbonate filters, and then resuspended in experimental media.

**Chemicals.** Radiolabeled PAH (9-<sup>14</sup>C- Phenanthrene) with a specific activity of 12.4 mCi mmol<sup>-1</sup> was purchased from Sigma. A phenanthrene stock solution of 10<sup>-4</sup> M was prepared in 100% methanol (Fisher Scientific).

**Phenanthrene accumulation studies.** The short- and long-term accumulation of phenanthrene was measured in marine diatoms exposed to radiolabeled phenanthrene for up to 11 days. Diatoms were resuspended in 250 mL synthetic ocean water (SOW, without addition of macronutrients, vitamins, and trace metals) and incubated at 18°C in the light ( $200 \mu\text{mol m}^{-2} \text{s}^{-1}$ ) in 300-mL glass BOD bottles with glass stoppers except where noted below for short-term treatments. Initial cell densities ranged from  $4 \times 10^4$  –  $6 \times 10^4$  and  $7 \times 10^5$  –  $9 \times 10^5$  cells mL<sup>-1</sup> for *T. weissflogii* and *T. pseudonana*, respectively (corresponding biomass of 12 – 18 mg L<sup>-1</sup> and 20 – 27 mg L<sup>-1</sup> for *T.*

*weissflogii* and *T. pseudonana*, respectively). Uptake experiments were begun with the addition of 50 – 200  $\mu\text{l}$  of  $^{14}\text{C}$  phenanthrene-methanol stock solution, yielding final phenanthrene concentrations of  $2 - 9 \times 10^{-8}$  M. Control bottles receiving methanol only indicated that the carrier of methanol has no negative effect on the growth of experimental cultures. Sampling times ranged from 1 min to 11 d. Short-term uptake sampling was conducted intensively in the first 4 – 5 h of exposure and long-term uptake sampling was conducted daily after the short-term sampling. At each sampling time, cell samples were collected by filtering 5 – 10 mL of cells on glass-fiber filters (Whatman, GF/F), and rinsed with 5 mL SOW. Unfiltered samples (1 mL) were collected simultaneously for total radioisotope analysis. Collected samples were put into 7 mL scintillation vials and 5 mL scintillation fluor (Scintisafe 30%, Fisher Scientific) was added. All vials were held at room temperature for more than 4 hours before analyzing for the radioactivity by scintillation counting with external standard ratio correction of quenching. The concentrations of  $^{14}\text{C}$  phenanthrene were calculated using the specific activity of the chemical and measured dpm.

**Short-term treatments.** The effects of various environmental factors, including DOC (dissolved organic carbon) concentrations and sources, temperature, and light (illumination) on short-term phenanthrene accumulation were examined in *T. weissflogii* and *T. pseudonana*. Three DOC sources were used, including natural seawater, humic acid (Aldrich), and algal exudate. The natural seawater was obtained from Cheesequake Creek (Raritan Bay, New Jersey) and Sandy Hook (New Jersey). Seawater from the two locations was filtered through 0.2  $\mu\text{m}$  polycarbonate filters to

remove suspended particles. Cheesequake seawater was diluted 1:1 with SOW. Various concentrations of humic acid ( $10 - 40 \text{ mg mL}^{-1}$ ) were prepared by dissolving humic acid into SOW followed by GF/F filtration. Algal exudate was obtained from the  $3 \mu\text{m}$  or  $0.2 \mu\text{m}$  filtrate (polycarbonate filters) of late exponential growth stage *T. weissflogii* cultures. Short-term phenanthrene accumulation was measured in 25%, 50%, and 100% of the  $3 \mu\text{m}$  algal culture filtrate and in 100% of the  $0.2 \mu\text{m}$  algal culture filtrate. Temperature effect experiments were performed at  $18 - 22^\circ\text{C}$  and  $4 - 6^\circ\text{C}$ . The effect of light was tested in foil-wrapped and illuminated BOD bottles containing the cell resuspension. In all of the various short-term treatments, control bottles were defined as the SOW experiment at  $18^\circ\text{C}$  under low illumination ( $60 \mu\text{mol m}^{-2}\text{s}^{-1}$ ). Experiments with diatoms obtained from the same parent culture are designated by number in Tables 2.2, 2.3 and 2.5.

**Algal characteristics measured.** Dry weights were determined gravimetrically by collecting algal cells on pre-weighed  $3 \mu\text{m}$  polycarbonate filters and drying at  $60^\circ\text{C}$ . Total lipid and particulate organic carbon (POC) samples were collected on pre-combusted GF/F filters ( $400^\circ\text{C}$ , 2 hr). Total lipid samples were determined gravimetrically or by charring method<sup>23</sup>. Particulate organic carbon samples were analyzed by Chesapeake Biological Laboratory (Exeter Analytical CE-440 Elemental Analyzer), Center for Environmental Science, University of Maryland. Diatom cell volumes and surface area were calculated based on 20 measures with a compound microscope assuming a cylindrical cell shape. The cell density of each sampling time

was determined by counting lugol-preserved cell samples with a Fuchs-Rosenthal counting chamber.

**Bioaccumulation model.** The bioaccumulation of phenanthrene in phytoplankton is conceptually modeled as accumulation into two compartments, cell surface and cell interior. The accumulation of phenanthrene by diatom cells can be described by a first-order, two-compartment kinetic model, using separate surface and interior uptake and depuration rate constants. Thus the experimental rate of phenanthrene accumulation in diatom cells is given by:

$$\frac{dC_p}{dt} = (k_u + k_{ad}) \cdot D \cdot W_d \cdot C_w - (k_{des} + k_G) \cdot C_{p,s} - (k_d + k_G) \cdot C_{p,i} \quad (2-1)$$

where  $C_p$  is the total activity of radiotracer in cells ( $\text{dpm mL}^{-1}$ ,  $C_p = C_{p,s} + C_{p,i}$ ),  $C_{p,s}$  is the activity of radiotracer in the surface compartment ( $\text{dpm mL}^{-1}$ ),  $C_{p,i}$  is the activity of radiotracer in the interior compartment ( $\text{dpm mL}^{-1}$ ),  $C_w$  is the dissolved activity of radiotracer ( $\text{dpm mL}^{-1}$ ),  $D$  is the cell density ( $\text{cell m}^{-3}$ ,  $D$  is a function of time),  $W_d$  is the dry weight of diatom cells ( $\text{kg cell}^{-1}$ ),  $k_u$  is the uptake rate constant to the interior ( $\text{m}^3 \text{kg}^{-1} \text{d}^{-1}$ ),  $k_d$  is the depuration rate constant from the interior ( $\text{d}^{-1}$ ),  $k_{ad}$  is the adsorption constant to the surface ( $\text{m}^3 \text{kg}^{-1} \text{d}^{-1}$ ),  $k_{des}$  is the desorption constant from the surface ( $\text{d}^{-1}$ ),  $k_G$  is growth rate constant ( $\text{d}^{-1}$ ), and  $t$  is the exposure time (d).

At steady-state, the partition coefficients in the cell surface and cell interior,  $K_s$  and  $K_i$ , and the overall kinetic bioconcentration factor ( $BCF$ ), a quantitative measure of bioaccumulation, are calculated using the following equations on a dry weight basis:

$$K_s = \frac{k_{ad}}{k_{des}} \quad (2-2)$$

$$K_i = \frac{k_u}{k_d} \quad (2-3)$$

$$BCF = K_v + K_i = \frac{C_{p\infty}}{C_{w\infty}} \quad (2-4)$$

where the partition coefficients and bioconcentration factor are in units of  $\text{m}^3\text{kg}^{-1}$ ,  $C_{p\infty}$  is the activity of radiotracer in the cells at steady-state ( $\text{dpm mL}^{-1}$ ), and  $C_{w\infty}$  is the dissolved activity of radiotracer at steady-state ( $\text{dpm mL}^{-1}$ ). The fraction of steady-state phenanthrene in cell surface,  $x_1$ , is calculated using the following equation:

$$x_1 = \frac{K_v}{K_v + K_i} \quad (2-5)$$

**Determination of  $k_{ad}$  and  $k_{des}$ .** Given the assumptions that during the short-term exposure (1) the sum of  $C_p$  and  $C_w$  is constant, (2) the accumulation in the cell interior is negligible, and (3) the cell density is constant (the  $k_G$  is zero), equation 2-1 can be simplified and solved as:

$$C_p = C_t \cdot \frac{D \cdot W_d \cdot k_{ad}}{D \cdot W_d \cdot k_{ad} + k_{des}} \left(1 - e^{-k_{des} D W_d + k_{ad} t}\right) \quad (2-6)$$

where  $C_t$  is the total activity of radiotracer ( $C_t = C_p + C_w$ ,  $\text{dpm mL}^{-1}$ ). Short-term phenanthrene accumulation data were fit to equation 2-6 in the form of  $y = a(1 - e^{-bt})$  using SigmaPlot to estimate the rate constants  $k_{ad}$  and  $k_{des}$ .

**Determination of  $k_u$  and  $k_d$ .** Long-term phenanthrene accumulation results were used to estimate the rate constants,  $k_u$  and  $k_d$ , by solving equation 2-1 using a numerical method. In this method, it was assumed that long-term steady state was reached after

seven days. The measured  $BCF$  was used to calculate  $K_i$  (see equation 2-4). Using  $K_i$  and equation 2-3,  $k_d$  was eliminated from equation 2-1. Equation 2-1 was then iterated using measured cellular radioactivities ( $C_p$ ), cell densities ( $D$ ), and growth rates ( $k_G$ ) for each time point and previously determined adsorption and desorption rate constants ( $k_{ad}$  and  $k_{des}$ ) to determine the long-term uptake rate constant,  $k_u$ . The long-term depuration rate constant  $k_d$  was then calculated with equation 2-3.

## 2.3 Results

### Diatom characteristics and growth

The characteristics of the experimental microalgae, *T. weissflogii* and *T. pseudonana*, including dry weight, lipid content, organic carbon content, and estimated ratio of cell surface area to cell volume ( $A/V$ ), are given in Table 2.1. The cellular dry weight, lipid content, organic carbon content, and cellular volumes of the two diatoms did not vary in the control SOW bottles over the long-term exposure time. Thus it is reasonable to use cell density measurements to monitor the biomass over the long term accumulation experiments. In the short-term experiments, it was assumed the cell density was constant in the first hour of exposure, which was confirmed by cell density measurements (data not shown). However, cell densities did increase during the long-term accumulation experiments (Figures 2.3 and 2.4). The growth rate constants derived from cell density measurements in long-term accumulation experiments were  $0.14 - 0.22 \text{ d}^{-1}$  and  $0.08 - 0.36 \text{ d}^{-1}$  for *T. weissflogii* and *T. pseudonana*, respectively, during the first 3 d. Diatom growth rate constants decreased gradually to less than  $0.01 \text{ d}^{-1}$  after the first 3 d.



### Overall phenanthrene accumulation dynamics

Representative phenanthrene accumulation curves are shown in Figures 2.1 – 2.4. Diatom-accumulated phenanthrene is presented as algal radioactivity (dpm mL<sup>-1</sup>) and cellular radioactivity (dpm cell<sup>-1</sup>). Total radioactivity (cell phase plus dissolved phase) in the medium remained stable over the short- and long-term exposure times (Figures 2.1A – 2.4A). Chemical analysis of accumulated phenanthrene measured by HPLC<sup>24</sup> showed no biodegradation of this PAH in the two diatoms tested during the time course of exposure (11 d). The short-term accumulation curves show that the phenanthrene concentrations in both *T. weissflogii* and *T. pseudonana* cells reached a short-term steady-state within 10 min at 18 – 22°C (Figures 2.1A and 2.2A), which was stable for several hours. It took longer (approximately 30 min) to reach short-term steady-state at 4 – 6°C (Figures 2.1B and 2.2B). The long-term accumulation curves (11-d exposure), however, showed that a slower uptake of phenanthrene followed the rapid sorption of the first hour (Figures 2.3 and 2.4), and a steady-state was reached within 5 to 7 days.

### Partition coefficients and overall bioconcentration factors

The surface ( $K_s$ ) and interior ( $K_i$ ) phenanthrene partition coefficients and overall bioconcentration factors (BCF) in the two diatoms are listed in Tables 2.2 and 2.3, and summarized in Table 2.4. Lipid-, organic carbon-, and dry weight-normalized BCFs for the two species are also shown in Table 2.4. The organic carbon normalized  $BCF_{oc}$  of 46.1 m<sup>3</sup>kg C<sup>-1</sup> and 32.7 m<sup>3</sup>kg C<sup>-1</sup> for *T. weissflogii* and *T. pseudonana*, respectively,

were more similar than the dry weight basis or the lipid normalized  $BCF_{lipid}$  (383  $m^3 kg lipid^{-1}$  and 142  $m^3 kg lipid^{-1}$  for *T. weissflogii* and *T. pseudonana*, respectively). This indicated that organic carbon rather than total lipid is the controlling phase for accumulation of phenanthrene. The relationship between  $BCF$  and organic carbon fraction,  $f_{oc}$ , will be interpreted in the discussion section.

### **Fraction of surface sorption**

The fractions of steady-state phenanthrene accumulated in the cell surface compartment ( $x_1$ ) were calculated using the average  $K_s$  and  $K_i$  (equation 2-5; Table 2.4). The  $x_1$  value in *T. weissflogii* (23%) is about half that in *T. pseudonana* (49%).

### **Kinetics parameters**

The average desorption rate constants,  $k_{des}$ , of up to 1273  $d^{-1}$  in *T. pseudonana* and 575  $d^{-1}$  in *T. weissflogii* at 18-22°C reflected the fast surface sorption curves observed in these experiments (Table 2.2; Figures 2.1 and 2.2). The depuration rate constants for the interior compartment,  $k_d$ , were similar (0.62  $d^{-1}$  and 0.56  $d^{-1}$  of *T. weissflogii* and *T. pseudonana*, respectively) in the two diatoms (Table 2.3) and much slower than  $k_{des}$ .

### **Illustration of two-compartment kinetic accumulation**

Modeled total, surface, and interior phenanthrene accumulation curves are shown in Figures 2.5 and 2.6. The modeling results show that phenanthrene in diatoms initially accumulated mainly in the cell surface ( $C_{p-s-model}$ ) and reached steady-state

within 10-20 min while accumulation in the cell interior ( $C_{p-i-model}$ ) increased very little (Figures 2.5A and 2.6A). Over the first 3 d of exposure, surface accumulation decreased with the decreasing dissolved phase concentration of phenanthrene as a result of the net accumulation of phenanthrene in the diatom internal compartments ( $C_{p-i-model}$ ). The cell interiors reached steady-state (hence overall equilibrium) within 5 to 7 d (Figures 2.5B and 2.6B).

### **Temperature effect**

As shown in Table 2.2, the average  $K_s$  increased 1.25 - 1.50 times as the temperature decreased from 18 – 22°C to 4 – 6°C for both of *T. weissflogii* and *T. pseudonana*. The average  $k_{des}$  of *T. weissflogii* (575 d<sup>-1</sup> at 18 – 22°C) decreased by a factor of 3.5 to 165 d<sup>-1</sup> while temperature decreased to 4 – 6°C. The same trend of temperature effect was found in *T. pseudonana*. The average  $k_{des}$  of *T. pseudonana* decreased a factor of 3.0 (1273 d<sup>-1</sup> and 429 d<sup>-1</sup> at 18 – 22°C and 4 – 6°C, respectively) at the lower temperature.

### **DOC treatment**

In all the short-term DOC effect experiments,  $K_s$  values were found to be slightly lower in the presence of humic acid, in natural seawater or with algal exudate than those in the DOC-free control treatments (Table 2.5). Although these short-term DOC experiments were only conducted once and interculture variability was significant, this trend was consistent in all experiments. The primary effect of DOC was to decrease the adsorption rate (desorption was not greatly effected, Table 2.5).

### **Light effect**

The light effect treatment results were indicated in the Table 2.2, showing there is no significant effect among the same experimental sets.

## **2.4 Discussion**

### **Two-compartment model**

The surface sorption and internal accumulation kinetics of phenanthrene are useful to evaluate the mechanisms of PAH accumulation in phytoplankton. Surface sorption was much faster than internal accumulation ( $k_{des}$  was 2 or 3 order magnitude higher than  $k_d$ ; Table 2.4), which confirms the applicability of using a two-compartment model to describe the bioaccumulation on phytoplankton and supports the equilibrium assumption regarding surface sorption<sup>7,8,9,10</sup>.

### **Surface sorption Kinetics**

In the phenanthrene accumulation experiments, the  $k_{des}$  values were 2.1 – 2.2 times greater in *T. pseudonana* than in *T. weissflogii* (Table 2.2) at 18 – 22°C, and 2.6 – 2.9 times greater at 4 – 6°C, possibly reflecting the fact that the ratio of cell surface area to cell volume of *T. pseudonana* is 2.8 times greater than that of *T. weissflogii* (Table 2.1). This result is consistent with the surface sorption mechanism and suggests that cell size could be one of the important factors controlling the kinetics of PAH accumulation in the cell surface compartment.

Surface sorption kinetics data are not available for comparison of phenanthrene bioaccumulation in phytoplankton with that of other HOCs. Skoglund et al (1996)<sup>9</sup> estimated  $K_s$  values from the earliest sampling point (30 min) in a series of bioaccumulation experiments of 40 representative PCB congeners in four freshwater unialgal species (two green algae, one diatom, and one cyanobacterium) and Dachs et al (1999)<sup>10</sup> estimated a  $k_{des}$  value of 288 d<sup>-1</sup> and  $K_s$  values from the first sampling point (15 min) in bioaccumulation experiments with 17 PCB congeners in a single algal species (marine prymnesiophyte). The time assumed to reach short-term steady-state in these two studies of PCB congeners (30 min) is consistent with short-term phenanthrene accumulation. The  $k_{des}$  value of 288 d<sup>-1</sup> for PCBs reported by Dachs et al (1999)<sup>10</sup> is somewhat lower than those for phenanthrene (1273 and 575 d<sup>-1</sup> in *T. pseudonana* and in *T. weissflogii*, respectively). However, the assumption of hydrophobicity-independent surface sorption kinetics for PCBs in the studies of Skoglund et al (1996)<sup>9</sup> and Dachs et al (1999)<sup>10</sup> may not hold for all HOCs. For example, Geyer et al (1984)<sup>19</sup> reported that the accumulation of lipophilic chemicals (hexachlorobenzene with log  $K_{ow}$  of 5.2) in a green algae species reach equilibrium faster than hydrophilic compounds (p-chloroaniline with log  $K_{ow}$  of 2.78) in 24 h exposures. This indicates that the hydrophobicity may affect the kinetics of HOC accumulation in phytoplankton. The variation of surface sorption kinetics among various HOCs with different hydrophobicities should be further investigated before extrapolating phenanthrene surface sorption kinetics data to other compounds.

### Temperature effect on surface sorption

Few studies on the effect of temperature on the bioaccumulation of HOCs in phytoplankton are available in the literature. The bioconcentration factors of chlorobenzene in the green alga, *Scenedesmus spp*, were reported to increase with increasing temperature from 4.5°C to 27.6°C<sup>15</sup>. This is inconsistent with our observations which showed that  $K_s$  increased 1.25 – 1.50 times as the temperature decreased from 18 – 22°C to 4 – 6°C for both of *T. weissflogii* and *T. pseudonana*. The temperature effect on  $K_s$  would be explained as the temperature effect on phenanthrene solubility, increasing temperature would lead to higher solubility and thus lower partition coefficients<sup>25</sup>. The temperature dependence of  $K_s$  can be applied to the bioaccumulation model according to the seasonal variation of surface water temperature. The temperature dependence of  $K_s$  and therefore the overall BCF of phenanthrene is a subject of further investigation.

No kinetics data concerning the effect of temperature on HOC bioaccumulation in phytoplankton are available for comparison with those observed in this study. The temperature effect on  $k_{des}$  may be due to a decrease in the diffusion coefficient of phenanthrene in seawater and in the cell surface with decreasing temperature. However, the surface sorption kinetics were still very fast (the average  $k_{ad}$  values are 165 d<sup>-1</sup> and 429 d<sup>-1</sup> of *T. weissflogii* and *T. pseudonana*, respectively) at the lower temperature, which is still likely faster than most other environmental and biological processes that could affect phenanthrene surface sorption in phytoplankton. Therefore, the temperature dependence of  $k_{des}$  could be negligible in most environmental situations. The

temperature dependence of the interior loss rate ( $k_d$ ), however, could be important and needs to be studied.

### **Internal accumulation kinetics**

In contrast to  $k_{dex}$  values, the long-term, internal compartment depuration rate constants ( $k_d$ ) were similar in both diatom species ( $0.62 \text{ d}^{-1}$  for *T. weissflogii* and  $0.56 \text{ d}^{-1}$  for *T. pseudonana* at  $18^\circ\text{C}$ ). The  $k_d$  values obtained from previous studies with different microalgae species exposed to PCBs and chlorobenzene<sup>8,10</sup> are similar to each other (around  $1 \text{ d}^{-1}$ ), except for the values obtained for the cyanobacterium *Anabaena* ( $0.27 \text{ d}^{-1}$  for hexachlorobenzene and  $2.7 \text{ d}^{-1}$  for 1,2,3,4-tetrachlorobenzene)<sup>8</sup> and to the  $k_d$  values for phenanthrene obtained in the current study. The similarity of  $k_d$  values among eukaryotic phytoplankton could simplify the input parameters in bioaccumulation models.

### **The fraction of surface sorption**

The proportion of phenanthrene accumulation in the cell surface fraction ( $x_1$ ) of *T. pseudonana* (49%) and *T. weissflogii* (23%) increased with the ratio of cell surface area to cell volume ( $A/V$ ), consistent with previous work<sup>8</sup>. To extend this relationship,  $x_1$  values for the two diatoms and a chlorophycean flagellate (*Dunaliella tertiolecta*) are plotted versus  $A/V$  values in Figure 2.7. The linear relationship between  $x_1$  and  $A/V$  indicates that in the two-compartment model, cell surface sorption is inversely related to phytoplankton cell size. The surface sorption fraction was as high as 85% in the cyanobacterium *Anabaena spp.* with an  $A/V$  value of  $1.35 \mu\text{m}^{-1}$ , indicating the

predominance of surface sorption<sup>8</sup>. By contrast, the  $x_1$  value in *T. weissflogii* ( $A/V = 0.59 \mu\text{m}^{-1}$ ) was 0.23, demonstrating the predominance of internal accumulation in this diatom. The size-dependence of cell surface and internal accumulation of HOCs may affect HOC trophic transfer and needs to be considered in the evaluation of bio-dilution. In the studies of the trophic transfer for trace metals, it has been reported that the soluble fraction of metal associated with the cytoplasm of phytoplankton cells is assimilated by herbivorous consumers such as copepods, while metals bound to phytoplankton cell membranes are not assimilated and are egested in fecal material<sup>26</sup>. If the relationship between cytoplasmic fractionation and assimilation efficiency for trace metal is applicable to the trophic transfer of HOCs, the size-dependence of cell surface and internal accumulation can be used to estimate the assimilation efficiency of HOCs in consumers such as copepods given the cell size distribution of a phytoplankton community. However, the applicability of using the relationship between cytoplasmic fractionation and assimilation efficiency for HOCs and the extent to which  $x_1$  values represent the cell fractionation controlling assimilation efficiency need to be further investigated and verified.

### **Bio-dilution**

Since the loss rates of cell surface phenanthrene in marine diatoms (up to  $1273 \text{ d}^{-1}$  and  $575 \text{ d}^{-1}$  in *T. pseudonana* and in *T. weissflogii*, respectively) are much faster than diatom growth rates, no bio-dilution of surface phenanthrene can occur. However, the growth of phytoplankton could be a significant factor in the accumulation of phenanthrene in the cell internal compartment since phytoplankton growth rates,  $k_G$ , are



often greater than the phenanthrene loss rates ( $k_d$ ) observed in this study (0.62 d<sup>-1</sup> and 0.56 d<sup>-1</sup> of *T. weissflogii* and *T. pseudonana*, respectively). Surface accumulation fractions ( $x_1$ ) and loss rate constants ( $k_d$ ) can be used in the quantitative evaluation of growth dilution on phenanthrene bioaccumulation in phytoplankton. The effect of growth on steady-state HOC bioaccumulation can be quantified with the following equation<sup>8</sup>:

$$\frac{BCF^G}{BCF^N} = \frac{\alpha + x_1}{\alpha + 1} \quad (2-7)$$

where  $BCF^G$  is the bio-dilution-influenced bioconcentration factor,  $BCF^N$  is the bioconcentration factor in the absence of any growth effect, and  $\alpha$  is the ratio of  $k_d$  to  $k_G$ . The ratio of  $BCF^G$  to  $BCF^N$  is the relative decrease in bioaccumulation caused by cell growth. Given that the  $k_d$  values of various HOCs in a range of algal species (about 1 d<sup>-1</sup>) are of the same order as growth rates, the fraction of surface accumulation becomes an important factor controlling the magnitude of bio-dilution. Assuming a  $k_d$  value of 1 d<sup>-1</sup> and a growth rate constant of 2 d<sup>-1</sup> (algal growth season), the bio-dilution decrease in BCF at steady-state would be 53% with an  $x_1$  of 0.2, 33% with an  $x_1$  of 0.5, and 13% with an  $x_1$  of 0.8. Thus, a reasonable range of the bio-dilution effect is 13% to 53% during an algal growth season. The cell size distribution of a phytoplankton community, which can affect  $x_1$ , needs to be considered in the evaluation of bio-dilution. Bio-dilution is expected to be significant in phytoplankton with major internal accumulation ( $x_1$  value of  $\leq 0.2$  for larger cells such as *T. weissflogii*). However, for cells with  $x_1$  values of 0.8 – 1.0, indicating the predominance of surface sorption and small cell size, it is reasonable to assume that HOC accumulation is near steady-state at

all times, even during the algal growth season (regardless of the value of the ratio of  $k_d$  to  $k_G$ ). The one-compartment model and equilibrium assumption is therefore reasonable for very small cells such as bacterio-plankton.

### **Overall organic carbon normalized $BCF_{oc}$**

The similarity of the organic carbon-normalized  $BCF_{oc}$ s for *T. weissflogii* and *T. pseudonana* suggests that organic carbon is the sorbing matrix for phenanthrene in these diatoms. This is consistent with recent studies indicating that organic carbon rather than total lipid is the controlling phase for the accumulation of PCBs in phytoplankton (uni-algal laboratory culture and natural assembles)<sup>9,17</sup>. The relationship between dry-weight-normalized bioconcentration factors and  $f_{oc}$  is plotted in Figure 2.8 for the diatoms and the chlorophycean flagellate (*D. tertiolecta*). The linear correlation between  $BCF$  and  $f_{oc}$  ( $r^2 = 0.95$ ) for two diatoms and one green alga confirms the organic carbon-dependence of phenanthrene bioaccumulation. Hence, normalization of  $BCF$  to the organic carbon content can minimize differences among algal species, and can be used to compare surface ( $K_s$ ) and interior ( $K_i$ ) phenanthrene partition coefficients. The average phenanthrene surface partition coefficient on a dry weight basis,  $K_s$ , in *T. weissflogii* is similar to that in *T. pseudonana* at 18 – 22°C (8.86 and 8.31  $m^3kg^{-1}$  for *T. weissflogii* and *T. pseudonana*, respectively). However, the average phenanthrene organic carbon-normalized surface partition coefficient,  $K_{s-OC}$ , in *T. pseudonana* (16.0  $m^3kgC^{-1}$ ) is significantly higher than that in *T. weissflogii* (10.6  $m^3kgC^{-1}$ ) at 18°C. This indicates that smaller cells such as *T. pseudonana* have a higher fraction of organic carbon in their cell surface than bigger cells.

Most previous studies of phenanthrene bioaccumulation in phytoplankton used exposure times of from 2 h to 48 h<sup>4,18,19</sup>. It is expected that reported phenanthrene *BCFs* might be underestimated because of the short time periods used to reach steady-state. The phenanthrene *BCFs* measured in *T. weissflogii* and *T. pseudonana* are generally in agreement with those previously determined for two species of chlorophycean microalgae (Table 2.6)<sup>4,18,19</sup>. However, this comparison of measurements on a dry weight basis must be evaluated with great care because the organic carbon fraction could vary among the algal species tested.

### **Bioavailability**

The effects of DOC on HOC bioavailability in phytoplankton have been studied with various concentrations of humic acid<sup>12</sup>, peat moss infusion<sup>11</sup>, and cell exudate<sup>1,13</sup>. The results from those studies indicate that the bioavailability of HOCs is reduced by DOC. The effect of the DOC-HOC association on HOC bioaccumulation can be described with a three-phase model, including particle, DOC, and free dissolved phases. The effect of DOC on bioaccumulation can then be quantified with the following equation<sup>27</sup>:

$$BCF_{obs} = \frac{BCF_{true}}{1 + DOC \times K_{DOC}} \quad (2-8)$$

where  $BCF_{obs}$  is the bioconcentration factor for an HOC in the presence of DOC in which the DOC-HOC association is defined in the dissolved phase,  $BCF_{true}$  is the intrinsic bioconcentration factor for an HOC in the absence of DOC,  $K_{DOC}$  is the partition coefficient of HOC in the DOC phase ( $m^3 kg C^{-1}$ ), and  $DOC$  is the concentration

of DOC ( $\text{mg C L}^{-1}$ ). Using our short-term DOC uptake results,  $K_{DOC}$  values were calculated using equation 2-8. For the experimental DOC concentrations (Cheesequake of  $5.65 \text{ mg C L}^{-1}$ , Sandy Hook of  $2.84 \text{ mg C L}^{-1}$ , algal exudate of  $17.5 \text{ mg C L}^{-1}$ , and humic acid of  $4.6 - 18.4 \text{ mg C L}^{-1}$  (based on 46% organic carbon<sup>28</sup>), the average calculated  $K_{DOC}$  values were  $13.1 \pm 8.4 \text{ m}^3 \text{ kgC}^{-1}$  for humic acid,  $32.2 \pm 15.9 \text{ m}^3 \text{ kgC}^{-1}$  for estuarine/coastal sea water (combine Cheesequake and Sandy Hook), and  $22.2 \pm 10.1 \text{ m}^3 \text{ kgC}^{-1}$  for algal exudate. The sorption of PAH to humic acid has been reported as  $\log K_{DOC} = 4.65 \text{ (L kg}^{-1}\text{)}$  for phenanthrene estimated from capacity retention factor measured in HPLC<sup>29</sup>, which is higher than the measured  $K_{DOC}$  for humic acid ( $\log K_{DOC} = 4.1$  in the unit of  $\text{L kgC}^{-1}$ ). In the studies of natural DOC, the  $K_{DOC}$  for HOC estimated directly from  $K_{ow}$  (1 order of magnitude lower than the  $K_{ow}$  values) can describe the observed distribution coefficients well in interpreting the effect of DOC on the measured PCB bioaccumulation factors in two diatoms and one cyanobacterium<sup>5</sup> and on the measured PAH partition coefficients from a sediment<sup>27</sup>. Koelmans and Heugens (1998)<sup>14</sup> reported that  $\log K_{DOC}$  ( $\text{L kg}^{-1}$ ) values for two chlorobenzenes and 4 PCBs in an algal exudate from a green algae are well correlated to  $\log K_{ow}$  with a slope of  $1 \pm 0.14$  and an intercept of  $-0.055$  ( $r^2 = 0.927$ ). These studies supported that  $\log K_{DOC}$  is linearly related to  $\log K_{ow}$  for those HOCs studied. Applying the relationship between  $\log K_{DOC}$  and  $\log K_{ow}$  and given the phenanthrene  $K_{ow}$  values of 4.57, the calculated  $K_{DOC}$  for natural sea water ( $\log K_{DOC} = 4.5$  in the unit of  $\text{L kgC}^{-1}$ ) would be higher than those used in previous studies<sup>5,27</sup>, and the calculated  $K_{DOC}$  for algal exudate ( $\log K_{DOC} = 4.3$  in the unit of  $\text{L kgC}^{-1}$ ) would be lower than that estimated from the regression equation in Koelmans and Heugens (1998)<sup>14</sup>. Calculated  $K_{DOC}$  values are of

the same order as the organic carbon-normalized  $BCF_{oc}$  measured for both diatoms tested ( $46.1 \text{ m}^3\text{kgC}^{-1}$  and  $32.7 \text{ m}^3\text{kgC}^{-1}$  for *T. weissflogii* and *T. pseudonana*, respectively). The similarity of  $K_{DOC}$  and  $BCF_{oc}$  of phenanthrene in this study indicates that dissolved organic carbon could play an important role in the bioaccumulation of phenanthrene if DOC and phytoplankton organic carbon concentrations are similar.

## 2.5 Conclusions

Surface sorption and internal accumulation kinetics of phenanthrene in two coastal marine diatoms were examined. The accumulation of phenanthrene in these diatoms is consistent with a two-compartment mechanism in which the compound first partitions in the cell surface and subsequently diffuses into the cell's interior. The surface sorption kinetics were found to be faster than most other environmental and biological process, supporting the equilibrium assumption. The bio-dilution from the growth of phytoplankton could be a significant factor in the internal accumulation of phenanthrene since the long-term loss rate constant,  $k_d$ , was found to be  $0.56 - 0.62 \text{ d}^{-1}$ , which is of the same order of magnitude as  $k_G$  in the phytoplankton growth season ( $1 - 3 \text{ d}^{-1}$  measured during spring and summer in Raritan Bay). The  $k_d$  values for phenanthrene we measured in diatoms are similar to those of other HOCs with a range of hydrophobicities and chemical structures, an observation that may help simplify modeling organic contaminant bioaccumulation. The similarity of organic carbon-normalized  $BCF_{oc}$ s for *T. weissflogii* and *T. pseudonana* suggests that organic carbon is the sorbing matrix for phenanthrene in these diatoms. The cell size (the ratio of cell surface area to cell volume,  $A/V$ ) could influence the phenanthrene accumulation

kinetics in the cell surface compartment and the relative contribution of cell surface sorption to overall bioaccumulation.

## References

- (1). Sijm, D.T.H.M.; Broersen, K.W.; de Roode, D.F.; Mayer, P. Bioconcentration kinetics of hydrophobic chemicals in different densities of *Chlorella pyrenoidosa*. *Environ Toxicol Chem.* **1998**, 17, 1695 -1704.
- (2). Koelmans, A.A.; van der Woude, H.; Hattink, J.; Niesten, D.J.M. Long-term bioconcentration kinetics of hydrophobic chemicals in *Selenastrum capricornutum* and *Microcystis aeruginosa*. *Environ Toxicol Chem.* **1999**, 18, 1164 -1172.
- (3). Swackhamer, D.L.; Skoglund, R.S. Bioaccumulation of PCBs by algae: kinetics versus equilibrium. *Environ Toxicol Chem.* **1993**, 12, 831 -838.
- (4). Halling-Sorenson, B.; Nyholm, N.; Kusk, K.O.; Jacobsson, E. Influence of Nitrogen Status on the Bioconcentration of Hydrophobic Organic Compounds to *Selenastrum carcornutum*. *Ecotoxicol Environ Saf.* **2000**, 45, 33 -42.
- (5). Stange, K.; Swackhamer, D.L. Factors affecting phytoplankton species-specific differences in accumulation of 40 polychlorinated biphenyls (PCBs). *Environ Toxicol Chem.* **1994**, 13, 1849 -1860.
- (6). Wang, K.; Rott, B.; Korte, F. Uptake and bioaccumulation of three PCBs by *Chlorella fusca*. *Chemosphere.* **1982**, 11, 525 -530.
- (7). Koelmans, A.A.; Jimenez, C.S.; Lijklema, L. Sorption of chlorobenzenes to mineralizing phytoplankton. *Environ Toxicol Chem.* **1993**, 12, 1425 -1439.
- (8). Koelmans, A.A.; Anzion, S.F.; Lijklema, L. Dynamics of organic micropollutant biosorption to cyanobacteria and detritus. *Environ Sci Technol.* **1995**, 29, 933 -940.
- (9). Skoglund, R.S.; Stange, K.; Swackhamer, D.L. A kinetics model for predicting the accumulation of PCBs in phytoplankton. *Environ Sci Technol.* **1996**, 30, 2113 -2120.
- (10). Dachs, J.; Eisenreich, S.J.; Baker, J.E.; Ko, F.; Jeremiason, J.D. Coupling of phytoplankton uptake and air-water exchange of persistent organic pollutants. *Environ Sci Technol.* **1999**, 33, 3653 -3660.
- (11). Richer, G.; Peters, R.H. Determinants of the short-term dynamics of PCB uptake by plankton. *Environ Toxicol Chem.* **1993**, 12, 207 -218.

- (12). Twiss, M.R.; Granier, L.; Lafrance, P.; Campbell, P.G.C. Bioaccumulation of 2,2',5,5'-tetrachlorobiphenyl and pyrene by picoplankton (*Synechococcus leopoliensis*, Cyanophyceae): influence of variable humic acid concentrations and pH. *Environ Toxicol Chem.* **1999**, 18, 2063 -2069.
- (13). Sijm, D.T.H.M.; Middelkoop, J.; Vrisekoop, K. Algal density dependent bioconcentration factors of hydrophobic chemicals. *Chemosphere.* **1995**, 31, 4001 - 4012.
- (14). Koelmans, A.A.; Heugens, E.H.W. Binding constants of chlorobenzenes and polychlorobiphenyls for algal exudates. *Wat Sci Tech.* **1998**, 37, 67 -73.
- (15). Koelmans, A.A.; Jimenez, C.S. Temperature dependency of chlorobenzene bioaccumulation in phytoplankton. *Chemosphere.* **1994**, 28, 2041 -2048.
- (16). Axelman, J.; Broman, D.; Naf, C. Field measurements of PCB partitioning between water and planktonic organisms: influence of growth, particles, and solute-solvent interactions. *Environ Sci Technol.* **1997**, 31, 665 -669.
- (17). Skoglund, R.S.; Swackhamer, D.L. Evidence for the use of organic carbon as the sorbing matrix in the modeling of PCB accumulation in phytoplankton. *Environ Sci Technol.* **1999**, 33, 1516 -1519.
- (18). Casserly, D.M.; Davis, E.M.; Downs, T.D.; Guthrie, R.K. Sorption of organics by *Selenastrum capricornutum*. *Water Res.* **1983**, 17, 1591 -1594.
- (19). Geyer, H.; Politzki, G.; Freitag, D. Prediction of ecotoxicological behavior of chemicals: relationship between n-octanol/Water partition coefficient and bioaccumulation of organic chemicals by alga *Chlorella*. *Chemosphere.* **1984**, 13, 269 - 284.
- (20). Mailhot, H. Prediction of algal bioaccumulation and uptake rate of nine organic compounds by ten physicochemical properties. *Environ Sci Technol.* **1987**, 21, 1009 - 1013.
- (21). Broman, D.; Naf, C.; Roiff, C.; Zebuhr, Y. Occurrence and dynamics of polychlorinated dibenzo-p-dioxins and dibenzofurans and polycyclic aromatic hydrocarbons in the mixed surface layer of remote coastal and offshore waters of the Baltic. *Environ Sci Technol.* **1991**, 25, 1850 -1864.
- (22). Price, N.M.; Harrison, G.I.; Hering, J.G.; Hudson, R.J.; Nirel, P.M.V.; Palenik, B.; Morel, F.M.M. Preparation and chemistry of artificial algal culture medium aquil. *Biological Oceanography.* **1988**, 6, 443 -461.
- (23). Marsh, J.B.; Weinstein, D.B. Simple charring method for determination of lipids. *J Lipid Res.* **1966**, 7, 574 -576.

- (24). Liang, W. PhD. Dissertation.. Bioavailability of polycyclic aromatic hydrocarbons(PAHs) to bacteria in estuarine sediment Rutgers University, 2001.
- (25). Schwarzenbach, R.P., Gschwend, P.M., Imboden, D.M. Environmental Organic Chemistry. Wiley-Interscience:New York, 1993.
- (26). Chang, S.I.; Reinfelder, J.R. Bioaccumulation, Subcellular Distribution, and Trophic Transfer of Copper in a Coastal Marine Diatom. *Environ Sci Technol.* **2000**, 34, 4931 -4935.
- (27). Mitra, S.; Dickhut, R.M. Three-Phase Modeling of Polycyclic Aromatic Hydrocarbon Association with Pore-Water\_Dissolved Organic Carbon. *Environ Toxicol Chem.* **1999**, 18, 1144 -1148.
- (28). Gustafsson, O.; Haghseta, F.; Chan, C.; Macfarlane, J.; Gschwend, P.M. Quantification of the dilute sedimentary soot phase: implication for PAH speciation and bioavailability. *Environ Sci Technol.* **1997**, 31, 203 -209.
- (29). Nielsen, T.; Siigur, K.; Helweg, C.; Jorgensen, O.; Hansen, P.E.; Kirso, U. Sorption of polycyclic aromatic compounds to humic acid as studied by high-performance liquid chromatography. *Environ Sci Technol.* **1997**, 31, 1102 -1108.



Table 2.1 Characteristic of tested algal cultures.

Culture	Dry weight	Total lipid		Organic carbon		Cell diameter	$A/V$
	$10^{-12}$ g cell <sup>-1</sup>	$10^{-12}$ g cell <sup>-1</sup>	wt %	$10^{-12}$ g cell <sup>-1</sup>	wt %	$\mu\text{m}$	$\mu\text{m}^{-1}$
<i>T. weissflogii</i>	300±30	30±2 <sup>a</sup>	10	250±50	83	8-10	0.59
<i>D. tertiolecta</i>	163±78 <sup>c</sup>	nd		24 <sup>c</sup>	15	6-9	1.16
<i>T. pseudonana</i>	30±2	3.5±0.2 <sup>b</sup>	12	15.7±3.2	52	2-3	1.66

<sup>a</sup>: Data were determined by charring method, phosphatidyl choline as standard (Marsh & Weinstein 1966).

<sup>b</sup>: Data were determined gravimetrically.

<sup>c</sup>: data provided by Antonietta Quigg (pers. comm.).  $A/V$ : the ratio of cell surface area to cell volume.

nd: not determined.

Table 2.2 Rate constants and dry weight-normalized partition coefficients. Short-term phenanthrene accumulation experiments were conducted in SOW at 18-22°C and 4-6°C.

Cultures	$C_T^a$	$k_{ad}$	$k_{des}$	$K_s$
	$10^{-9}M$	$m^3 kg^{-1} d^{-1}$	$d^{-1}$	$m^3 kg^{-1}$
<b><i>T. weissflogii</i> 18-22 °C</b>				
1	34.6	5652	807	7.01
2	34.6	7111	761	9.34
3	34.9	9262	884	10.48
5	31.5	4727	532	8.88
	42.0	4489	504	8.90
6	24.9	3409	384	8.87
	44.5	3450	361	9.55
	90.8	2862	311	9.21
7	25.8	4762	633	7.53
<b>Average</b>		<b>5080±2027</b>	<b>575±208</b>	<b>8.86±1.04</b>
<b>4-6 °C</b>				
5	45.3 <sup>b</sup>	2041	171	11.94
7	25.1	1810	163	11.10
	34.1	1793	172	10.42
	48.7	1690	153	11.08
<b>Average</b>		<b>1834±148</b>	<b>165±9</b>	<b>11.13±0.62</b>
<b><i>T. pseudonana</i> 18-22 °C</b>				
8	44.6	11090	1406	7.83
	90.0	8971	1122	7.99
9	20.7	11335	1436	7.89
	39.0	11374	1261	9.02
	80.8	11186	1257	8.90
	20.0 <sup>b</sup>	10187	1254	8.12
	39.0 <sup>b</sup>	9767	1175	8.31
78.2 <sup>b</sup>	10779	1275	8.45	
<b>Average</b>		<b>10575±861</b>	<b>1273±105</b>	<b>8.31±0.45</b>
<b>4-6 °C</b>				
8	45.0	6420	517	12.41
	93.2	6717	547	12.28
9	21.0 <sup>b</sup>	3824	310	12.31
	41.8 <sup>b</sup>	5612	453	12.40
	79.1 <sup>b</sup>	4257	315	13.50
<b>Average</b>		<b>5366±1285</b>	<b>429±111</b>	<b>12.58±0.52</b>

<sup>a</sup>:  $C_T$  is the total phenanthrene concentration at the start of each experiment.

<sup>b</sup>: Conducted in complete darkness.

Table 2.3 Uptake rate constants, depuration rate constants, dry weight-normalized partition coefficients in cell interior, and the overall dry weight-normalized bioconcentration factors. Long-term phenanthrene accumulation experiments were conducted in the continuous light at 18°C.

Cultures	$C_T^a$	$k_u$	$k_d$	$K_i$	$BCF$
	$10^{-9}M$	$m^3 kg^{-1} d^{-1}$	$d^{-1}$	$m^3 kg^{-1}$	$m^3 kg^{-1}$
<i>T. weissflogii</i>					
6	24.9	17.05	0.69	24.6	33.5
	44.5	17.25	0.64	27.0	36.6
	90.8	19.06	0.54	35.6	44.8
<b>Average</b>		<b>17.79±1.11</b>	<b>0.62±0.08</b>	<b>29.1±5.8</b>	<b>38.3±5.9</b>
<i>T. pseudonana</i>					
9	20.7	5.66	0.68	8.3	16.2
	39.0	4.55	0.58	7.9	16.9
	80.8	3.72	0.41	9.1	17.9
<b>Average</b>		<b>4.64±0.97</b>	<b>0.56±0.14</b>	<b>8.4±0.6</b>	<b>17.0±0.9</b>

<sup>a</sup>:  $C_T$  is the total phenanthrene concentration at the start of each experiment.

Table 2.4 Phenanthrene loss rate constants, partition coefficients, fraction of surface accumulation( $x_1$ ), and overall bioconcentration factors in *T. pseudonana*, *T. weissflogii*, and *D. tertiolecta*.  $K_s$ ,  $K_i$ , and  $BCF$  are dry weight-normalized partition coefficients.  $BCF_{oc}$  and  $BCF_{lipid}$  are normalized to cellular organic carbon or lipid content, respectively.

Culture	$k_{des}$	$K_s$	$n$	$k_d$	$K_i$	$n$	$x_1$	$BCF$	$BCF_{oc}$	$BCF_{lipid}$
	$d^{-1}$	$m^3kg^{-1}$		$d^{-1}$	$m^3kg^{-1}$		(%)	$m^3kg^{-1}$	$m^3kg^{-1}$	$m^3kg^{-1}$
<i>T. weissflogii</i>	575±208	8.86±1.04	9	0.62±0.08	29.1±5.8	3	23	38.3±5.9	46.1±12	383±74
<i>D. tertiolecta</i>	nd	1.68±0.04	3	0.37±0.03	2.9±0.9	3	36	4.6±1.1	32.2±16	nd
<i>T. pseudonana</i>	1273±105	8.31±0.45	8	0.56±0.14	8.4±0.6	3	49	17.0±0.9	32.7±7	141±14

nd: not determined

Table 2.5 Rate constants and dry weight-normalized partition coefficients of phenanthrene *T. weissflogii* in the presence of DOC. Short-term phenanthrene accumulation experiments were conducted at 18–22°C.

Cultures	Experimental conditions		$k_{ad}$	$k_{des}$	$K_s$
	Media	$C_T^a$ $10^{-9}M$	$m^3 kg^{-1} d^{-1}$	$d^{-1}$	$m^3 kg^{-1}$
<i>T. weissflogii</i>					
1	HA-40 mg L <sup>-1</sup>	39.5	5320	840	6.34
	HA-20 mg L <sup>-1</sup>	36.2	5347	824	6.49
	HA-10 mg L <sup>-1</sup>	36.6	5676	882	6.43
	SOW	34.6	5652	807	7.01
2	Cheesequake	33.9	4489	576	7.79
	Sandy Hook	32.8	6314	773	8.17
	SOW	34.6	7111	761	9.34
3	Cheesequake	36.8	5492	617	8.90
	50% Cheesequake	38.9	6991	689	10.14
	SOW	34.9	9262	884	10.48
4	Exudate 100%	34.5	nd	nd	9.34 <sup>b</sup>
	Exudate 50%	34.7	nd	nd	9.39 <sup>b</sup>
	Exudate 25%	35.2	nd	nd	9.89 <sup>b</sup>
	Exudate 0.2 $\mu m$	37.4	nd	nd	10.89 <sup>b</sup>
	SOW	33.8	nd	nd	11.27 <sup>b</sup>

<sup>a</sup>:  $C_T$  is the total phenanthrene concentration at the start of each experiment.

<sup>b</sup>:  $K_s$  values were calculated as the measured cellular phenanthrene divided by dissolved phenanthrene.

nd: not determined.

Table 2.6 Phenanthrene dry weight normalized *BCFs* in various phytoplankton species.

Species	Exposure time	Reported <i>BCF</i>	<i>BCF</i> (m <sup>3</sup> kg <sup>-1</sup> ) <sup>a</sup>	Reference
<i>Selenastrum capricornutum</i>	24 hr	23,800 mg(water)/mg(TSS)	23.8	Casserly <i>et al.</i> , 1983
<i>Chlorella fusca</i>	24 hr	1,760 ml(water)/g(wet algae)	8.8 <sup>b</sup>	Geyer <i>et al.</i> , 1984
<i>Selenastrum capricornutum</i>	2 hr	4.24 liter/kg (in log scale)	17.4	Halling-Sorensen <i>et al.</i> , 2000
<i>Thalassiosira weissflogii</i>	1 hr		8.86	this study
<i>T. weissflogii</i>	11 days		38.3	this study
<i>Thalassiosira pseudonana</i>	1 hr		8.31	this study
<i>T. pseudonana</i>	11 days		17.0	this study

<sup>a</sup>: All data of *BCF/BF* were converted to dry weight-normalized of m<sup>3</sup>/kg for comparison.

<sup>b</sup>: To calculate the *BCF* on dry weight basis the reported *BCF* was multiplied by 5 (Geyer *et al.*, 1984).

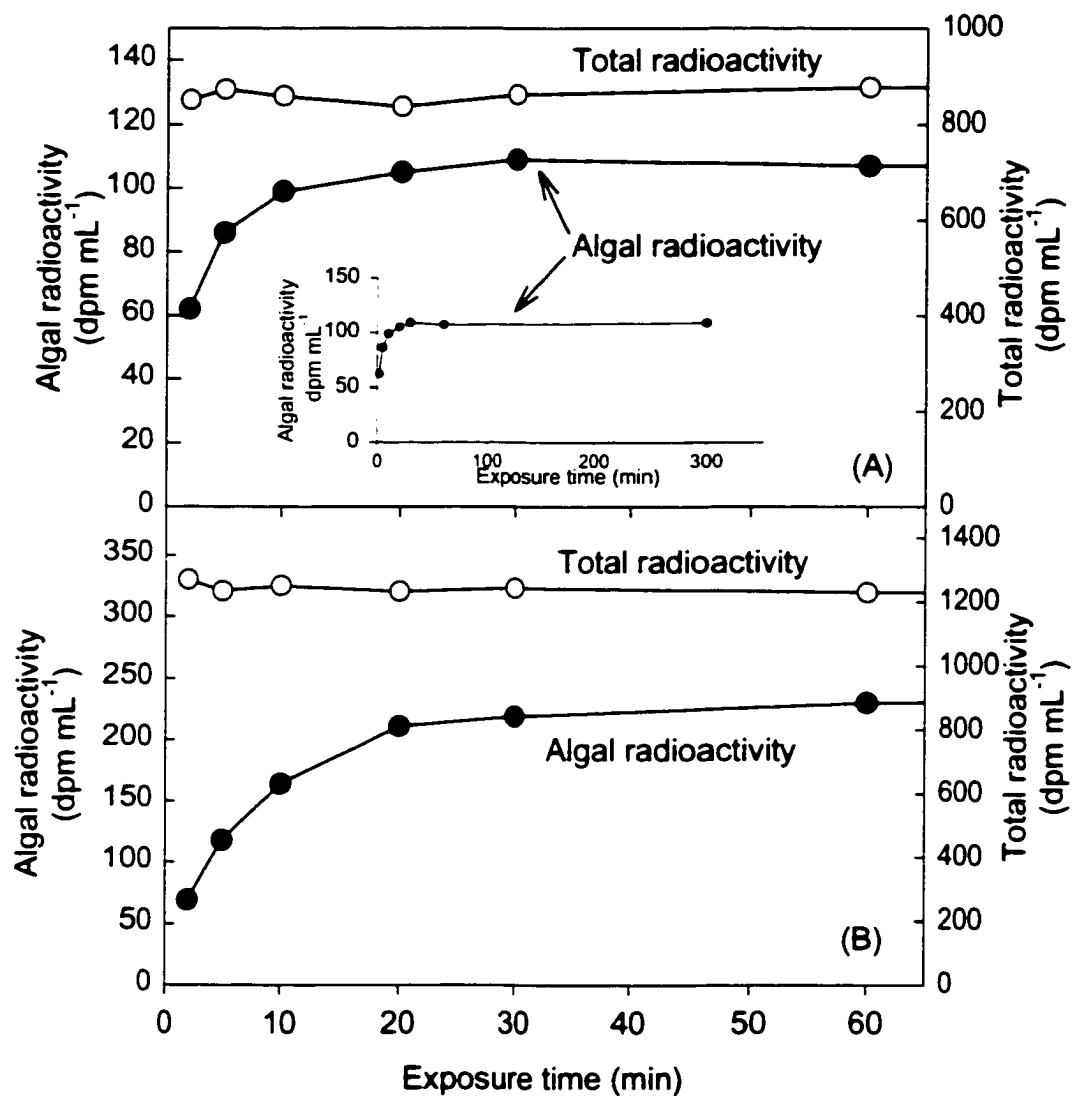


Figure 2.1 Short-term phenanthrene uptake in *T. weissflogii*. The total and algal  $^{14}\text{C}$ -phenanthrene radioactivities over the exposure time are shown. (A) Experiment was conducted at 18-22°C with a total phenanthrene concentration of  $3.46 \times 10^{-8}$  M. (B) Experiment was conducted at 4-6°C with a total phenanthrene concentration of  $4.53 \times 10^{-8}$  M.

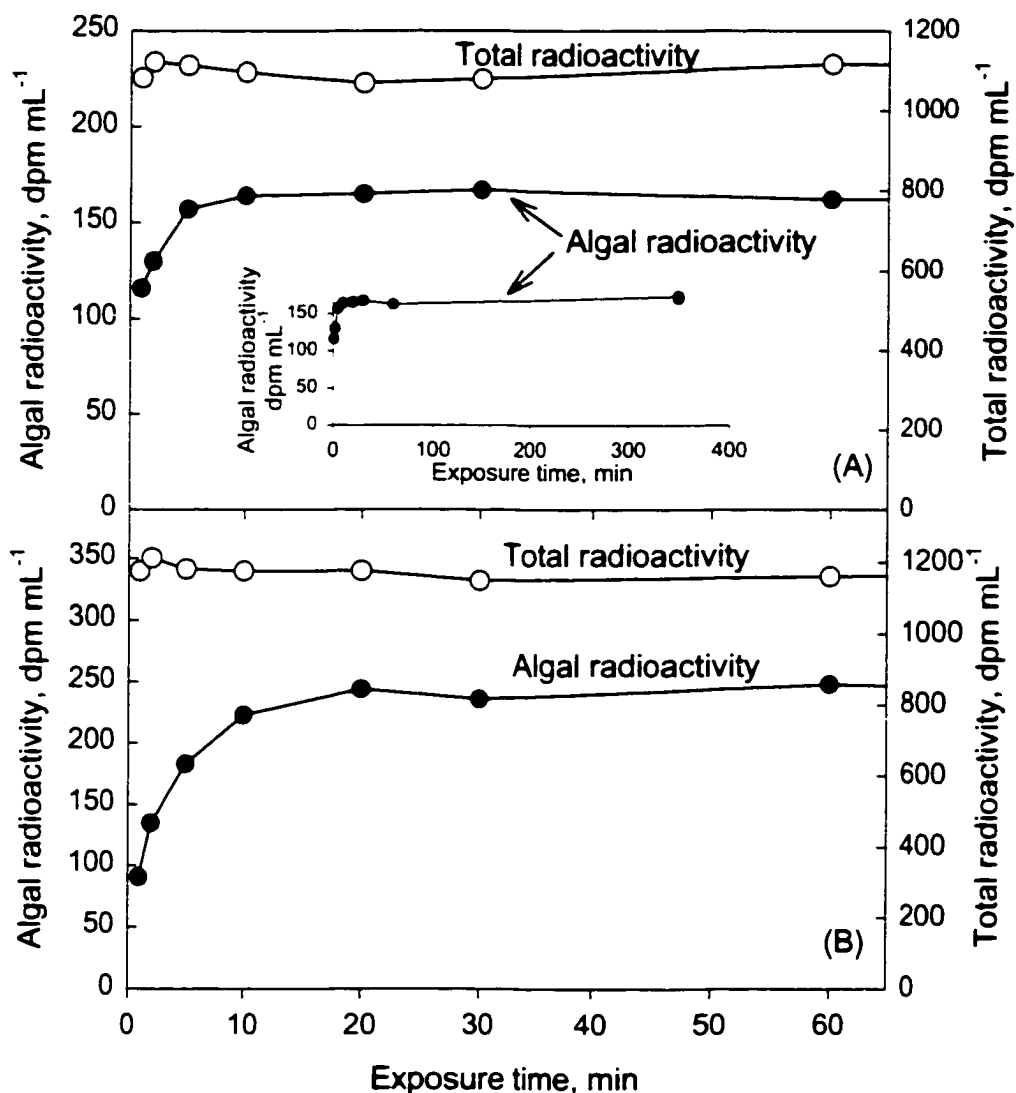


Figure 2.2 Short-term phenanthrene uptake in *T. pseudonana*. The total and algal  $^{14}\text{C}$ -phenanthrene radioactivities over the exposure time are shown. (A) Experiment was conducted at 18-22°C with a total phenanthrene concentration of  $3.90 \times 10^{-8}$  M. (B) Experiment was conducted at 4-6°C with a total phenanthrene concentration of  $4.18 \times 10^{-8}$  M.



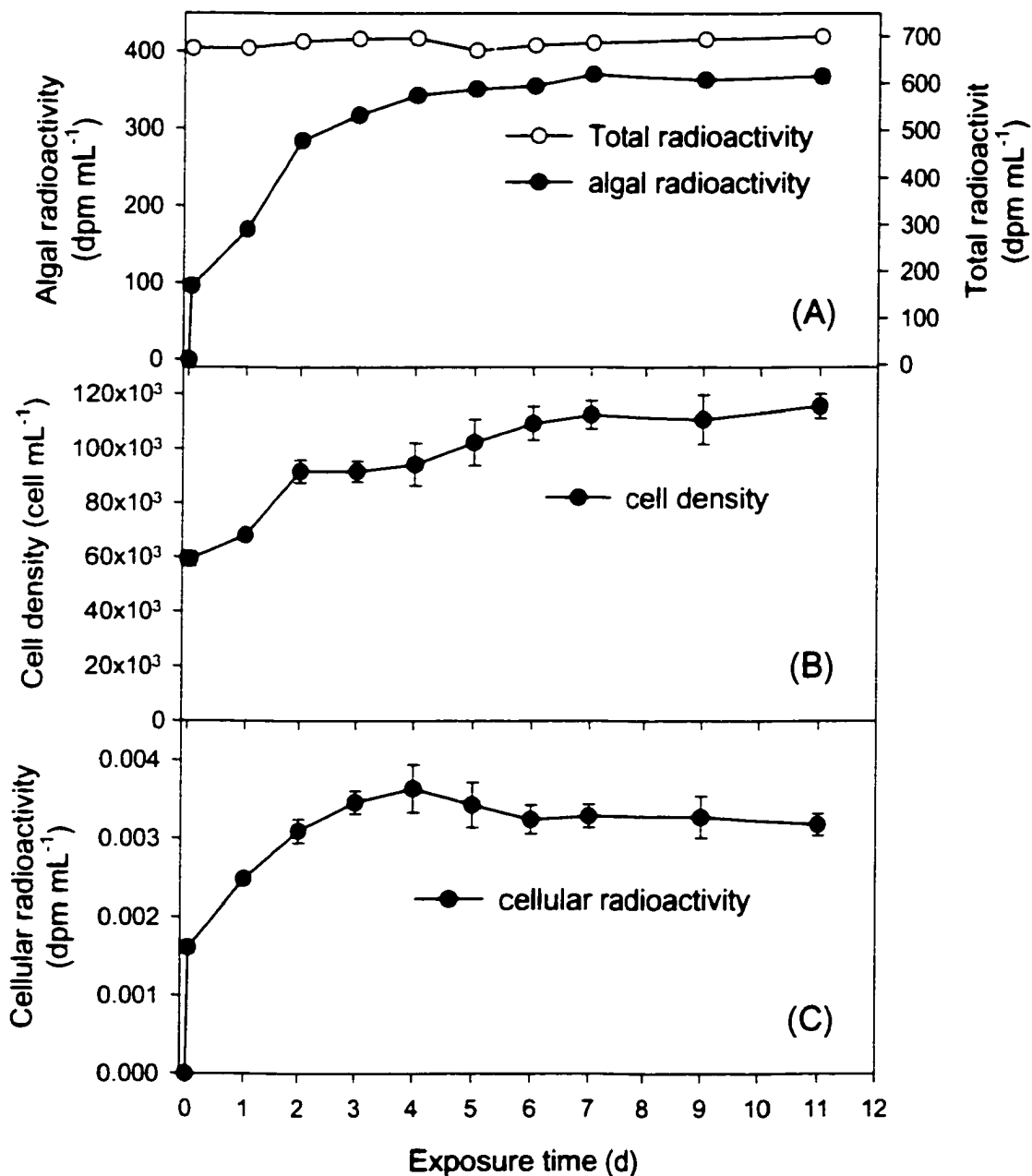


Figure 2.3 Long-term phenanthrene uptake in *T. weissflogii* at 18°C with  $2.49 \times 10^{-8}$  M phenanthrene. (A) The total and algal  $^{14}\text{C}$ -phenanthrene radioactivities, (B) cell density, and (C) cellular radioactivity over the exposure time are shown.

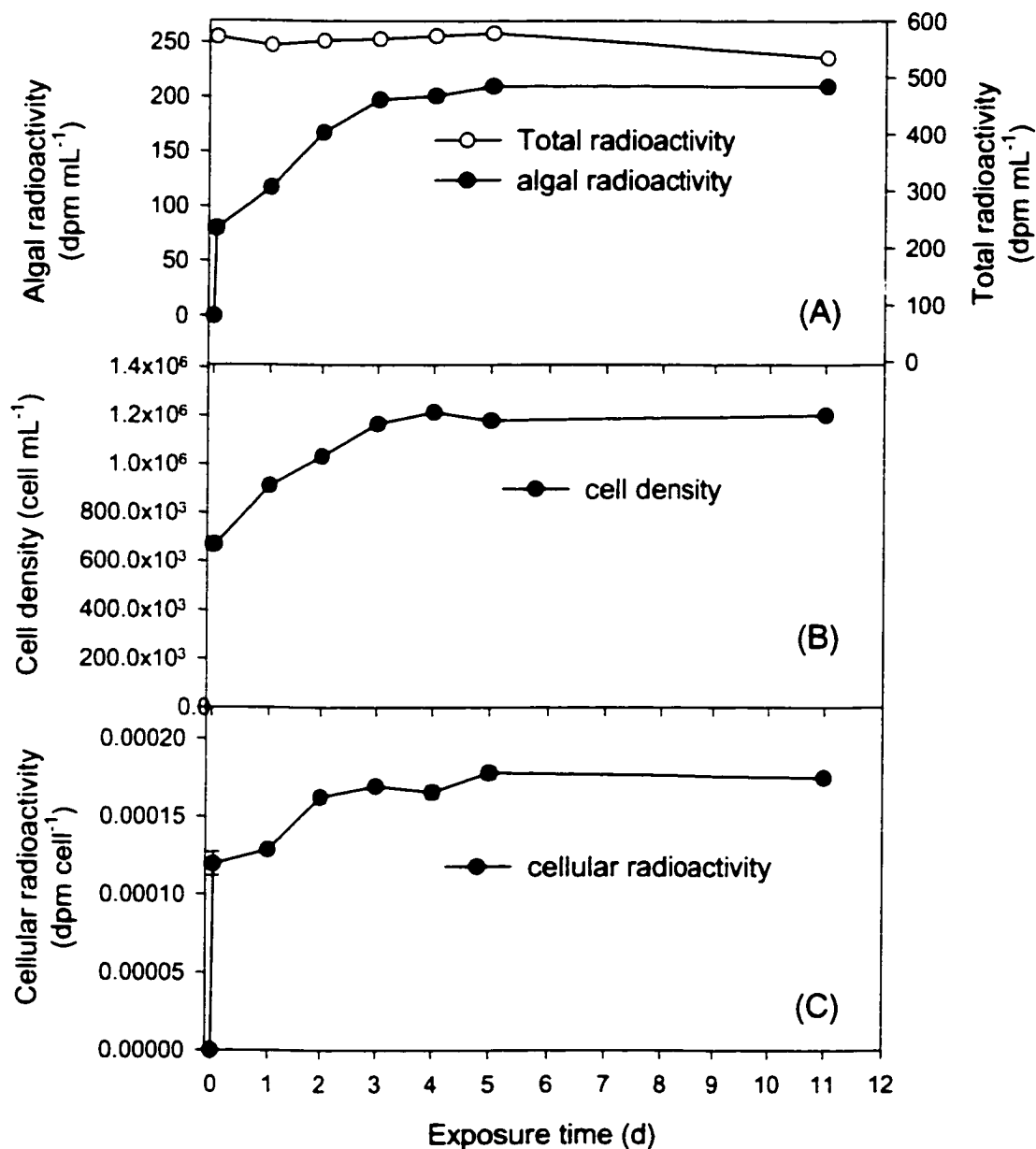


Figure 2.4 Long-term phenanthrene uptake in *T. pseudonana* at 18°C with  $2.07 \times 10^{-8}$  M phenanthrene. (A) The total and algal  $^{14}\text{C}$ -phenanthrene radioactivities, (B) cell density, and (C) cellular radioactivity over the exposure time are shown.

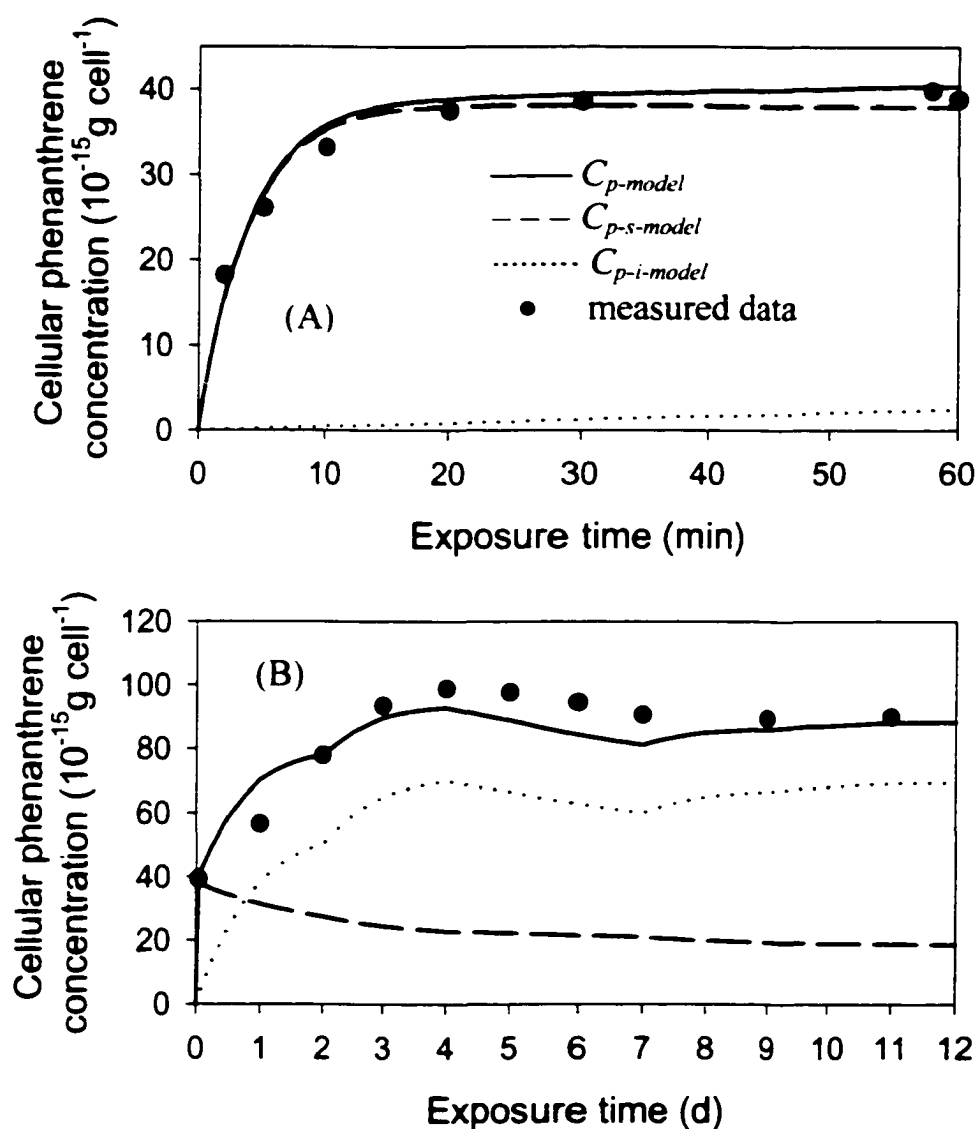


Figure 2.5 Cellular phenanthrene concentrations in *T. weissflogii* over (A) the first hour of exposure, and (B) 11 d of exposure in unit of  $10^{-15} \text{ g cell}^{-1}$ . The dots ( $\bullet$ ) are measured data, the lines are model results. Experiment was conducted at  $18^\circ\text{C}$  with a total phenanthrene concentration of  $9.08 \times 10^{-8} \text{ M}$ .

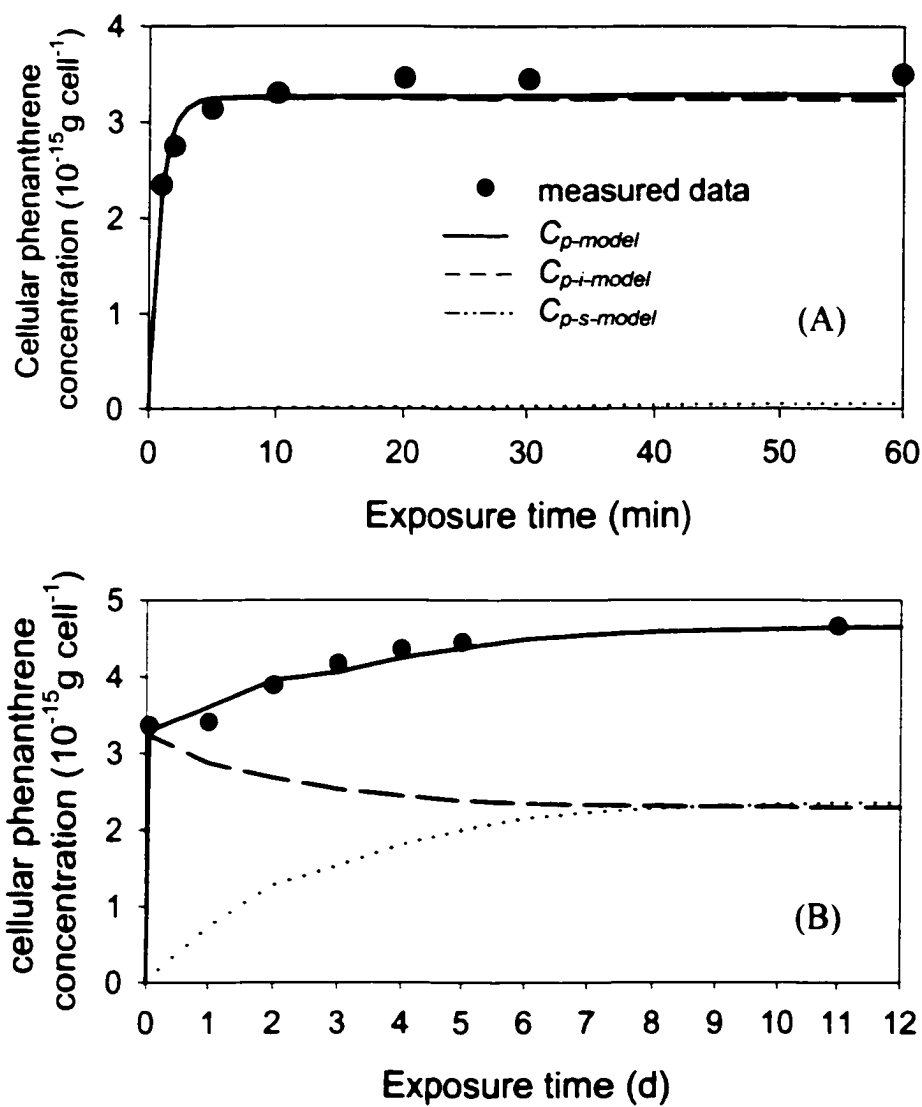


Figure 2.6 Cellular phenanthrene concentrations in *T. pseudonana* over (A) the first hour of exposure, and (B) 11 d of exposure in unit of  $10^{-15} \text{ g cell}^{-1}$ . The dots (●) are measured data, the lines are model results. Experiment was conducted at  $18^\circ\text{C}$  with a total phenanthrene concentration of  $80.8 \times 10^{-8} \text{ M}$ .

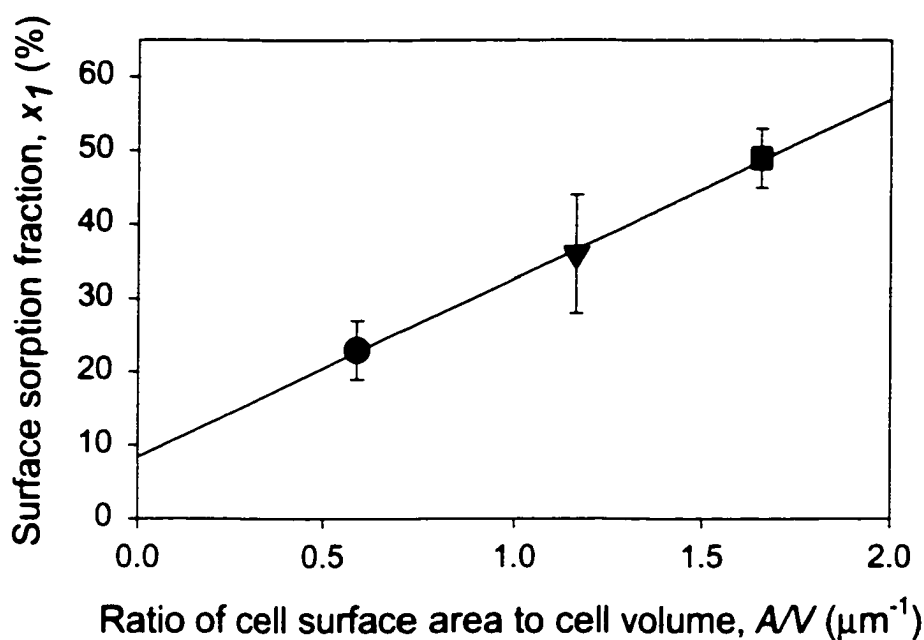


Figure 2.7 The relationship between surface sorption fraction of phenanthrene and cell surface area to volume ratio in the phenanthrene accumulation in *T. weissflogii* (●), *T. pusedonana* (■), and *T. tertiolecta* (▼). The line describes the regression result  $x_1 = 24.26 A/V + 8.419$  ( $r^2 = 0.99$ ).

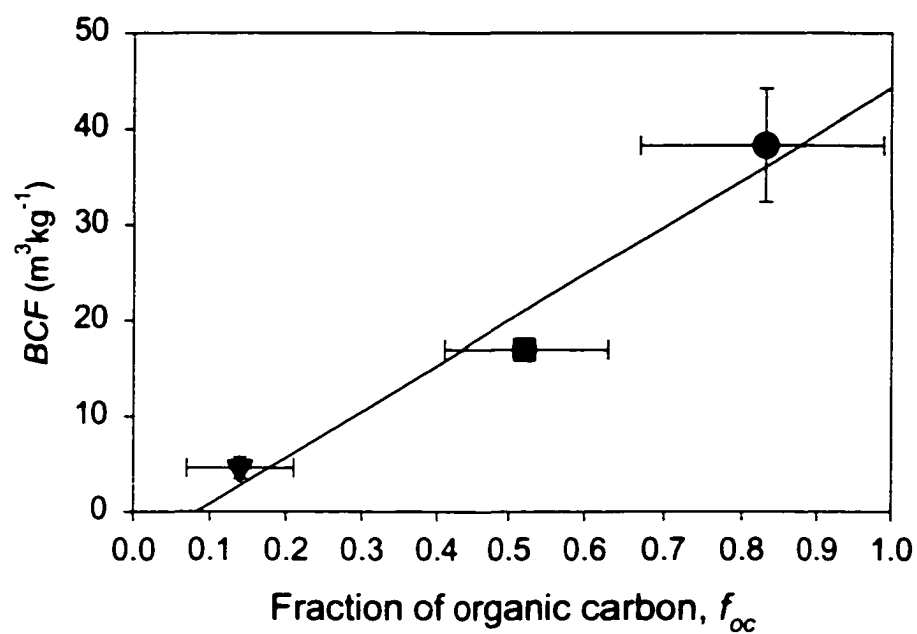


Figure 2.8 Dependence of phenanthrene dry weight-normalized  $BCF$  on the fraction of organic carbon in *T. weissflogii* (●), *T. pusedonana* (■), and *T. tertiolecta* (▼).

### **Chapter 3. Polycyclic Aromatic Hydrocarbons (PAHs) in the Air, Water, and Suspended particle of the NY/NJ Hudson River Harbor Estuary**

#### **Abstract**

Simultaneous measurements of polycyclic aromatic hydrocarbons (PAHs) in the air, water, and suspended particulate matter of Raritan Bay, New Jersey, were made during four field campaigns in April, August, and October 2000 and in April 2001. Gas phase and atmospheric particle PAH concentrations measured during the cruise of Oct/2000 (average total PAHs concentrations of  $10.08 \text{ ng m}^{-3}$  and  $98.13 \text{ ng m}^{-3}$  in particle and gas phases, respectively) were highest among these four cruises, but both the dissolved and suspended particulate phase PAH concentrations in water were highest during the cruise of Apr/2000 ( $60.37 \text{ ng L}^{-1}$  and  $92.49 \text{ ng L}^{-1}$  in dissolved and suspended particulate phases, respectively). Calculated organic carbon normalized partition coefficients ( $K_{oc}$ ) were 1-3 orders of magnitude higher than those predicted from an organic carbon partitioning model for low to intermediate molecular weight PAHs including phenanthrene, methylphenanthrenes, and pyrene. Log  $K_{oc}$  values were weakly correlated with PAH hydrophobicity (octanol water partition coefficient,  $K_{ow}$ ) in Apr/2000 and Apr/2001, but not in Aug/2000 and Oct/2000 (PAHs  $n = 13$ ). The higher than expected PAH  $K_{oc}$  values and their weak correlations with  $K_{ow}$  indicate the presence of a particulate phase (possibly soot particles) to which PAHs sorbed more strongly compared to organic carbon. Using an extended soot carbon-partitioning equation, 5–10% of phenanthrene was estimated to associate with organic carbon in the

suspended particulate phase, suggesting the predominance of soot-like phase in the total suspended particulate phenanthrene in Raritan Bay. This indicates the importance of measuring the environmental soot abundance to predict field observations. However, monitoring the organic carbon associated PAH, as a surrogate of phytoplankton associated PAHs, is still needed because phytoplankton is the first entry into the food web. The total suspended matter (TSM), chlorophyll-a (Chl a), total particulate lipid (TLP), particulate organic carbon (POC), and particulate organic nitrogen (PON) were highest in April and August and lowest in October. Phosphate, nitrate, and nitrite concentrations were lowest in April.

### 3.1 Introduction

Polycyclic aromatic hydrocarbons (PAHs) are members of a class of organic chemicals consisting of two or more fused benzene rings in linear, angular and cluster arrangements and are pollutants of concern due to their carcinogenic nature. PAHs are found ubiquitously in aquatic environments, even in remote areas<sup>1</sup>. Moreover, urban and industrial developments contribute to increased PAH loading in coastal areas<sup>2,3,4</sup>. Sorption is a key process controlling the fate of many hydrophobic organic compounds (HOCs) such as PAHs in aquatic environments. The partitioning of HOCs between the dissolved and suspended particulate phases can be quantified with a partition coefficient:

$$K_p = \frac{C_p}{C_d \cdot TSM} \quad (3-1)$$



where  $K_p$  is the water-partile partition coefficient ( $L\ kg^{-1}$ ),  $C_p$  is the concentration of PAH in the particulate phase ( $ng\ L^{-1}$ ),  $C_d$  is the concentration of PAH in the dissolved phase ( $ng\ L^{-1}$ ), and TSM is the total suspended matter in the water column ( $kg\ L^{-1}$ ). Laboratory studies have indicated that sorption coefficients normalized to organic carbon ( $K_{oc}$ ) are relatively invariant for natural sediments and soil<sup>5,6,7</sup>. Assuming organic carbon is the only PAH-sorbing matrix in suspended particles,  $K_{oc}$  values can be calculated from field measurements given the weight fraction of organic carbon ( $f_{oc}$ ) in the sorbents:

$$K_{oc} = \frac{K_p}{f_{oc}} \quad (3-2)$$

Our laboratory studies (Chapter 2) indicated that organic carbon-normalized phenanthrene bioconcentration factors ( $BCF_{oc}$ ) are similar among two marine diatoms and one green alga ( $32.2 - 46.1\ m^3\ kgC^{-1}$ ). Skoglund and Swackhamer (1999)<sup>8</sup> reported empirical evidence supporting the use of organic carbon as the sorbing matrix for polychlorinated biphenyls (PCBs) in phytoplankton.

The  $K_{oc}$  values for a range of compounds have been found to be correlated to their octanol-water partition coefficients ( $K_{ow}$ ). Several organic carbon-partitioning models have been reported that provide reasonable estimates of  $K_{oc}$  from  $K_{ow}$  values<sup>5,6,7</sup>. For example, Karickhoff (1981)<sup>6</sup> found the following relationship between the  $K_{oc}$  and  $K_{ow}$  for five PAHs in soils and sediments:

$$\log K_{oc} = 0.989 \log K_{ow} - 0.346 \quad (r^2 = 0.997) \quad (3-3)$$

Several recent field observations of PAHs have reported that  $K_{oc}$  values for PAHs are much higher than predictions based on the organic carbon-partitioning equations<sup>1,9,10</sup>.

For example, the measured  $K_{oc}$  values in New York-New Jersey Harbor Estuary were found to be one order of magnitude higher than those predicted from the simple organic carbon-partitioning model<sup>4</sup>. These elevated observed  $K_{oc}$  values have led to the proposition that the presence of soot-like particles, which have a high affinity for PAHs<sup>9,11,10</sup>, could affect PAH partitioning. An extended partitioning equation for PAHs including partitioning with soot-like particles has been reported<sup>9</sup>:

$$K_d = f_{oc} K_{oc} + f_{sc} K_{sc} \quad (3-4)$$

where  $f_{sc}$  is the weight fraction of soot carbon in particles and  $K_{sc}$  is soot carbon normalized partition coefficient. The elevated  $K_d$  values for phenanthrene and fluoranthene in a marine sediment<sup>9</sup> and for fluoranthene and pyrene in estuarine suspended particles<sup>10</sup> can be quantitatively explained with the extended soot carbon-partitioning model.

The objectives of this study were (1) to measure concentrations of PAHs in the air, water, and suspended particulate matters in Raritan Bay, (2) to calculate the water-particulate partition coefficients of PAHs, and (3) to examine whether a simple organic carbon-partitioning model can be applied to PAHs measured in Raritan Bay.

### 3.2 Materials and methods

**Sampling sites.** Simultaneous air and water samples were taken aboard the R/V Walford at a site (40.30°N/74.05°W) in the Raritan Bay, New Jersey (Figure 3.1), during six cruises from October 1999 through April 2001 (sampling site switched to 40.29°N/73.57°W on April 24 and 25, 2001), including the first two pilot cruises of Oct/1999 and Dec/1999 in 1999. The New York-New Jersey Harbor Estuary and the

Lower Hudson River Estuary have been reported to be impacted greatly by anthropogenic input of PAHs due to their proximity to urban and industrial regions<sup>2-4</sup>.

**PAH measurements.** Details of sample preparation, extraction and analysis are presented in previous studies<sup>2-4</sup> and summarized here. Air samples were collected using modified high volume air samplers (Tisch Environmental). Quartz fiber filters (QF/F, Whatman) were used to capture the particulate phase and polyurethane foam plugs (PUFs) were used to capture the gas phase. Water samples were collected using an Infiltrax 100 water sampler (Axys Environmental System Ltd) at a depth of 1.5 m. Glass fiber filters (GF/F, Whatman) were used to collect the suspended matter phase and XAD resin (Amberlite) cartridges were used to capture dissolved phase.

Phytoplankton samples were collected for PAH analysis during the Apr/2000, Aug/2000, Oct/2000, and Apr/2001 cruises using a plankton net sampler (64  $\mu\text{m}$  Nitex mesh). Precombusted GF/F (47 mm) was used to collect the concentrated phytoplankton suspension (50 – 400 ml). The volumes for plankton net samples were estimated indirectly via the chl-a measurements of the plankton net samples and suspended particulate matter. All samples were stored frozen until analysis.

Samples were spiked with deuterated anthracene-*d*<sub>10</sub>, fluoranthene-*d*<sub>10</sub>, and benzo[*e*]pyrene-*d*<sub>12</sub> as surrogate standards and extracted using a Soxhlet apparatus for 24 hours using the following solvents for different sample media: QF/F in dichloromethane; PUF in petroleum ether; XAD-2 resin and GF/F in acetone: hexane (1:1 by volume). The extracts were concentrated and reduced in volume to approximately 1 ml. The concentrated extract was fractionated and cleaned up on a

column of 3% water-deactivated alumina. The PAH fraction was eluted with 2:1 dichloromethane: hexane, and concentrated to 0.1 to 0.2 ml. All samples were analyzed on a Hewlett-Packard 6890 gas chromatograph (GC) coupled to a Hewlett Packard 5973 mass selective detector (MSD). The column used was a 30 m × 0.25 mm i.d., J&W Scientific 122-5062 DB-5 (5% diphenyl-dimethylpolysiloxane) capillary column. The identity and subsequent retention time of each PAH was confirmed by the use of a calibration standard which contained known concentrations of surrogate compounds, internal standard compounds, and all of the PAH compounds of interest in this study. The mass of each PAH was determined by isotopic dilution with a series of internal standards (phenanthrene-*d*<sub>10</sub>, pyrene-*d*<sub>10</sub>, and benzo[*a*]pyrene-*d*<sub>12</sub>) added to the samples prior to instrumental analysis.

**Meteorological measurements.** Air temperature, wind speeds and directions were recorded on the R/V Walford.

**CTD measurements.** Water profiles of temperature, pH, dissolved oxygen (DO), and salinity were obtained by CTD-(Conductivity, Temperature, Depth) -transmissometer-fluorometer profiler on each sampling cruise.

**Total Suspended matter measurements.** Seawater was pumped through ¼" Tygon tubing from a depth of 1.5 m, the same depth of the Infiltrax 100 samplers (PAH water samples). A 350 µm Nitex mesh was used to exclude meso-zooplankton and other large particles. For the analysis of total suspended matter (TSM), total particulate lipid (TPL),

chlorophyll a (Chl a), particulate organic carbon (POC), and particulate organic nitrogen (PON), 200 – 500 ml of pumped seawater were filtered through pre-combusted (450°C for 2 hr) glass-fiber filters (GF/F, Whatman) in triplicate. After filtration, filters were rinsed with 20 ml 0.7 M ammonium formate solution and stored frozen until analysis.

In the laboratory, TSM was determined gravimetrically (48 hr, 60°C) using a balance with an accuracy of 1 µg. Pigment was extracted with 90% acetone. The extracts were filtered and the filtrate was used to determine the concentrations of chlorophyll a and phaeopigment (following acidification with 0.1 N HCl) using a spectrophotometer<sup>12</sup>. Lipid was extracted with a mixture of methanol and chloroform. After filtration and purifying the filtrate with 0.04% MgCl<sub>2</sub> salt solution, the pure extract in chloroform was blow down to dryness in a N<sub>2</sub> stream. The lipid content was determined either by charring method<sup>13</sup> or gravimetrically using a balance with an accuracy of 1 µg. POC and PON analyses were conducted by the Chesapeake Biological Laboratory using an Exeter Analytical CE-440 Elemental Analyzer.

#### **Dissolved inorganic nutrients and dissolved organic carbon measurements.**

Seawater was passed through pre-combusted GF/F filters. The filtrates were collected in acid-cleaned polyethylene bottles and stored frozen until analysis. Nitrate (NO<sub>3</sub><sup>-</sup>), nitrite (NO<sub>2</sub><sup>-</sup>), ammonium (NH<sub>4</sub><sup>+</sup>), and phosphate (PO<sub>4</sub><sup>-3</sup>) were analyzed in duplicate by the standard seawater analytical procedures<sup>14,15</sup>. Dissolved organic carbon (DOC) analyses were conducted by the Chesapeake Biological Laboratory using a Shimadzu 5000 total carbon analyzer.

**Phytoplankton and bacterioplankton enumeration.** Phytoplankton samples for species composition were collected with a plankton net (64  $\mu\text{m}$  Nitex mesh). A concentrated phytoplankton sample (40 ml) was preserved with formaldehyde for microscopic examination. Phytoplankton species were identified and counted and the sizes of the dominant species were estimated.

Unfiltered seawater (40 ml) was preserved with formaldehyde for bacteria counting. These samples were stained with DAPI, filtered on black 0.22  $\mu\text{m}$  polycarbonate filters, and counted using epifluorescence microscopy<sup>16</sup>.

**Phytoplankton growth rates.** Phytoplankton growth rates were estimated from incubations of meso-zooplankton-free seawater. Three 500-ml acid-cleaned polycarbonate bottles were filled with pumped seawater, sieved through a 350  $\mu\text{m}$  Nitex mesh to remove zooplankton. These bottles were incubated on deck, submerged in a cooler filled with surface seawater, for 4 – 7 h. The light intensity was adjusted to simulate that at a depth of 1.5 m with neutral density screening. Chl a and POC samples were collected at the end of each incubation and growth rate estimated from changes in biomass.

### 3.3 Results

#### **Meteorological and CTD measurements**

Meteorological data, including air temperature, wind speeds and wind directions, and CTD measurements, including water temperature, dissolved oxygen,

salinity, pH, and derived water column stratification status, are presented in Tables 3.1 and 3.2, respectively. Air temperature ranged from 8 to 23°C and mean wind speeds ranged from 0.2 to 10 m s<sup>-1</sup> (Table 3.1). For the water column parameters, the water temperature showed a seasonal pattern and ranged from 8°C (Dec/1999, Apr/2000, and Apr/2001) to 23°C (Aug/2000). Salinity, which ranged from 22 to 30 and pH, which ranged from 7.0 to 8.6, showed no seasonal pattern. Water temperature and salinity profiles showed stratification with mixing depths of 2 – 3 m in Dec/1999, Apr/2000, Aug/2000, and Apr/2001, and well-mixed water columns in Oct/1999 and Oct/2000. DO profiles showed super-saturated or saturated DO in the surface water and decreasing of DO with depth. The tidal chart for Sandy Hook is presented in Table 3.3.

#### **Total suspended particulate matter measurements**

The suspended particulate matter parameters (TSM, Chl a, TPL, POC, and PON) for each sampling cruise are presented in Table 3.4. A seasonal pattern was found among suspended particulate related parameters (Figure 3.2), with low concentrations in Oct/1999, Dec/1999, and Oct/2000 (fall and winter), and high concentrations in Apr/2000, Aug/2000, and Apr/2001 (spring and summer). The daily and in some cases hourly variation in the measured parameters reflects the small-scale spatial and temporal variability present in the Raritan Bay (Table 3.4). The calculated organic carbon fractions ( $f_{oc}$ ) and C/N ratios are also presented in Table 3.4.

### **Inorganic dissolved nutrients**

Dissolved nutrient measurements are presented in Table 3.5. Nitrate measurements ranged from 2 to 36  $\mu\text{M}$ , showing low concentrations in Apr/2000 and Apr/2001 (spring) and higher concentrations during fall and winter (Figure 3.3A). Nitrite and phosphate measurements followed similar patterns as nitrate with nitrite ranging from 0.3 to 4.0  $\mu\text{M}$  and phosphate ranging from 0.54 to 4.0  $\mu\text{M}$  (Figures 3.3B & 3.3C). Ammonium measurements ranged from 3.0 to 145  $\mu\text{M}$ , showing up to 145  $\mu\text{M}$  in Apr/2000 cruise and lowest down to 2.6  $\mu\text{M}$  in Apr/2001 (Figure 3.3D).

### **Phytoplankton community**

In the phytoplankton community, diatoms were found to dominate in all samples. Five dominant diatom genera were selected to quantify relative abundance in the phytoplankton community (Figure 3.4). *Skeletonema* spp and *Asterionella* spp were numerically most abundant in Oct/1999 Apr/2000, Aug/2000, and Apr/2000 while *Chaetoceros* spp and *Pseudo-nitzschia* spp were most abundant in Oct/2000. However, with using the cell volume to calculate relative abundance, *Conscinodiscus* spp, which has a diameter of 100 to 150  $\mu\text{m}$ , makes a major contribution in the phytoplankton biomass in August and October (Figure 3.4). Among the phytoplankton community, green algae and dinoflagellates were occasionally found (<1% cell counted).

### **Phytoplankton growth rates**

Short-term incubation results (Chl a & POC) are listed in Tables 3.6 and 3.7. Phytoplankton growth rates ranged from 0 to 3  $\text{d}^{-1}$ . The August 23, 2000 incubation



showed a significant decrease in Chl *a* measurement accompanied by increases in both phaeopigment and POC measurements. These results, and those for the previous two days, show the growth of a phytoplankton bloom and its apparent crash on August 23.

### **Bacterial enumeration**

The bacterial abundance was found to range from 1.0 to 5.3 cells $\times 10^6$  mL<sup>-1</sup>, and no seasonal pattern was found (Table 3.4). Assuming a carbon concentration of  $20 \times 10^{-15}$  g C cell<sup>-1</sup>, it is approximately 20 – 106  $\mu$ g C L<sup>-1</sup> for the bacteria. Given *POC* measurements of sampling cruises, the relative contribution of bacteria to total *POC* ranged from 2 to 9%.

### **PAH measurements**

The abbreviations and related information for the 36 PAHs are listed in Table 3.8. The average concentrations of PAHs in air from the four cruises are shown in Figures 3.5 – 3.8. Both the gas and particle phase PAHs concentrations in air were higher in Oct/2000 than during other seasons. The total atmospheric PAH concentrations in Oct/2000 averaged 10 ng m<sup>-3</sup> and 98 ng m<sup>-3</sup> on particles and in the gas phase, respectively. Lower atmospheric PAH concentrations were found in both Apr/2000 and Apr/2001 (averages of 1.5 ng m<sup>-3</sup> and 1.6 ng m<sup>-3</sup> on particles in Apr/2000 and Apr/2001, respectively, and 12 ng m<sup>-3</sup> and 19 ng m<sup>-3</sup> in the gas phase in Apr/2000 and Apr/2001, respectively).

Both the dissolved and suspended particulate phase PAH concentrations in water were highest in the cruise of Apr/2000 (60 ng L<sup>-1</sup> and 92 ng L<sup>-1</sup> in dissolved and

suspended particulate phases, respectively). Consistently lower concentrations were found in Apr/2001, Aug/2000, and Oct/2000 (22 – 23 ng L<sup>-1</sup> and 16 – 25 ng L<sup>-1</sup> in dissolved and suspended particulate phases, respectively).

### **PAH measurements in water from plankton net samples**

The average PAH concentrations from plankton net samples were lower than those from the in-situ pump (Figure 3.9), indicating that the plankton net did not collect all suspended particle associated PAHs. In Oct/2000 and Apr/2001, POC was measured in plankton net samples. The organic carbon-normalized suspended particle phase concentrations were similar or lower than in-situ pump samples (Figure 3.10).

### **PAH profile distribution**

The comparisons among the PAH concentration profiles of the gas, air particle, dissolved, and suspended particulate phases were made to examine the linkage of each other. The average PAH concentration profiles (Figures 3.5 – 3.8) from each cruise were used for the comparison. The air particle phase and water suspended particulate phase were statistically correlated ( $r^2 = 0.68 \sim 0.88$ ,  $n = 27$ ,  $p = 0.001$ ) in the four cruises, suggesting the two particle phases are closely coupled. In water, dissolved and suspended particulate phases are correlated for the low molecular weight PAHs (MW = 166 ~ 219,  $r^2 = 0.73 \sim 0.92$ ,  $n = 14$ ,  $p = 0.001$ ). However, the gas phase and dissolved phase were not significantly correlated except in Apr/2001 for low molecular weight PAHs (MW = 166 ~ 198,  $r^2 = 0.88$ ,  $n = 8$ ,  $p = 0.001$ ).

### Organic carbon-normalized PAH partition coefficients

To determine whether the simple organic carbon-partitioning equation can be applied to PAHs measured in Raritan Bay, the PAH  $K_{oc}$  values, estimated using equation 3-3, were plotted against  $K_{ow}$  ( $n = 13$ ) (Figure 3.11). The PAHs selected were based on the availability of  $K_{ow}$  values in the literature<sup>18,19</sup> and the magnitude of dissolved phase concentrations, excluding those below detection limit. It has been reported that the estimated  $\log K_{ow}$  values for nine selected PAHs are within 0.15 to 0.26 log units over a temperature range of 10 – 25°C<sup>20</sup>. Since the temperature dependence of  $K_{ow}$  for PAHs is relatively minor,  $K_{ow}$  were not corrected for temperature in this study. The regression lines showed weak correlations of  $\log K_{oc}$  values with  $\log K_{ow}$  for PAHs in Apr/2000 ( $r^2 = 0.4 \sim 0.5$ ,  $p = 0.02 \sim 0.01$ ) and Apr/2001 ( $r^2 = 0.2 \sim 0.45$ ,  $p = 0.2 \sim 0.01$ ), and no correlations in Aug/2000 and Oct/2000 ( $r^2 < 0.1$ ,  $p > 0.2$ ). The average slopes in Apr/2000 and Apr/2001 are 0.49 and 0.44, and the average intercepts are 3.33 and 3.5. Predicted PAH  $K_{oc}$  values using the organic carbon-partitioning model<sup>6</sup> (equation 3-3) is presented as a dotted line. The field measured  $K_{oc}$  values were higher than those predicted with this model except for benzo[*e*]pyrene ( $\log K_{ow} = 6.44$ ). These correlation slopes are clearly far from one. However, theoretically, the slope should be close to one at equilibrium for OC<sup>4</sup> or other PAH-sorbing particles such as soot<sup>21</sup>. The results in this study might indicate the PAHs are not at equilibrium between the water and the particles as was suggested by Achman et al<sup>22</sup>. They might also indicate that other factors are controlling the partitioning of PAHs on particles, such as DOC, phytoplankton growth, or soot-like particles.

### **Relationship between $K_d$ and $f_{oc}$**

The field  $K_d$  values calculated using equation 3-1 for phenanthrene, pyrene, methylphenanthrenes, and benzo[e]pyrene were used to examine the linear correlation between  $K_d$  and  $f_{oc}$ . Those field  $K_d$  values for four cruises were plotted against measured  $f_{oc}$  values (Figure 3.12). Predicted  $K_d$  values for phenanthrene, pyrene, methylphenanthrenes, and benzo[e]pyrene using equations 3-2 and 3-3 were also plotted for comparison the field values. The laboratory derived phenanthrene  $BCF_{oc}$  value of  $36,300 \text{ L kg C}^{-1}$  used to predict the field  $K_p$  values were also shown in Figure 3.12A. Very weak correlations were found between field  $K_p$  and  $f_{oc}$  values ( $r^2 < 0.2$ , except  $r^2 = 0.37$  for methylphenanthrenes in Oct/2000 and  $r^2 = 0.34$  for benzo[e]pyrene in Apr/2001). It is clear that the field measured phenanthrene  $K_p$  values were 1 to 2 orders of magnitude higher those predicted from laboratory phenanthrene  $BCF_{oc}$  and from the organic carbon-partitioning model. The methylphenanthrenes and pyrene  $K_p$  values against  $f_{oc}$ , shown in Figures 3.12A and 3.12B, present the same pattern as phenanthrene. For benzo[e]pyrene, however, the  $K_d$  values were similar to the predicted values.

## **3.4 Discussion**

### **Inorganic dissolved nutrients**

Dissolved nutrient concentrations measured in Raritan Bay are consistent with reports of the New Jersey Department of Environmental Protection<sup>23</sup>, indicating that Raritan Bay is characterized by relatively nutrient rich water.

### **Phytoplankton community**

This diatom-dominated phytoplankton community found in Raritan Bay is consistent with other reports. Diatoms such as *Skeletonema costatum* and *Thalassiosira* spp were reported to be dominant compared to all other species enumerated through most of 1991–1992<sup>24</sup>. A moderate bloom of diatoms, including *Rhizosolenia*, *Asterionella*, and *Skeletonema* spp, was detected in May, 1999 (DEP report, 2000)<sup>25</sup>, which is consistent with the results for Apr/2000 and Apr/2001 which show that *Asterionella* and *Skeletonema* dominated in Raritan Bay.

### **Extended soot carbon partitioning model**

Empirical models are frequently used to predict  $K_{oc}$  and  $K_p$  values for HOCs such as PAHs and PCBs from  $K_{ow}$  values. The relationship between  $\log K_{oc}$  and  $\log K_{ow}$  for PAHs in Raritan Bay showed a weak correlation (Figure 3.11), raising questions about the validity of the organic carbon-partitioning model in predicting PAH  $K_{oc}$  from  $K_{ow}$ , particularly in August and October of 2000. Moreover, the field  $K_p$  values for PAHs such as phenanthrene, methylphenanthrenes, and pyrene were higher than predictions based on organic matter partitioning (Figure 3.12). These higher than expected  $K_p$  results are consistent with previous reports<sup>9,10</sup>, which indicated the presence of soot-like particles to which PAHs are significantly more associated than with natural organic matter.

Because the soot carbon fractions,  $f_{sc}$ , were not measured, the modified  $K_d$  cannot be quantified using the extended soot carbon-partitioning model. However, this model can be used to estimate the relative fractions of organic carbon- and soot carbon-

associated PAHs for phenanthrene, pyrene, methylphenanthrene, and benzo[*e*]pyrene. The relative fractions of organic carbon associated PAHs were calculated by dividing the product of predicted  $K_{oc}$  value from equation 3-3 and field measured  $f_{oc}$  value by the field measured  $K_p$  values from equation 3-1. The laboratory determined phenanthrene  $BCF_{oc}$  of 36,300 L kg C<sup>-1</sup> was also used to quantify the phytoplankton associated phenanthrene fraction in the field samples. For phenanthrene, organic carbon or phytoplankton account for only 5–10% of the total phenanthrene in suspended particulate matter in Raritan Bay. The results for methylphenanthrenes and pyrene also indicated that about 10% of the two PAHs were associated with natural organic carbon. These calculations indicate that a significant fraction of particulate PAHs are associated with some phase other than organic matter or phytoplankton. The elevated PAH  $K_d$  values in marine sediments (phenanthrene and fluoranthene)<sup>9</sup>, estuarine suspended particles (fluoranthene and pyrene)<sup>10</sup>, and recipient water of an aluminum reduction plant (17 PAHs individuals)<sup>26</sup> have been quantitatively explained with extended, soot carbon-partitioning models. In Raritan Bay, soot particles may account for a large portion of this PAH-binding phase and the environmental behavior and effects of soot particles require further study.

### **Atmospheric deposition**

The air particle phase and water suspended particulate phase were statistically correlated ( $r^2 = 0.68 \sim 0.88$ ,  $n = 27$ ) in the four cruises, suggesting that the two particle phases are linked and that atmospheric deposition of PAH-associated particles could affect PAH concentration in these surface water. Atmospheric deposition of soot-like

aerosols has been shown to contribute significantly to surface microlayer particle-associated PAH concentration in the urban Elizabeth River estuary (Southern Chesapeake)<sup>27</sup>. The wet or dry atmospheric deposition of aerosol-bound PAHs is expected to be most important for the higher molecular weight PAHs such as benzo[*b*]fluorene, chrysene, and benzo[*a*]pyrene which are predominantly in the aerosol phase to the total PAH input to Raritan Bay<sup>4</sup>. Atmospheric deposition may also include a significant load from deposition to the adjacent watersheds and subsequent runoff.

The dissolved phase PAHs accumulated in surface waters via the air-water exchange, could partition onto suspended particles. Gigliotti et al (2002)<sup>4</sup> reported that gas phase absorption dominates the total PAH inputs to Raritan Bay for low molecular weight PAHs such as phenanthrene and methylphenanthrenes. It is expected that gas absorption would contribute to soot-associated PAHs in Raritan Bay.

### **Re-distribution**

In their study of the soot-water distribution coefficients of PAHs on diesel particulate matter, Bucheli and Gustafsson (2000)<sup>11</sup> reported that PAHs can actively distribute from the aqueous phase to soot phase, suggesting that the observed PAH distribution is not merely a result of the initial, permanent occlusion during soot formation (combustion). This suggested that the sorption of PAHs on soot particles could play a crucial role in the fate and transport of PAHs in aquatic environments. Laboratory determined water-soot partition coefficients for PAHs ( $K_{sc}$ ) are 1 to 3 orders of magnitude higher than  $K_{oc}$  values<sup>11,28</sup>. Since  $f_{oc}$  values are typically only a factor of 10 – 20 higher than  $f_{sc}$  values in estuarine suspended particulate matter<sup>10</sup> and

harbor sediments<sup>9</sup>, soot partitioning could realistically account for at least as much as the organic carbon associated particulate PAHs. This indicates the importance of monitoring the environmental soot abundance,  $f_{sc}$ .

### **Resuspension and runoff**

The relatively high concentrations of perylene found in the suspended particulate phase compared to the other three phases, is consistent with a previous report<sup>4</sup>. Gigliotti et al (2002)<sup>4</sup> suggest that resuspension likely accounts for the high concentrations of perylene measured in the suspended particulate phases due to the observation of perylene-rich in situ sediment samples. It is likely that sediment transport processes (resuspension) would also contribute other PAHs to the water column. In an estuary, tidally-driven resuspension of sediment-associated PAHs could be important.

Dachs et al (1997)<sup>29</sup> attributed suspended particulate associated perylene measured from an estuary in the western Mediterranean to a naturally derived origin. Arzayus et al (2001)<sup>30</sup> also suggested that sediment-associated perylene measured in Chesapeake Bay is derived from the diagenetic alteration of terrestrial organic matter and terrestrial runoff could be the mode of entry of perylene. These two results indicate that runoff is the possible source of some PAHs. Budzinski et al (1997)<sup>31</sup> also suggested that perylene can be used as a useful tracer of water to elucidate the riverine inputs to deep-sea sediments.

### **Bioaccumulation of PAHs**



In this study, the organic carbon or phytoplankton  $BCF_{oc}$ -associated phenanthrene only contributes 5–10% in the total suspended particulate phenanthrene in Raritan Bay based on the extended soot carbon-partitioning model. However, it is believed that phytoplankton plays a crucial role in the fate and transport of HOCs in aquatic environments because it is the primary entrance into the food chain<sup>32</sup>. Moreover, PAH bioaccumulation is of great concern because of the potential environmental health risk. It is reasonable to use the extended soot carbon partitioning model to predict and explain the field observations. However, to predict PAH trophic transfer, the phytoplankton-associated PAH needs to be quantified to represent the bioavailable fraction of the total measured suspended particulate associated PAH. Even though the extended partitioning model could estimate the partitioning of PAHs in aquatic environments, organic matter partitioning model and bioaccumulation models<sup>33</sup> are needed to predict the bioavailability of PAHs in surface water.

### 3.5 Conclusions

The measured phenanthrene partition coefficients as well as methylphenanthrene and pyrene are 2 to 3 orders of magnitude higher than those predicted by the organic carbon partitioning model or laboratory determined  $BCF_{oc}$ , suggesting the need for extending the organic carbon partitioning model to include an additional phase such as soot. The sources of soot-associated PAHs in Raritan Bay could include atmospheric deposition, resuspension of sediments, and riverine runoff, resulting in a heterogeneous mixture of suspended particles. It is reasonable to use the extended soot carbon partitioning model to estimate the total particulate PAH. However, out of concern over

the environmental health risk, the bioaccumulation model, which predicts the phytoplankton partitioning of PAHs, is needed to estimate the bioaccumulation of PAHs through the food web.

## References

- (1). Broman, D.; Naf, C.; Roiff, C.; Zebuhr, Y. Occurrence and dynamics of polychlorinated dibenzo-p-dioxins and dibenzofurans and polycyclic aromatic hydrocarbons in the mixed surface layer of remote coastal and offshore waters of the Baltic. *Environ Sci Technol.* **1991**, 25, 1850 -1864.
- (2). Gigliotti, C.L.; Dachs, J.; Nelson, E.D.; Brunciak, P.A.; Eisenreich, S.J. Polycyclic aromatic hydrocarbons in the New Jersey coastal atmosphere. *Environ Sci Technol.* **2000**, 34, 3547 -3554.
- (3). Nelson, E.D.; Macconnell, L.L.; Baker, J.E. Diffusive exchange of gaseous polycyclic aromatic hydrocarbons and polychlorinated biphenyls across the air-water interface of the Chesapeake bay. *Environ Sci Technol.* **1998**, 32, 912 -919.
- (4). Gigliotti, C.L.; Brunciak, P.A.; Dachs, J.; Glenn IV, T.R.; Nelson, E.D.; Totten, L.A.; Eisenreich, S.J. Air-water exchange of polycyclic aromatic hydrocarbons in the NY-NJ harbor estuary. *Environ Toxicol Chem.* **2002**, 21, 235 -244.
- (5). Karickhoff, S.W.; Brown, D.S. Sorption of hydrophobic pollutants on natural sediments. *Wat Res.* **1979**, 13, 241 -248.
- (6). Karickhoff, S.W. Semi-empirical estimation of sorption of hydrophobic pollutants on natural sediments and soils. *Chemosphere.* **1981**, 10, 833 -846.
- (7). Karickhoff, S.W. Organic pollutants sorption in aquatic systems. *J Hydraulic Engineering.* **1984**, 110, 707 -735.
- (8). Skoglund, R.S.; Swackhamer, D.L. Evidence for the use of organic carbon as the sorbing matrix in the modeling of PCB accumulation in phytoplankton. *Environ Sci Technol.* **1999**, 33, 1516 -1519.
- (9). Gustafsson, O.; Haghseta, F.; Chan, C.; Macfarlane, J.; Gschwend, P.M. Quantification of the dilute sedimentary soot phase: implication for PAH speciation and bioavailability. *Environ Sci Technol.* **1997**, 31, 203 -209.
- (10). Zhou, J.L.; Fileman, T.W.; Evans, S.; Donkin, P.; Readman, J.W.; Mantoura, R.F.C.; Rowland, S. The partition of fluoranthrene and pyrene between suspended

particles and dissolved phase in the Humber estuary: a study of the controlling factors. *The Science of the Total Environment*. **1999**, 243/244, 305 -321.

(11). Buchell, T.D.; Gustafsson, O. Quantification of the soot-water distribution coefficient of PAHs provides mechanistic basis for enhanced sorption observations. *Environ Sci Technol*. **2000**, 34, 5144 -5151.

(12). Eaton AD, Clesceri LS, and Greenberg AE, editors. Standard Methods for Examination of Water and Wastewater. 19th ed. APHA, AWWA, WEF: 1995.

(13). Marsh, J.B.; Weinstein, D.B. Simple charring method for determination of lipids. *J Lipid Res*. **1966**, 7, 574 -576.

(14). Parsons, R.T., Maita, Y., Lalli, C.M. A manual of chemical and biological methods for seawater analysis. Pergamon Press:Oxford, New York, Toronto, 1984.

(15). Grasshoff, K., Ehrhardt, M., Kremling, K. ; Grasshoff K, Ehrhardt M, and Kremling K, editors. Methods of seawater analysis. Verlag Chemie GmbH:Weinheim, 1983.

(16). Porter, K.G.; Feig, Y.S. The use of DAPI for identifying and counting aquatic microflora. *Limnol Oceanogr*. **1980**, 25, 943 -948.

(17). Broman, D.; Naf, C.; Axelman, J.; Bandh, C.; Pettersen, H.; Johnstone, R.; Wallberg, P. Significance of bacteria in marine waters for the distribution of hydrophobic organic contaminants. *Environ Sci Technol*. **1996**, 30, 1238 -1241.

(18). Ruepert, C.; Grinwis, A.; Govers, H. Prediction of partition coefficients of unsubstituted polycyclic aromatic hydrocarbons from C<sub>18</sub> chromatographic and structural properties. *Chemosphere*. **1985**, 14, 279 -291.

(19). Miller, M.M.; Wasik, S.P.; Huang, G.; Shiu, W.; Mackay, D. Relationships between octanol-water partition coefficient and aqueous solubility. *Environ Sci Technol*. **1985**, 19, 522 -529.

(20). Lie, Y.D.; Wania, F.; Shiu, W.Y.; Boocock, D.G.B. HPLC-based method for estimating the temperature dependence of n-octanol-water partition coefficients. *J Chem Eng Data*. **2000**, 45, 738 -742.

(21). Walters, R.W.; Luthy, R.G. Equilibrium adsorption of polycyclic aromatic hydrocarbons from water onto activated carbon. *Environ Sci Technol*. **1984**, 18, 395 -403.

(22). Achman, D.R.; Hornbuckle, K.C.; Eisenreich, S.J. Volatilization of polychlorinated biphenyls from Green Bay, Lake Michigan. *Environ Sci Technol*. **1993**, 27, 75 -87.

- (23). New Jersey ambient monitoring program report on marine and coastal water quality 1993-1997. New Jersey Department of Environmental Protection. 1999;
- (24). Lansdale, D.J.; Cosper, E.M.; Doall, M. Effects of zooplankton size-structure and biomass in the lower Hudson River estuary. *Estuaries*. **1996**, 19, 874 -889.
- (25). Annual summary of phytoplankton blooms and related conditions in the New Jersey coastal waters summer of 1999. State of New Jersey, Department of Environmental Protection. 2000;
- (26). Nas, K.; Axelman, J.; Naf, C.; Broman, D. Role of soot carbon and other carbon matrices in the distribution of PAHs among particles, DOC, and the dissolved phase in the effluent and recipient waters of an aluminum reduction plant. *Environ Sci Technol*. **1998**, 32, 1786 -1792.
- (27). Liu, K.; Dickhut, R.M. Surface microlayer enrichment of polycyclic aromatic hydrocarbons in southern Chesapeake Bay. *Environ Sci Technol*. **1997**, 31, 2777 - 2781.
- (28). Accardi-Dey, A.; Gschwend, P.M. Assessing the combined roles of natural organic matter and black carbon as sorbents in sediments. *Environ Sci Technol*. **2002**, 36, 21 -29.
- (29). Dachs, J.; Bayona, J.M.; Raoux, C.; Albaiges, J. Spatial, vertical distribution and budget of polycyclic aromatic hydrocarbons in the western Mediterranean seawater. *Environ Sci Technol*. **1997**, 31, 682 -688.
- (30). Arzayus, K.M.; Dickhut, R.M.; Canuel, E.A. Fate of atmospherically deposited polycyclic aromatic hydrocarbons (PAHs) in Chesapeake Bay. *Environ Sci Technol*. **2001**, 35, 2178 -2183.
- (31). Budzinski, H.; Jones, I.; Bellocq, J.; Pierard, C.; Garrigues, P. Evaluation of sediment contamination by polycyclic aromatic hydrocarbons in the Gironde estuary. *Mar Chem*. **1997**, 58, 85 -97.
- (32). Swackhamer DL, Skoglund RS. ; Baker R, editors. *Organic Substances And Sediments In Water*. Boca Roton FL: Lewis Publisher, CRC Press INC., 1991; The role of phytoplankton in the partitioning of hydrophobic organic contaminants in water. p. 91-105.
- (33). Skoglund, R.S.; Stange, K.; Swackhamer, D.L. A kinetics model for predicting the accumulation of PCBs in phytoplankton. *Environ Sci Technol*. **1996**, 30, 2113 -2120.

Table 3.1 Air temperature, wind direction, and wind speeds measured in Raritan Bay.

Sampling Date		Air Temp (°C)	Wind speed (m s <sup>-1</sup> )	Wind direction	Wind direction (degree)
Oct-20-1999	PM	12.4	2.8	SE	135
Dec-3-1999	PM	10.6	2.4	SW	240
Apr-19-2000	AM	9.0	7.3	NE	60
	PM	10.0	6.2	W	270
Apr-20-2000	AM	14.5	4.4	SE	135
	PM	14.5	5.7	SE	130
Apr-21-2000	AM	8.2	10.0	SE	120
Aug-21-2000	AM	19.6	2.1	NE	30
	PM	22.2	1.8	SW	225
Aug-22-2000	AM	22.0	1.5	SW	225
	PM	23.7	2.6	SE	135
Aug-23-2000	AM	22.4	5.5	SE	150
	PM	23.0	6.4	SE	150
Oct-25-2000	AM	17.5	0.8	SW	255
	PM	21.2	2.1	SE	135
Oct-26-2000	AM	12.5	0.4	SW	225
	PM	15.3	1.1	SW-NE-SE	225-45-120
Oct-27-2000	AM	15.8	0.7	SW	225
	PM	20.0	0.2	S-SW-NE	180-225-45
Apr-24-2001	AM	22.8	1.9	SW	225
	PM	25.0	3.8	SW	225
Apr-25-2001	AM	9.3	3.8	NE	45
Apr-26-2001	AM	13.9	2.2	NE-E-SE	45-90-135
	PM	16.5	1.8	SE	150

Table 3.2 Water temperature, dissolved oxygen (DO), salinity, pH, and water column stratification status in Raritan Bay.

Sampling Date	Temp (°C)	DO (%Satuation)	Salinity	pH	Water Column Characteristics
Oct-20-1999	14.5 ~ 15.5	70 ~ 130	23.0 ~ 25.5	7.8 ~ 7.9	No stratification
Dec-3-1999	8.6 ~ 9.3	85 ~ 95	23.3 ~ 26.5	7.9 ~ 8.0	Weak Stratification, mixing depth 2m
Apr-19-2000	8.4 ~ 8.8	95 ~ 100	23.0 ~ 24.0	8.3 ~ 8.5	Weak Stratification, mixing depth 2m
Apr-20-2000	8.6 ~ 9.8	85 ~ 110	21.0 ~ 23.5	8.1 ~ 8.6	Stratification, mixing depth 2m
Apr-21-2000	8.8 ~ 9.0	86 ~ 87	23.0 ~ 24.0	8.1-8.3	No stratification
Aug-21-2000	21~21.5	76~86	21.1-22.4	8.0-8.1	Stratification, mixing depth 2-3m
Aug-22-2000	21.5~23	75~100	22.2~23.5	7.9~8.3	Stratification, mixing depth 2-3m
Aug-23-2000	21.1~21.8	80~130	21.8~24.5	8.3~8.6	Stratification, mixing depth 3~4m
Oct-25-2000	15.1~15.3	89~100	25.5~26.5	7.7~7.8	No stratification
Oct-26-2000	15.4~15.7	87~100	25.5~26.5	7.5~7.8	No stratification
Oct-27-2000	15.6~15.8	60~70	26.5~27	7.7~8.2	No stratification
Apr-24-2001	8~11.5	100~160	22~25	7.0~8.0	Weak Stratification, mixing depth 2-3m
Apr-25-2001	6.5~7.5	100~110	30.4~30.8	7.0~7.5	No stratification
Apr-26-2001	8~9.5	100~165	25~30.5	7.0~7.6	Stratification, mixing depth 4-5m

Table 3.3 Tide chart in Raritan bay presented at local time.

Cruise	Date	Low	High	Low	High
Oct/1999	Oct-20		04:39	11:02	16:58
Dec/1999	Dec-3		04:21	10:41	16:36
Apr/2000	Apr-19		09:09	15:25	21:30
	Apr-20		09:50	16:02	22:10
	Apr-21		10:32	16:38	22:50
Aug/2000	Aug-21	06:28	12:49	19:13	
	Aug-22	07:18	13:43	20:26	
	Aug-23	08:25	14:42	21:41	
Oct/2000	Oct-25		06:59	13:13	19:15
	Oct-26		07:45	14:03	20:01
	Oct-27		08:28	14:50	20:45
Apr/2001	Apr-24	03:22	09:11	15:23	21:20
	Apr-25	04:03	09:51	16:01	21:57
	Apr-26	04:45	10:36	16:41	22:41

Table 3.4 Total suspended matter (TSM), chlorophyll a (Chl a), total particulate lipid (TPL), particulate organic carbon (POC), organic carbon fraction ( $f_{oc}$ ), particulate organic nitrogen (PON), C/N ratio, and bacteria abundance measured in Raritan Bay surface water. Values are mean  $\pm$  SD of triplicate samples for suspended matter measurements, mean  $\pm$  SD of 10 countings for bacteria abundance.

Cruises	Date (mm/dd)	Time	TSM (mg L <sup>-1</sup> )	Chl a ( $\mu$ g L <sup>-1</sup> )	TPL ( $\mu$ g L <sup>-1</sup> )	POC ( $\mu$ g L <sup>-1</sup> )	$f_{oc}$ (%)	PON ( $\mu$ g L <sup>-1</sup> )	C/N	Bacteria (cell $\times 10^6$ L <sup>-1</sup> )	
Oct/1999	10/20	13:00	ns	5.7 $\pm$ 0.7	136 $\pm$ 32	495 $\pm$ 133	39	91 $\pm$ 29	6.30	1.0 $\pm$ 0.2	
		16:00	ns	2.7 $\pm$ 0.1	117 $\pm$ 38	361 $\pm$ 21	12	61 $\pm$ 4	7.00	2.5 $\pm$ 0.4	
Dec/1999	12/03	11:30	ns	2.9 $\pm$ 0.2	88 $\pm$ 5	447 $\pm$ 8		69 $\pm$ 2	7.47	2.0 $\pm$ 0.4	
		14:30	ns	2.0 $\pm$ 0.2	80 $\pm$ 4	392 $\pm$ 14	16	58 $\pm$ 4	7.93	1.7 $\pm$ 0.4	
Apr/2000	04/19	11:00	9.8 $\pm$ 0.6	3.2 $\pm$ 0.0	268 $\pm$ 45	1496 $\pm$ 409	15.3	792 $\pm$ 481	2.21	1.0 $\pm$ 0.2	
		13:30	19.3 $\pm$ 0.0	25.1 $\pm$ 1.4	503 $\pm$ 13	2231 $\pm$ 55	11.6	641 $\pm$ 20	4.06	1.2 $\pm$ 0.4	
		16:00	18.7 $\pm$ 0.1	24.3 $\pm$ 8.8	479 $\pm$ 62	3095 $\pm$ 575	16.6	1473 $\pm$ 571	2.45	1.6 $\pm$ 0.4	
	04/20	9:00	11.7 $\pm$ 0.5	6.4 $\pm$ 1.1	220 $\pm$ 29	1156 $\pm$ 71	9.9	346 $\pm$ 67	3.90	1.8 $\pm$ 0.3	
		13:00	8.0 $\pm$ 0.3	8.8 $\pm$ 0.8	209 $\pm$ 4	1054 $\pm$ 57	13.2	373 $\pm$ 55	3.30	2.5 $\pm$ 0.3	
		16:30	10.2 $\pm$ 0.3	23.4 $\pm$ 7.1	456 $\pm$ 43	1920 $\pm$ 102	18.8	504 $\pm$ 53	4.45	2.9 $\pm$ 0.5	
	04/21	9:00	13.6 $\pm$ 0.0	6.7 $\pm$ 0.5	211 $\pm$ 28	1500 $\pm$ 345	11.0	623 $\pm$ 387	2.81	1.3 $\pm$ 0.3	
		11:30	12.9 $\pm$ 2.7	3.9 $\pm$ 0.2	236 $\pm$ 43	1176 $\pm$ 73	9.1	470 $\pm$ 56	2.92	1.4 $\pm$ 0.3	
	Aug/2000	08/21	10:00	3.4 $\pm$ 1.0	5.2 $\pm$ 1.0	115 $\pm$ 4	515 $\pm$ 58	15.1	104 $\pm$ 19	5.78	3.2 $\pm$ 0.7
			13:30	2.4 $\pm$ 0.2	4.9 $\pm$ 0.2	113 $\pm$ 20	547 $\pm$ 160	22.8	115 $\pm$ 41	5.55	2.6 $\pm$ 0.5
			16:00	3.0 $\pm$ 0.1	5.1 $\pm$ 0.3	112 $\pm$ 19	501 $\pm$ 89	16.7	99 $\pm$ 21	5.90	2.3 $\pm$ 0.3
		08/22	9:00	2.9 $\pm$ 0.1	14.1 $\pm$ 1.1	205 $\pm$ 9	857 $\pm$ 127	29.6	194 $\pm$ 24	5.16	2.2 $\pm$ 0.3
12:30			2.7 $\pm$ 0.2	9.0 $\pm$ 0.8	202 $\pm$ 80	677 $\pm$ 31	25.1	139 $\pm$ 32	5.68	2.0 $\pm$ 0.4	
15:30			3.2 $\pm$ 0.2	10.6 $\pm$ 0.8	225 $\pm$ 37	753 $\pm$ 33	23.5	139 $\pm$ 5	6.32	2.0 $\pm$ 0.3	
08/23		9:00	6.8 $\pm$ 0.1	45.9 $\pm$ 3.8	500 $\pm$ 16	1783 $\pm$ 33	26.2	397 $\pm$ 28	5.24	3.4 $\pm$ 0.4	
		11:30	7.9 $\pm$ 1.3	47.5 $\pm$ 7.5	636 $\pm$ 38	2226 $\pm$ 86	28.2	476 $\pm$ 15	5.46	3.1 $\pm$ 0.4	
		15:30	4.0 $\pm$ 0.2	20.0 $\pm$ 1.0	300 $\pm$ 39	963 $\pm$ 32	24.1	198 $\pm$ 4	5.67	2.3 $\pm$ 0.4	
Oct/2000		10/25	9:30	2.4 $\pm$ 0.1	3.1 $\pm$ 0.6	143 $\pm$ 44	492 $\pm$ 22	20.5	105 $\pm$ 12	5.47	2.7 $\pm$ 0.9
			14:00	2.0 $\pm$ 0.3	3.5 $\pm$ 0.5	89 $\pm$ 4	408 $\pm$ 25	20.4	80 $\pm$ 7	5.95	2.6 $\pm$ 1.0
			16:00	2.5 $\pm$ 0.2	4.4 $\pm$ 0.1	100 $\pm$ 9	422 $\pm$ 5	16.9	82 $\pm$ 2	6.01	2.6 $\pm$ 0.7
	10/26	9:00	1.7 $\pm$ 0.1	2.0 $\pm$ 0.1	57 $\pm$ 2	260 $\pm$ 12	15.3	54 $\pm$ 8	5.61	2.7 $\pm$ 0.7	
		13:00	2.6 $\pm$ 0.6	4.7 $\pm$ 0.2	91 $\pm$ 6	388 $\pm$ 2	14.9	85 $\pm$ 7	5.32	2.6 $\pm$ 0.4	
		16:30	2.8 $\pm$ 0.3	5.8 $\pm$ 0.1	99 $\pm$ 1	485 $\pm$ 6	17.3	92 $\pm$ 5	6.15	2.9 $\pm$ 0.7	
	10/27	9:00	2.1 $\pm$ 0.1	2.2 $\pm$ 0.1	61 $\pm$ 6	266 $\pm$ 10	12.7	55 $\pm$ 2	5.65	2.8 $\pm$ 0.4	
		13:00	2.3 $\pm$ 0.2	3.3 $\pm$ 0.1	68 $\pm$ 3	327 $\pm$ 31	14.2	96 $\pm$ 25	3.98	3.3 $\pm$ 0.6	
		16:00	2.2 $\pm$ 0.1	3.6 $\pm$ 0.1	75 $\pm$ 9	350 $\pm$ 54	15.9	106 $\pm$ 42	3.85	2.9 $\pm$ 0.7	
	Apr/2001	04/24	9:00	5.4 $\pm$ 0.4	5.1 $\pm$ 0.1	184 $\pm$ 5	636 $\pm$ 13	11.8	191 $\pm$ 4	3.89	4.1 $\pm$ 1.3
			13:30	11.9 $\pm$ 1.0	57.8 $\pm$ 3.8	1130 $\pm$ 54	2338 $\pm$ 82	19.6	423 $\pm$ 79	6.45	5.3 $\pm$ 1.5
			16:00	10.0 $\pm$ 0.6	30.6 $\pm$ 2.3	802 $\pm$ 45	2836 $\pm$ 27	28.4	579 $\pm$ 27	5.72	3.4 $\pm$ 0.6
04/25		9:00	2.7 $\pm$ 0.1	6.2 $\pm$ 0.3	153 $\pm$ 4	482 $\pm$ 14	17.9	162 $\pm$ 10	3.48	3.5 $\pm$ 0.7	
		11:30	4.7 $\pm$ 0.6	6.3 $\pm$ 1.1	196 $\pm$ 7	641 $\pm$ 12	13.6	201 $\pm$ 15	3.72	3.3 $\pm$ 0.7	
04/26		8:30	3.1 $\pm$ 0.3	5.3 $\pm$ 0.3	166 $\pm$ 19	497 $\pm$ 29	16.0	162 $\pm$ 22	3.58	2.7 $\pm$ 0.9	
		11:30	4.6 $\pm$ 0.2	8.1 $\pm$ 1.0	644 $\pm$ 20	975 $\pm$ 51	21.2	221 $\pm$ 14	5.15	3.1 $\pm$ 0.5	
		16:00	5.4 $\pm$ 0.2	6.5 $\pm$ 0.4	445 $\pm$ 52	783 $\pm$ 24	14.5	205 $\pm$ 10	4.46	2.6 $\pm$ 0.3	

ns: no sample



Table 3.5 Dissolved nutrients, including phosphate, nitrate, nitrite, and ammonium concentrations measured in Raritan Bay surface water. Values are presented as mean  $\pm$  SD of duplicate measurements or a single measurement.

Cruises	Date (mm/dd)	Time	Phosphate ( $\mu$ M)	Nitrate ( $\mu$ M)	Nitrite ( $\mu$ M)	Ammonium ( $\mu$ M)
Oct 1999	10/20	13:00	1.34 $\pm$ 0.13	32.4 $\pm$ 1.81	3.1 $\pm$ 0.03	17.5 $\pm$ 0.7
		16:00	2.53 $\pm$ 0.13	28.6 $\pm$ 0.01	2.6 $\pm$ 0.09	18.9 $\pm$ 0.7
Dec 1999	12/03	11:30	3.22 $\pm$ 0.02	32.4 $\pm$ 1.81	2.8 $\pm$ 0.01	24.8 $\pm$ 1.2
		14:30	3.20 $\pm$ 0.02	31.3 $\pm$ 0.30	2.7 $\pm$ 0.01	21.6 $\pm$ 0.4
Apr 2000	04/19	11:00	1.44 $\pm$ 0.07	19.5 $\pm$ 0.31	1.4 $\pm$ 0.01	21.2 $\pm$ 0.1
		13:30	1.06 $\pm$ 0.01	18.1 $\pm$ 0.30	1.4 $\pm$ 0.06	9.56 $\pm$ 0.43
		16:00	1.01 $\pm$ 0.01	18.5	1.4 $\pm$ 0.01	76.8 $\pm$ 2.1
	04/20	9:00	1.72 $\pm$ 0.01	18.1	1.3 $\pm$ 0.01	19.7 $\pm$ 2.0
		13:00	1.7 $\pm$ 0.01	21.9	1.3 $\pm$ 0.01	na
		16:30	0.77 $\pm$ 0.03	15.3	1.2 $\pm$ 0.01	6.35 $\pm$ 0.5
	04/21	9:00	1.84 $\pm$ 0.03	18.5	1.2 $\pm$ 0.01	29.2 $\pm$ 0.3
		11:30	1.70 $\pm$ 0.03	19.4	1.2 $\pm$ 0.01	145.7 $\pm$ 4.3
Aug 2000	08/21	10:00	3.13 $\pm$ 0.03	23.4	2.1 $\pm$ 0.04	22.8 $\pm$ 0.7
		13:30	3.30 $\pm$ 0.02	23.7	2.3 $\pm$ 0.01	23.1 $\pm$ 0.6
		16:00	3.18 $\pm$ 0.03	23.2	2.3 $\pm$ 0.01	21.7 $\pm$ 0.6
	08/22	9:00	2.96 $\pm$ 0.01	23.0	2.4 $\pm$ 0.01	18.0 $\pm$ 0.3
		12:30	3.06 $\pm$ 0.02	23.9	2.3 $\pm$ 0.01	17.2 $\pm$ 0.3
		15:30	2.84 $\pm$ 0.03	24.5	2.2 $\pm$ 0.01	19.8 $\pm$ 0.1
	08/23	9:00	2.27 $\pm$ 0.03	27.3	3.4 $\pm$ 0.06	14.8 $\pm$ 0.8
		11:30	1.32 $\pm$ 0.03	21.7	3.2 $\pm$ 0.01	5.1 $\pm$ 1.1
		15:30	1.30 $\pm$ 0.02	17.0	2.4 $\pm$ 0.04	4.4 $\pm$ 0.1
Oct 2000	10/25	9:30	3.87 $\pm$ 0.03	32.5	3.5 $\pm$ 0.06	25.2 $\pm$ 1.5
		14:00	4.03 $\pm$ 0.02	37.9	3.9 $\pm$ 0.01	25.9 $\pm$ 0.8
		16:00	3.94 $\pm$ 0.01	33.9 $\pm$ 0.15	3.5 $\pm$ 0.01	25.3 $\pm$ 1.2
	10/26	9:00	3.84 $\pm$ 0.03	31.2	3.3 $\pm$ 0.01	30.1 $\pm$ 2.0
		13:00	3.99 $\pm$ 0.10	35.9	3.7 $\pm$ 0.01	24.4 $\pm$ 2.5
		16:30	3.70 $\pm$ 0.03	32.5	3.4 $\pm$ 0.01	23.2 $\pm$ 0.4
	10/27	9:00	3.80 $\pm$ 0.03	27.1 $\pm$ 0.3	3.1 $\pm$ 0.01	28.7 $\pm$ 0.6
		13:00	3.94 $\pm$ 0.10	32.6 $\pm$ 0.5	3.4 $\pm$ 0.03	26.3 $\pm$ 0.6
		16:00	4.10 $\pm$ 0.01	26.2	3.4 $\pm$ 0.01	27.3 $\pm$ 0.1
Apr 2001	04/24	9:00	1.17 $\pm$ 0.11	15.2 $\pm$ 0.4	0.67 $\pm$ 0.08	15.1 $\pm$ 0.1
		13:30	0.54 $\pm$ 0.03	3.2 $\pm$ 0.3	0.31 $\pm$ 0.02	4.1 $\pm$ 0.2
		16:00	0.59 $\pm$ 0.06	7.1 $\pm$ 0.3	0.48 $\pm$ 0.03	6.5 $\pm$ 0.1
	04/25	9:00	0.77 $\pm$ 0.03	2.0 $\pm$ 0.3	0.25 $\pm$ 0.01	2.6 $\pm$ 0.1
		11:30	0.75 $\pm$ 0.05	3.8 $\pm$ 0.3	0.37 $\pm$ 0.01	4.3 $\pm$ 0.1
	04/26	8:30	1.12 $\pm$ 0.03	6.8 $\pm$ 0.5	0.55 $\pm$ 0.03	8.0 $\pm$ 0.1
		11:30	0.75 $\pm$ 0.01	4.1 $\pm$ 0.4	0.42 $\pm$ 0.02	8.6 $\pm$ 0.1
		16:00	1.13 $\pm$ 0.05	9.0 $\pm$ 0.7	0.69 $\pm$ 0.03	9.3 $\pm$ 0.1

na: not available

Table 3.6 Chlorophyll a (Chl a) and phaeopigment measured and growth rate ( $\mu$ ,  $d^{-1}$ ) estimated in the short-term incubation experiments. Values are mean  $\pm$  SD of triplicate samples.

Cruises	Date	Time (h)	Chl a ( $\mu\text{g L}^{-1}$ )			Phaeopigment ( $\mu\text{g L}^{-1}$ )	
			Start	End	$\mu$ , $d^{-1}$	Start	End
Oct 1999	Oct. 20	6	5.7 $\pm$ 0.7	5.3 $\pm$ 0.9	0	0.38 $\pm$ 0.68	0.20 $\pm$ 0.19
Dec. 1999	Dec. 3	3	2.9 $\pm$ 0.2	2.6 $\pm$ 0.2	0	0.21 $\pm$ 0.01	0.02 $\pm$ 0.21
Apr/2000	Apr. 19	7	3.2 $\pm$ 0.0	3.1 $\pm$ 0.2	0	3.2 $\pm$ 0.77	3.8 $\pm$ 0.74
	Apr. 20	8	6.4 $\pm$ 1.1	8.7 $\pm$ 1.1	0.92	3.8 $\pm$ 0.57	3.4 $\pm$ 0.55
	Apr. 21	3.5	6.7 $\pm$ 0.5	5.9 $\pm$ 0.5	0	5.3 $\pm$ 1.41	4.5 $\pm$ 1.28
Aug 2000	Aug. 21	7	5.2 $\pm$ 1.0	12.7 $\pm$ 0.3	3.1	1.65 $\pm$ 0.32	1.20 $\pm$ 0.15
	Aug. 22	7	14.1 $\pm$ 1.1	24.3 $\pm$ 2.8	1.9	4.35 $\pm$ 0.61	14.8 $\pm$ 1.05
	Aug. 23	7.5	45.9 $\pm$ 3.8	22.2 $\pm$ 2.8	-2.3	7.72 $\pm$ 3.58	37.5 $\pm$ 7.15
Oct 2000	Oct. 25	7	3.1 $\pm$ 0.6	2.3 $\pm$ 0.7	0	0.22 $\pm$ 0.63	4.24 $\pm$ 0.89
	Oct. 26	7	2.0 $\pm$ 0.4	3.1 $\pm$ 0.5	1.5	0.04 $\pm$ 0.06	0 $\pm$ 0
	Oct. 27	7	2.2 $\pm$ 0.1	3.1 $\pm$ 0.3	1.4	0.07 $\pm$ 0.03	0 $\pm$ 0
Apr 2001	Apr. 24	7	5.0 $\pm$ 0.1	5.9 $\pm$ 0.2	0.5	0.44 $\pm$ 0.04	0.01 $\pm$ 0.34
	Apr. 25	3	6.2 $\pm$ 0.3	5.8 $\pm$ 0.3	0	0.20 $\pm$ 0.06	0.37 $\pm$ 0.05
	Apr. 26	8	5.3 $\pm$ 0.3	5.6 $\pm$ 0.1	0	0.69 $\pm$ 0.26	0.19 $\pm$ 0.12

Table 3.7 Particulate organic carbon (POC) and particulate organic nitrogen (PON) measured and growth rate ( $\mu$ ,  $d^{-1}$ ) and C/N ratio estimated in the short-term incubation experiments. Values are mean  $\pm$  SD of triplicate samples.

Cruises	Date (mm/dd)	Time (h)	POC ( $\mu g L^{-1}$ )			PON ( $\mu g L^{-1}$ )		C/N ratio	
			Start	End	$\mu$ , $d^{-1}$	Start	End	Start	End
Oct/1999	10/20	6	495 $\pm$ 133	ns		91 $\pm$ 29	ns	6.30	
Dec/1999	12/03	3	447 $\pm$ 8	ns		69 $\pm$ 2	ns	7.47	
Apr/2000	04/19	7	1496 $\pm$ 409	1377 $\pm$ 53	0	792 $\pm$ 481	851 $\pm$ 76	2.21	1.89
	04/20	8	1156 $\pm$ 71	1271 $\pm$ 56	0.28	346 $\pm$ 67	295 $\pm$ 24	3.90	5.03
	04/21	3.5	1500 $\pm$ 345	1391 $\pm$ 76	0	623 $\pm$ 387	648 $\pm$ 88	2.81	2.50
Aug 2000	08/21	7	515 $\pm$ 58	1050 $\pm$ 186	2.4	104 $\pm$ 19	77 $\pm$ 20	5.78	6.59
	08/22	7	857 $\pm$ 127	2197 $\pm$ 401	3.2	194 $\pm$ 24	76 $\pm$ 11	5.16	6.39
	08/23	7.5	1783 $\pm$ 33	4107 $\pm$ 743	2.7	397 $\pm$ 28	153 $\pm$ 15	5.24	6.45
Oct 2000	10/25	7	492 $\pm$ 22	638 $\pm$ 39	0.9	105 $\pm$ 12	100 $\pm$ 13	5.47	7.44
	10/26	7	260 $\pm$ 12	630 $\pm$ 103	3.0	54 $\pm$ 8	146 $\pm$ 40	5.61	5.03
	10/27	7	266 $\pm$ 10	417 $\pm$ 15	1.5	55 $\pm$ 2	73 $\pm$ 10	5.65	6.66
Apr 2001	04/24	7	636 $\pm$ 13	818 $\pm$ 153	0.9	191 $\pm$ 4	176 $\pm$ 65	3.89	5.42
	04/25	3	482 $\pm$ 14	590 $\pm$ 46	1.6	162 $\pm$ 10	198 $\pm$ 19	3.48	3.48
	04/26	8	497 $\pm$ 29	649 $\pm$ 60	0.8	162 $\pm$ 22	154 $\pm$ 20	3.58	4.92

ns: no sample

Table 3.8 PAHs measured in Raritan Bay.

	PAH	Abbreviation	$\log K_{ow}^b$	MW <sup>d</sup>
1	Fluorene	FLUOR	4.18	166
2	Phenanthrene	PHEN	4.57	178
3	Anthracene	ANTHR	4.54	178
4	1Methylfluorene	1MeFLUOR	4.97	180
5	Dibenzothiophene	DBT		184
6	4,5Methylenephenanthrene	4,5MePHEN	5.25	190
7	Methylphenanthrenes <sup>a</sup>	MePHENs	5.07 <sup>c</sup>	192
8	Methyldibenzothiophenes	MeDBTs		198
9	Fluoranthene	FLANT	5.22	202
10	Pyrene	PYR	5.18	202
11	3,6-Dimethylphenanthrene	3,6DmePHGN		206
12	Benzo[a]fluorene	BaF	5.69	216
13	Benzo[b]fluorene	BbF	5.69	216
14	Retene	RET		234
15	Benzo[b]naphtho[2,1-d]thiophene	BNT		234
16	Cyclopenta[cd]pyrene	CPcdPYR		226
17	Benz[a]anthracene	BaA	5.84	228
18	Chrysene/Triphenylene	CHRY	5.84	228
19	Naphacene	NAPTHA	5.84	228
20	Benzo[b+k]fluoranthene	BbkFLANT	6.44	252
21	Benzo[e]pyrene	BeP	6.44	252
22	Benzo[a]pyrene	BaP	6.44	252
23	Perylene	PERYL	6.44	252
24	Indeno[1,2,3-cd]pyrene	INDENO	7.04	276
25	Benzo[g,h,i]perylene	BghiERYN	7.04	276
26	Dibenzo[a,h+a,c]anthracene	DBA	7.11	278
27	Coronene	COR	7.65	300

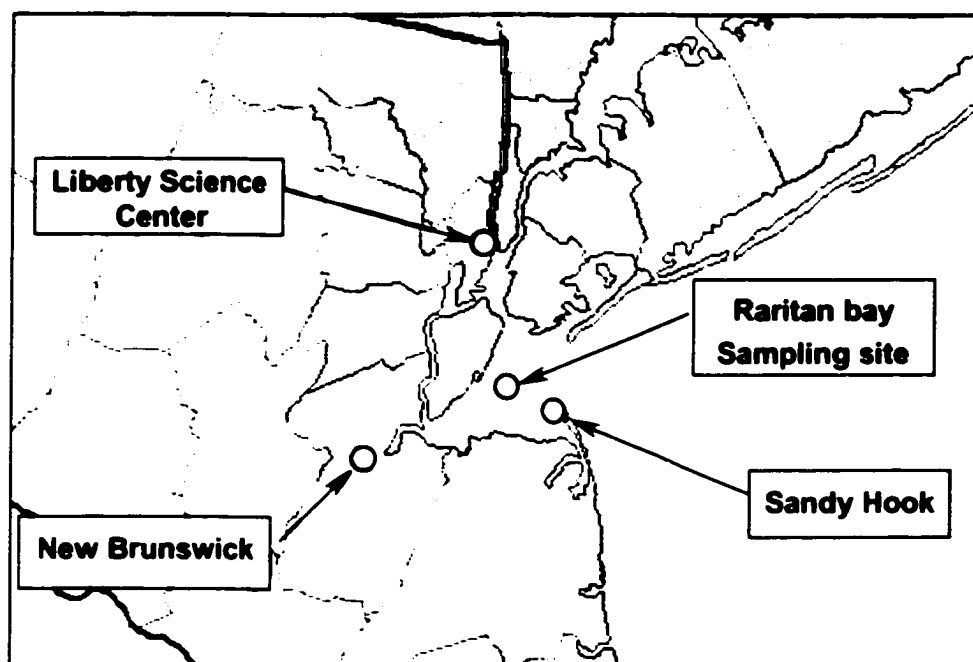
<sup>a</sup> methylphenanthrenes include 1-methylphenanthrene, 2-methylphenanthrene, 1-methylanthracene, 2-methylanthracene, and 9-methylanthracene

<sup>b</sup>  $\log K_{ow}$  values were obtained from Ruepert et al (1985) and Miller et al (1985)

<sup>c</sup>  $\log K_{ow}$  value is that of 9-methylanthracene of 5.07

([www.es.lancs.ac.uk/kcjgroup/5.html](http://www.es.lancs.ac.uk/kcjgroup/5.html))

<sup>d</sup> MW= molecular weight



Shaded areas indicate urban areas by population density  
*Adapted map courtesy of The National Atlas, USGS*

Figure 3.1 The sampling site in the Raritan bay, New Jersey.

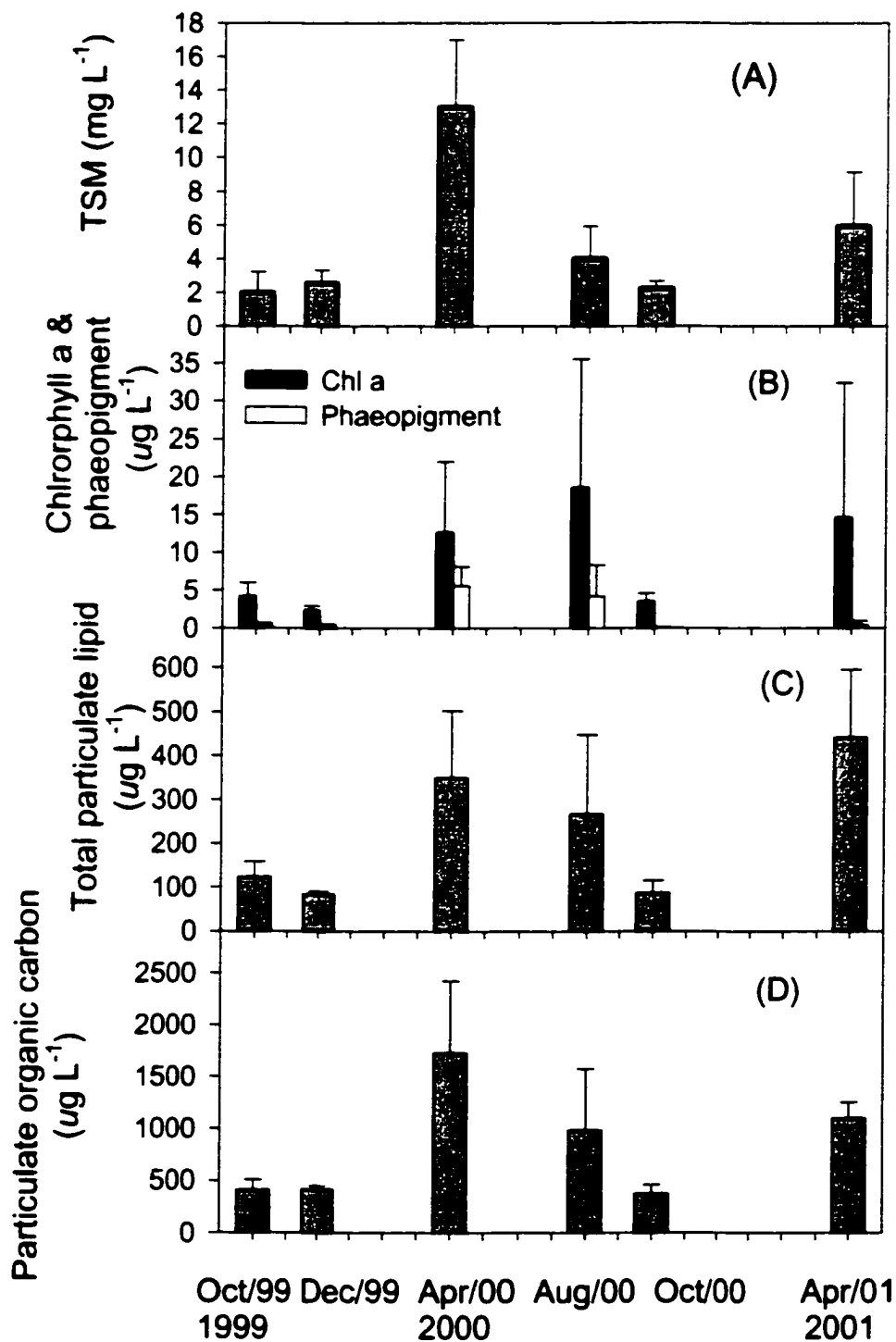


Figure 3.2 Average concentrations of (A) total suspended matter, (B) chlorophyll a & phaeopigment, (C) total particulate lipid, and (D) particulate organic carbon of each sampling cruise in Raritan Bay.

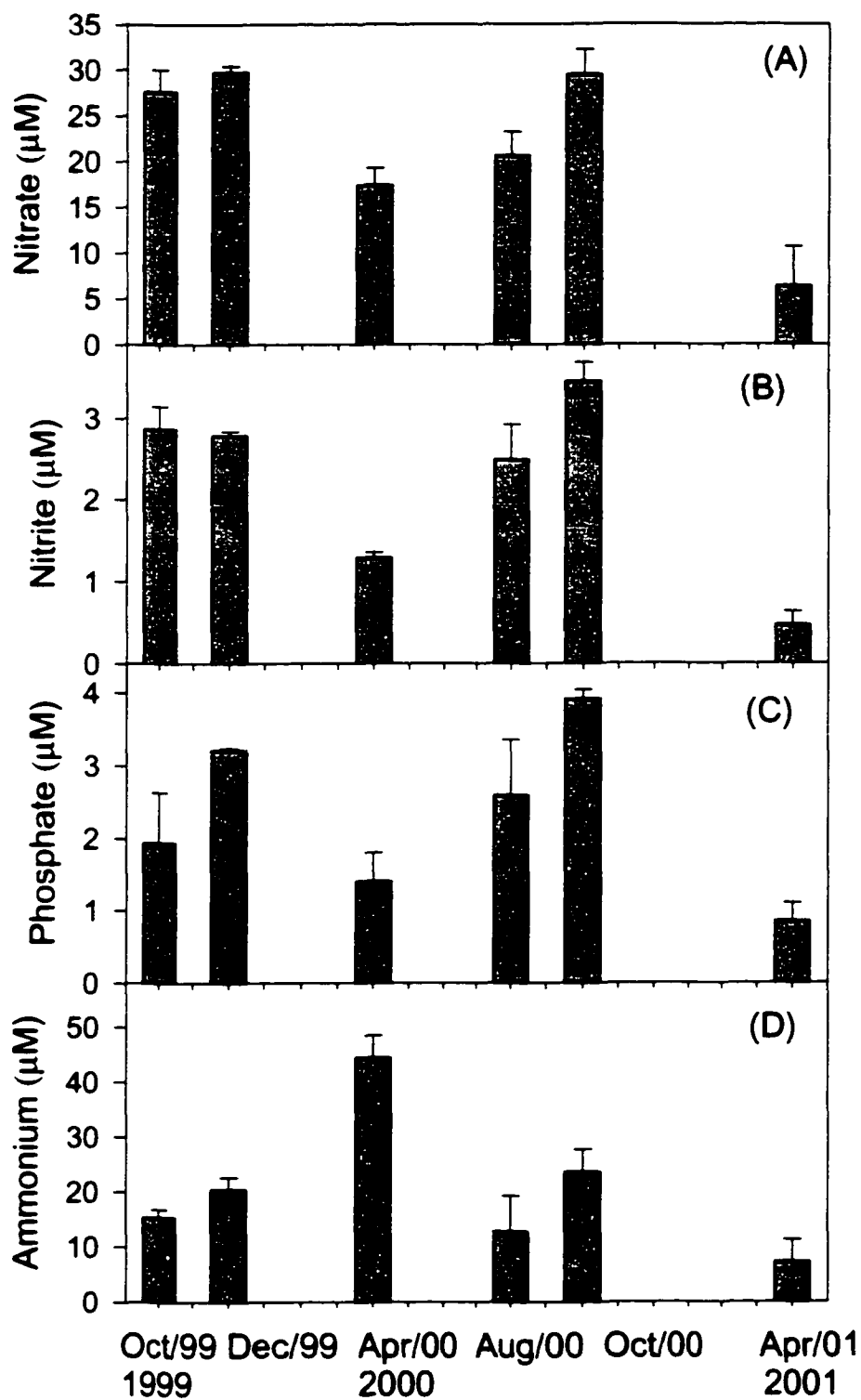


Figure 3.3 Average concentrations of (A) nitrate, (B) nitrite, (C) phosphate, and (D) ammonium of each sampling cruise in Raritan Bay.

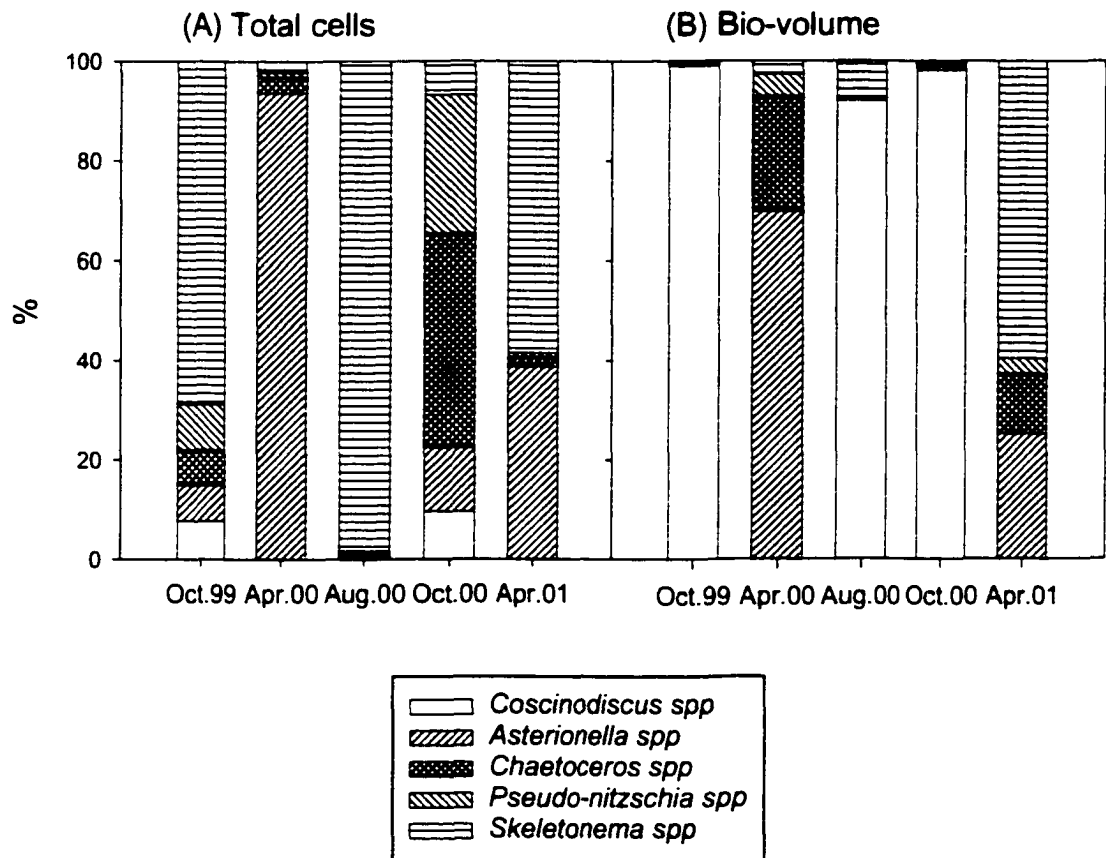


Figure 3.4 The relative abundance (%) of 5 dominant phytoplankton genera in the Raritan Bay with respect to the (A) total cells counted and (B) total bio-volume.



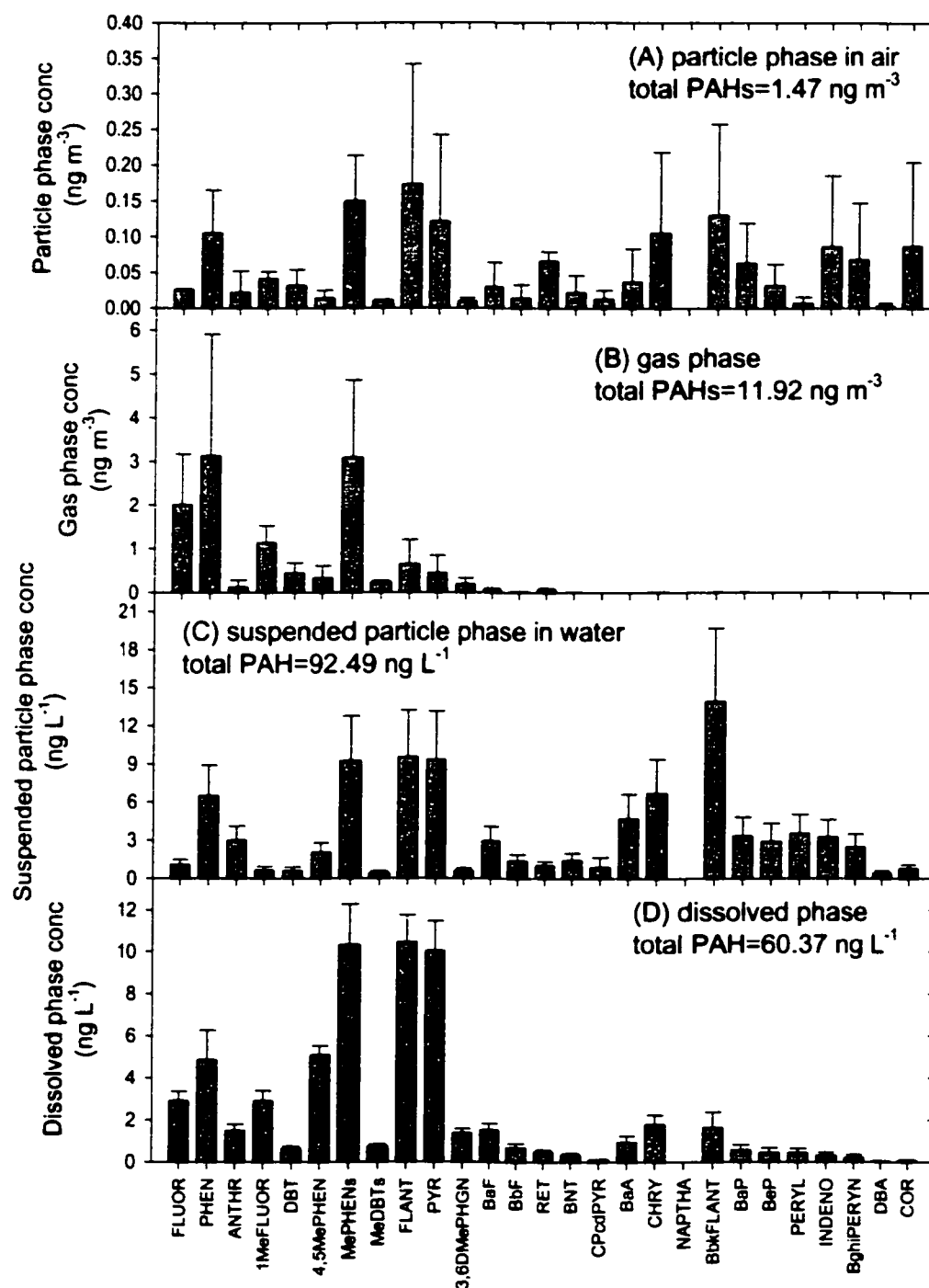


Figure 3.5 Average PAH concentrations in (A) atmospheric particles, (B) gas phase (C) suspended particles in water, and (D) dissolved phases measured in the cruise of Apr/2000 from Raritan Bay. Error bars are standard deviation of 5 measurements.

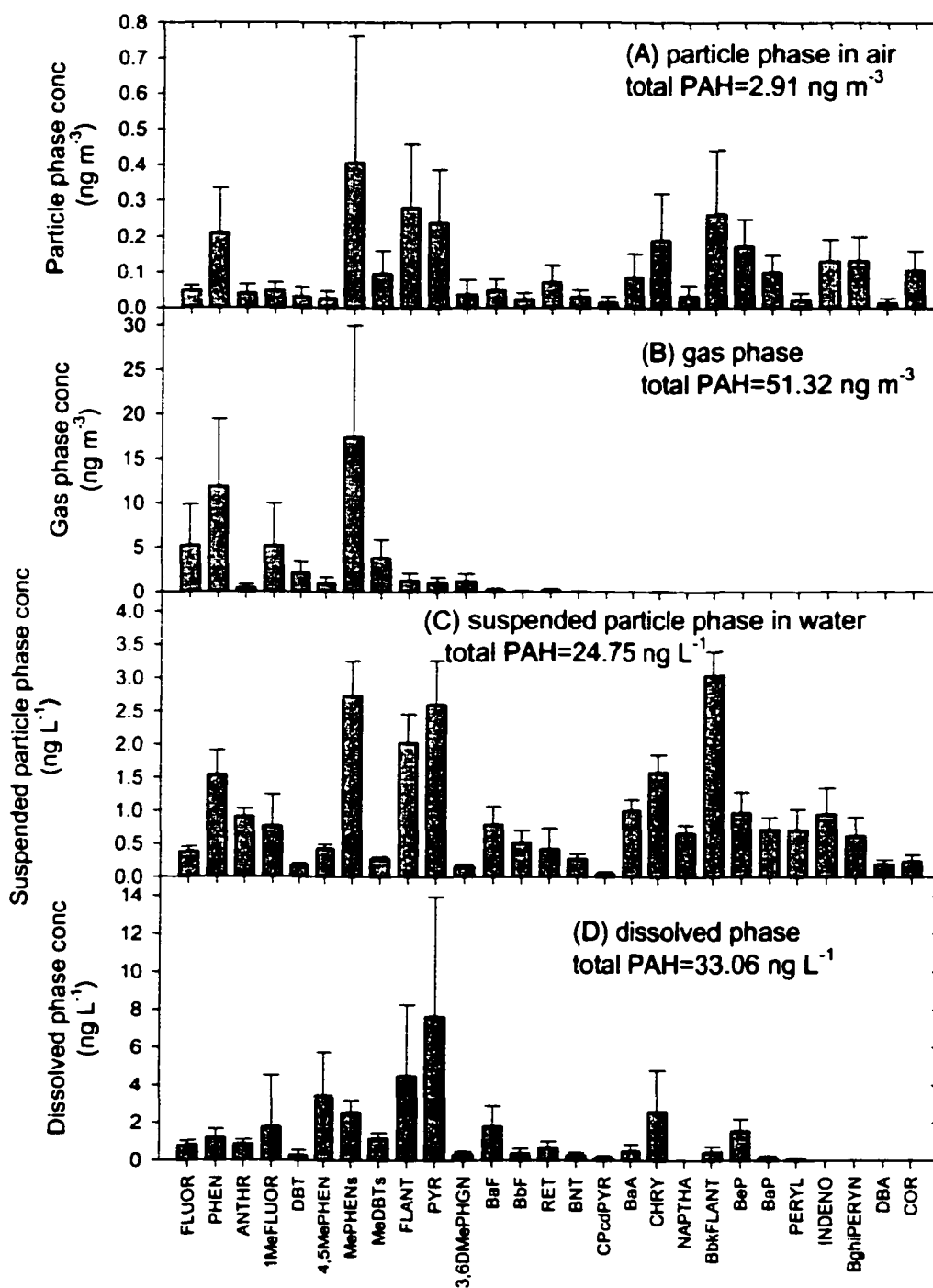


Figure 3.6 Average PAH concentrations in (A) atmospheric particles, (B) gas phase (C) suspended particles in water, and (D) dissolved phases measured in the cruise of Aug/2000 from Raritan Bay. Error bars are standard deviation of 6 measurements.

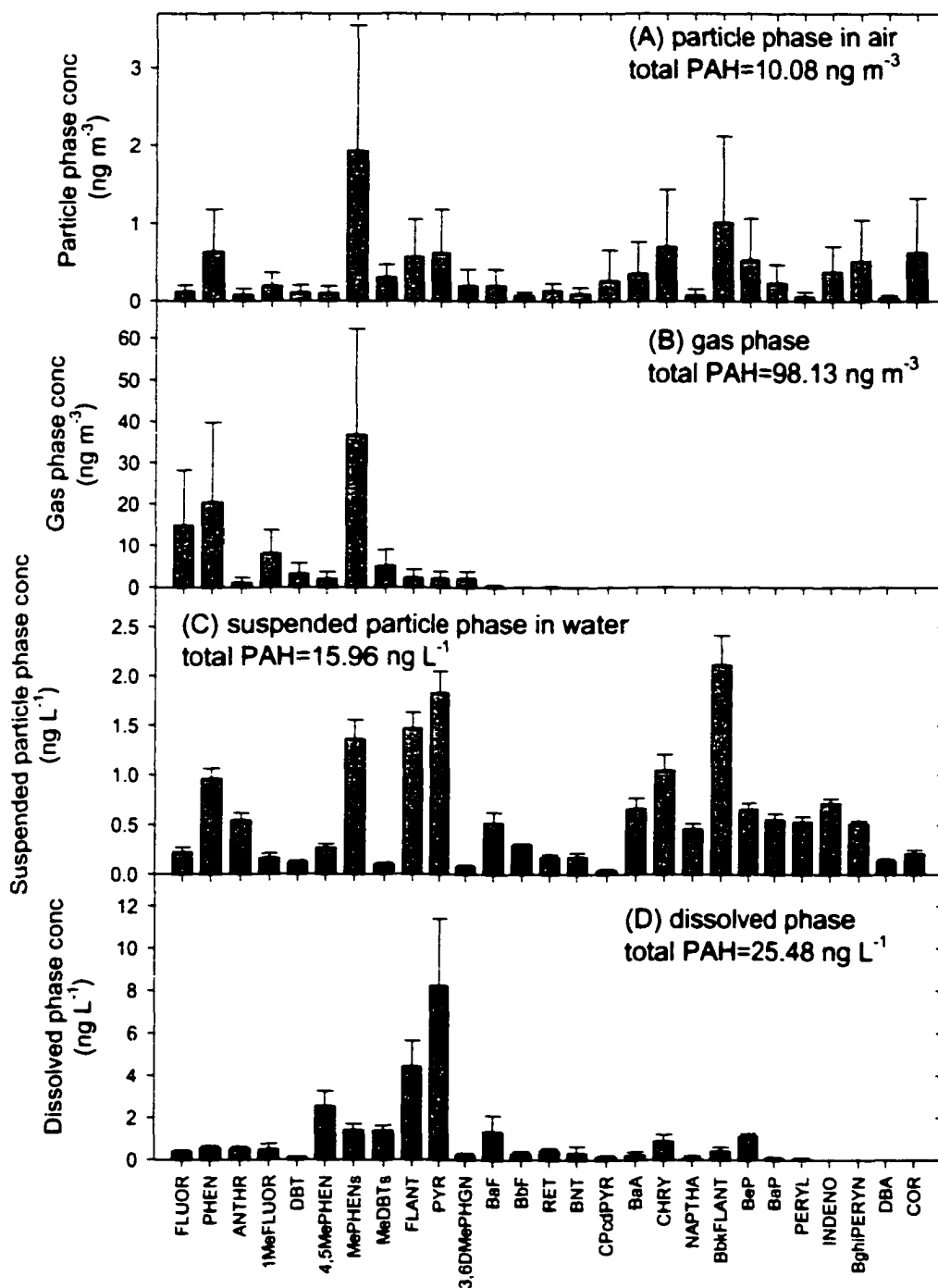


Figure 3.7 Average PAH concentrations in (A) atmospheric particles, (B) gas phase (C) suspended particles in water, and (D) dissolved phases measured in the cruise of Oct/2000 from Raritan Bay. Error bars are standard deviation of 6 measurements.

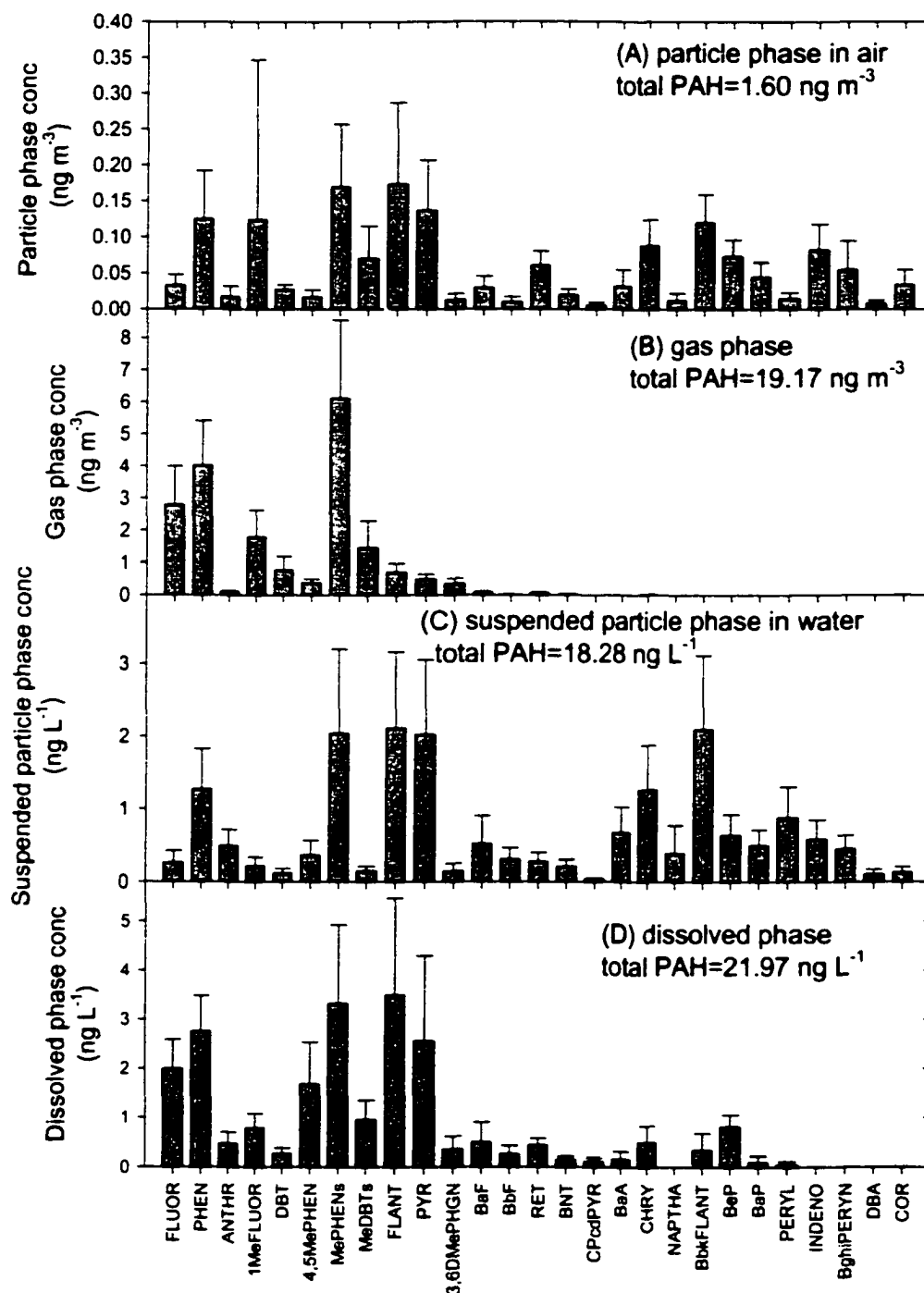


Figure 3.8 Average PAH concentrations in (A) atmospheric particles, (B) gas phase (C) suspended particles in water, and (D) dissolved phases measured in the cruise of Apr/2001 from Raritan Bay. Error bars are standard deviation of 6 measurements.

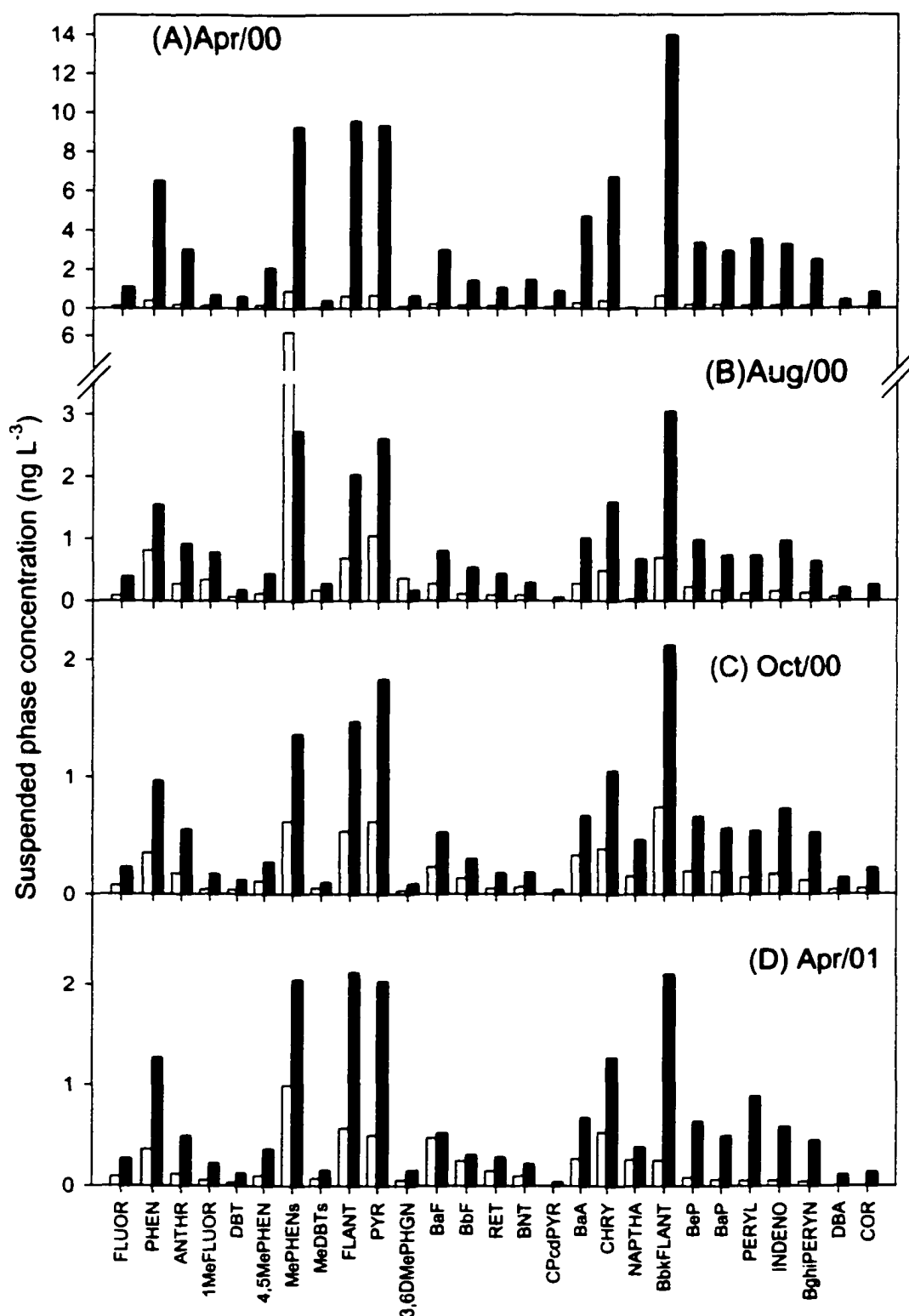


Figure 3.9 Average PAH concentrations in suspended particulate phase measured in the four cruises from Raritan Bay. (A) Apr/2000, (B) Aug/2000, (C) Oct/2000, and (D) Apr/2001.

■ present Infiltrax samples □ present plankton net samples

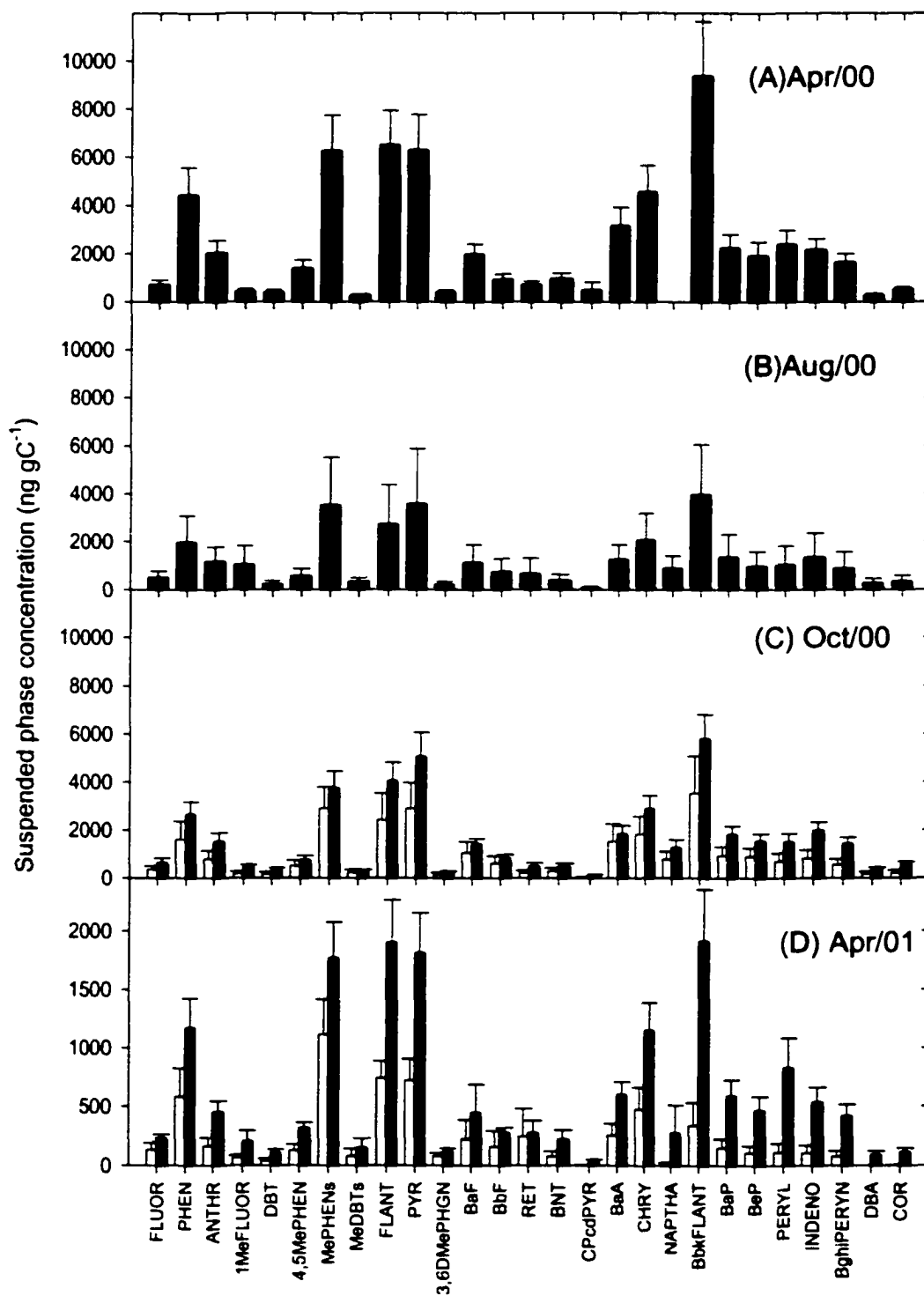


Figure 3.10 Average organic carbon normalized PAH concentrations in suspended particulate phase measured in the four cruises from Raritan Bay. (A) Apr/2000, (B) Aug/2000, (C) Oct/2000, and (D) Apr/2001.

■ present Infiltrax samples □ present plankton net samples

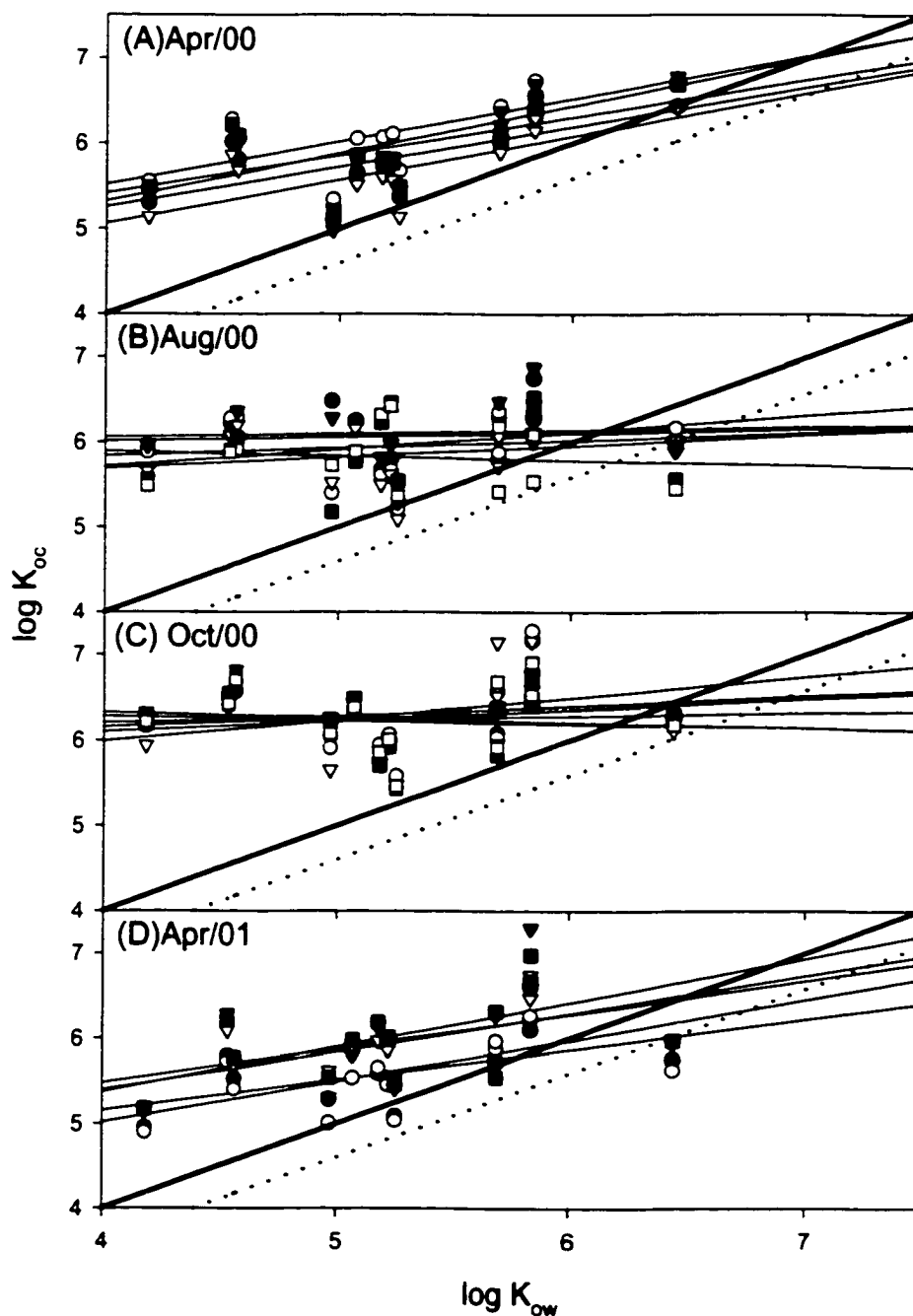


Figure 3.11  $\log K_{oc}$  versus  $\log K_{ow}$  for PAHs measured in the four cruises from Raritan Bay. (A) Apr/2000, (B) Aug/2000, (C) Oct/2000, and (D) Apr/2001. Thin lines represent regressions of  $\log K_{oc}$  versus  $\log K_{ow}$  for each sampling time during seasonal field campaigns. Thick Solid lines represent 1:1 slope lines, and dotted lines represent equation 3-3. PAHs ( $\log K_{ow}$ ) include fluorene (4.18), anthracene(4.54), phenanthrene (4.57), 1methylfluorene(4.97), methylphenanthrenes(5.07), pyrene(5.18), fluoranthene(5.22), 4,5methylenephenanthrene(5.25), benzo[a]fluorene(5.69), benzo[b]fluorene(5.69), benz[a]anthracene(5.84), chrysene/Triphenylene(5.84), and benzo[e]pyrene(6.44); see Table 3.8 for refs.

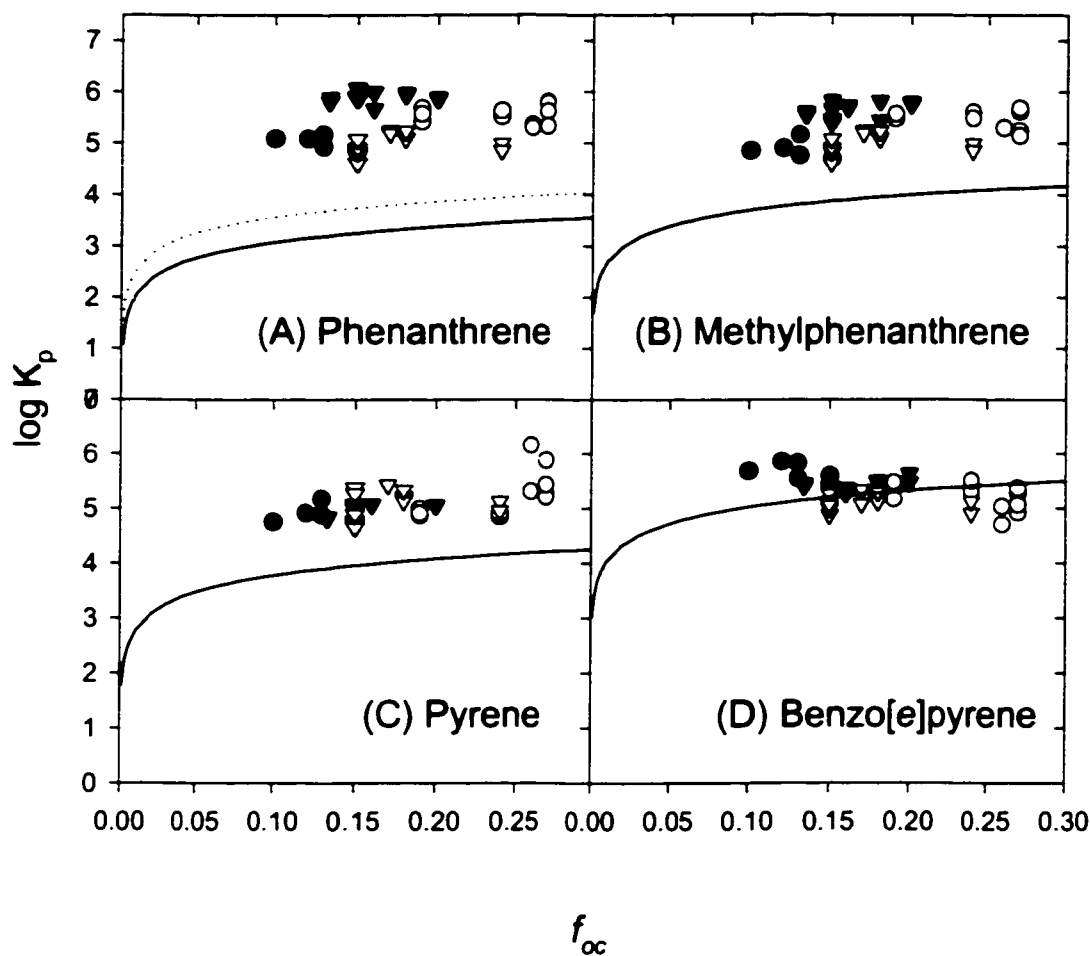


Figure 3.12 The partition coefficients of (A) phenanthrene, (B) methylphenanthrenes, (C) pyrene, and (D) benzo[e]pyrene as a function of organic carbon fractions measured in Apr/2000(●), Aug/2000(○), Oct/2000(▼), and Apr/2001(▽) from Raritan Bay.  $K_p$  values were calculated using equation 3-1. The solid lines were calculated from the equation  $K_p = f_{oc} K_{oc}$ , and the  $K_{oc}$  values were calculated using equation 3-3. Dotted line was calculated from the equation  $K_p = f_{oc} BCF_{oc}$ , where  $BCF_{oc}$  is the phenanthrene bioconcentration factor of 36,000 measured in laboratory experiments (Chapter 2). PAHs ( $\log K_{ow}$ ) include phenanthrene (4.57), methylphenanthrenes(5.07), pyrene(5.18), and benzo[e]pyrene(6.44).



## **Chapter 4. Modeling air-water exchange and phytoplankton bioaccumulation of phenanthrene: a field test in Raritan Bay, New Jersey, USA**

### **Abstract**

A dynamic model that couples air-water exchange and phytoplankton accumulation of semivolatile organic compounds was applied to the common polycyclic aromatic hydrocarbon phenanthrene in Raritan Bay, New Jersey, to investigate the mutual interactions between the two processes. Air, water, and phytoplankton polycyclic aromatic hydrocarbon (PAH) concentrations were measured in Raritan Bay during four cruises in April, August, and October 2000, and April 2001. Air-water exchange fluxes ranged from  $-1850$  to  $1600 \text{ ng m}^{-2} \text{ d}^{-1}$  in April of both 2000 and 2001, but showed net absorption ( $-50$ – $1000 \text{ ng m}^{-2} \text{ d}^{-1}$ ) in August and October. Bioaccumulation fluxes into phytoplankton ranged from  $16 \text{ ng m}^{-2} \text{ d}^{-1}$  (Oct/2000) to  $527 \text{ ng m}^{-2} \text{ d}^{-1}$  (Apr/2000), reflecting higher biomass-dependent water-phytoplankton exchange in April. Annual dynamic simulations of the coupled air-water-phytoplankton exchange using over-water gas phase phenanthrene concentrations as input over-estimated the dissolved phase concentrations in summer and fall. However, predicted dissolved phase phenanthrene concentrations from the dynamic simulation using an monthly sampling database from a shore-based sampling site (Sandy Hook) are in agreement with measured data, suggesting long-term high frequent sampling network is important in monitoring the hydrophobic organic pollutants such as phenanthrene.

## 4.1 Introduction

Phytoplankton bioaccumulation and air-water exchange are two important physical-biological processes controlling the fate and transport of hydrophobic organic compounds (HOCs) in aquatic environments. The accumulation of dissolved phase HOCs by phytoplankton is an important removal mechanism of these compounds that may lead to their transport to bottom sediments with settling cells or ingestion by higher organisms, such as zooplankton, in the first step of bioconcentration up the food web<sup>1,2,3,4</sup>. Air-water exchange (gas sorption or volatilization) is an important process in determining a chemical's loading and fate and transport in aquatic environments<sup>5,6,7,8,9</sup>. However, in some cases air-water exchange may be the dominant process controlling water concentrations as was found for toxaphene in Lake Superior<sup>8</sup>.

It is expected that dissolved HOC concentrations will reflect the net balance between air-water exchange (gas sorption and volatilization) and phytoplankton accumulation processes. However, studies on the mutual influence between air-water and water-phytoplankton processes are limited<sup>10,11</sup>. A dynamic modeling simulation that coupled air-water exchange and phytoplankton uptake of a polychlorinated biphenyl (PCB 52) applied to experimental data from two remote lakes confirmed that air-water exchange input effectively support the PCB concentration in phytoplankton<sup>10</sup>.

It has been reported that the New York-New Jersey Harbor Estuary and the Lower Hudson River Estuary were impacted greatly by anthropogenic inputs of polycyclic aromatic hydrocarbons (PAHs) due to their proximity to urban and industrial regions<sup>9,12</sup>. To evaluate the impact of air-water exchange on concentrations of PAHs (dissolved and suspended particulate phases) in Raritan Bay, this study will (1) estimate the fluxes

among the air, water, suspended particle compartments, and (2) test a dynamic model of air-water-phytoplankton exchange, by comparing model results with field measurements. Phenanthrene is selected in this study because of its ubiquity in coastal aquatic environments<sup>13</sup> and the availability in bioaccumulation kinetics parameters (Chapter 2).

#### 4.1.1 Model description

**Phytoplankton accumulation.** The accumulation of phenanthrene by phytoplankton is described by a first-order, two-compartment kinetic model, using separate surface and interior uptake and depuration rate constants:

$$\frac{dC_p}{dt} = (k_u + k_{ad}) \cdot C_w - (k_{des} + k_G) \cdot C_{p,s} - (k_d + k_G) \cdot C_{p,i} \quad (4-1)$$

where  $C_p$  is the PAH concentration in phytoplankton ( $\text{ng kgC}^{-1}$ ),  $C_{p,s}$  and  $C_{p,i}$  are the PAH concentrations in the surface compartment and interior compartment ( $\text{ng kgC}^{-1}$ ), respectively.  $C_w$  is the dissolved PAH concentration ( $\text{ng m}^{-3}$ ),  $k_u$  is the uptake rate constant to the interior ( $\text{m}^3 \text{kgC}^{-1} \text{d}^{-1}$ ),  $k_d$  is the depuration rate constant from the interior ( $\text{d}^{-1}$ ),  $k_{ad}$  is the adsorption constant to the surface ( $\text{m}^3 \text{kgC}^{-1} \text{d}^{-1}$ ),  $k_{des}$  is the desorption constant from the surface ( $\text{d}^{-1}$ ), and  $k_G$  is the phytoplankton growth rate constant ( $\text{d}^{-1}$ ).

The flux between water and phytoplankton is described as the following equation<sup>10</sup>:

$$F_{p-w} = h_{mix} \cdot k_{ad} \cdot POC \cdot (C_{p,s} \frac{k_{des}}{k_{ad}} - C_w) + h_{mix} \cdot k_u \cdot POC \cdot (C_{p,i} \frac{k_d + k_G}{k_u} - C_w) \quad (4-2)$$

where  $F_{p-w}$  is the PAH flux between water and phytoplankton ( $\text{ng m}^{-2} \text{d}^{-1}$ ),  $h_{mix}$  is the mixing depth (m), and  $POC$  (particulate organic carbon) represents phytoplankton biomass ( $\text{kgC m}^{-3}$ ). Since  $k_{des} \gg k_G$ ,  $k_G$  is not included in the surface flux term.  $F_{p-w}$  is

positive when the flux is from phytoplankton to water (depuration), and is negative during bioaccumulation.

**Air-Water Exchange.** The air-water exchange flux can be obtained from a two-layer model:

$$F_{A-W} = k_{ol} \cdot (C_w - \frac{C_A}{H'}) \quad (4-3)$$

where  $F_{A-W}$  is the PAH flux between air and water ( $\text{ng m}^{-2} \text{d}^{-1}$ ),  $k_{ol}$  is the overall mass transfer coefficient ( $\text{m d}^{-1}$ ),  $C_A$  is the PAH concentration in the gas phase ( $\text{ng m}^{-3}$ ).  $H'$  is the dimensionless Henry's law constant corrected for temperature and salinity. A positive  $F_{A-W}$  indicates net volatilization out of water column and a negative  $F_{A-W}$  indicates net absorption into water column. Details on calculation methods and corrections used for estimation of  $H'$  and  $k_{ol}$  are available in the literature<sup>9,14,15</sup>

The reciprocal of  $k_{ol}$  is the total resistance to mass transfer across the air-water interface, which can be expressed as:

$$\frac{1}{k_{ol}} = \frac{1}{k_w} + \frac{1}{k_a H'} \quad (4-4)$$

where  $k_w$  is the mass transfer coefficient across the water layer ( $\text{m d}^{-1}$ ) and  $k_a$  is the mass transfer coefficient across the air layer ( $\text{m d}^{-1}$ ). The  $k_w$  for  $\text{CO}_2$  and  $k_a$  for  $\text{H}_2\text{O}$  have been described empirically as a function of wind speed<sup>14,16</sup>, and used to estimate  $k_w$  and  $k_a$  for phenanthrene:

$$k_{w,\text{CO}_2} = 0.45 \cdot u_{10}^{1.64} \quad (4-5)$$

$$k_{a,\text{H}_2\text{O}} = 0.2 \cdot u_{10} + 0.3 \quad (4-6)$$

where  $u_{10}$  is the wind speed ( $\text{m s}^{-1}$ ) at a height of 10 m. Using the difference in diffusivity between phenanthrene and  $\text{H}_2\text{O}$ , and between phenanthrene and  $\text{CO}_2$ , mass transfer coefficients for phenanthrene can be calculated from equations 4-5 and 4-6 as the following equations<sup>5</sup>:

$$k_{w,\text{phenanthrene}} = k_{w,\text{CO}_2} \cdot \left( \frac{Sc_{\text{phenanthrene}}}{Sc_{\text{CO}_2}} \right)^{-0.5} \quad (4-7)$$

$$k_{a,\text{phenanthrene}} = k_{a,\text{H}_2\text{O}} \cdot \left( \frac{D_{a,\text{phenanthrene}}}{D_{a,\text{H}_2\text{O}}} \right)^{0.61} \quad (4-8)$$

where  $Sc_{\text{phenanthrene}}$  is the Schmidt number for phenanthrene, which was determined by dividing the kinematic viscosity of water by the diffusivity of phenanthrene;  $Sc_{\text{CO}_2}$  is the Schmidt number for  $\text{CO}_2$  of 600 at 20 °C.  $D_{a,\text{phenanthrene}}$  and  $D_{a,\text{H}_2\text{O}}$  are the diffusivities of phenanthrene and  $\text{H}_2\text{O}$ , respectively, in the air layer. The calculations of diffusivities for phenanthrene and  $\text{H}_2\text{O}$  in water and air layers can be found in the literature<sup>14,15</sup>. The temperature dependent Schmidt number for  $\text{CO}_2$  ranges from 1300 to 550 at 8–24°C<sup>16,17</sup>. Using a constant  $Sc_{\text{CO}_2}$  of 600 would result in a 10% underestimation of the air-water exchange fluxes for phenanthrene at low temperature (8–10°C). The temperature dependent  $H'$  was corrected for temperature and salinity<sup>9</sup>.

## 4.2 Materials and methods

**Sampling and site characteristics.** Samples were taken aboard the R/V Walford at a site (40.30°N/74.05°W) in the Raritan Bay, New Jersey, during four intensive sampling cruises (April, August, October 2000, and April 2001).

**Phenanthrene measurements.** Simultaneous air and water samples were taken aboard the R/V Walford. Details of sample preparation, extraction and analysis are presented in previous studies<sup>9,12</sup> and Chapter 3. Physical-chemical properties of phenanthrene are listed in Table 4.1.

**Phytoplankton measurements** Additional suspended matter related measurements were collected for total suspended matter (TSM) and particulate organic carbon (POC). In this study, POC represents the phytoplankton biomass. It is assumed that a large part of POC in Raritan Bay derived from primary production, consists of both live phytoplankton and its detritus. Phytoplankton growth rates were estimated from short-term incubations of meso-zooplankton-free sea water. The estimated phytoplankton growth rates were adjusted to represent in situ growth rates by considering day/night period and the grazing effect.

**Phytoplankton kinetic parameters.** The phenanthrene kinetic parameters in phytoplankton were obtained from laboratory batch experiments (Chapter 2) and are listed in Table 4.2. The phenanthrene kinetics parameters were selected based on a phytoplankton cell size of 10  $\mu\text{m}$  in diameter to reflect the phytoplankton community in Raritan Bay, which were dominated by *Skeletonema* spp and *Asterionella* spp.

## 4.3 Results

### Instantaneous air-water exchange fluxes

Prior to evaluating the dynamic modeling, it is useful to evaluate whether there is a net flux of PAH between the air and surface water in Raritan Bay. If there is a net flux, the direction and magnitude can be used to evaluate the impact of air-water exchange to the surface water and phytoplankton concentrations. Air-water exchange fluxes for phenanthrene were calculated using equation 4-3 with the paired gas and dissolved phase phenanthrene concentrations at each sampling time during each cruise. The phenanthrene concentrations, air temperature, wind speed, and salinity are listed in Table 4.3. The calculated air-water exchange fluxes for phenanthrene in the four cruises as well as phenanthrene concentrations are shown in Figure 4.1. Phenanthrene fluxes varied from negative to positive in Apr/2000 and Apr/2001 ( $-1850$  to  $1600$   $\text{ng m}^{-2} \text{d}^{-1}$  and  $-600$  to  $400$   $\text{ng m}^{-2} \text{d}^{-1}$ , respectively), reflecting the spatial and temporal variability of phenanthrene concentrations, temperature, and wind speed in Raritan Bay (Table 4.3 and Figure 4.1). Net gas absorption fluxes ( $-50$  to  $-1000$   $\text{ng m}^{-2} \text{d}^{-1}$ ) were found in Aug/2000 and Oct/2000. The majority (2/3) of phenanthrene fluxes calculated in Aug/2000 and Oct/2000 have a net absorption flux, indicating Raritan Bay acted as a sink of phenanthrene, especially during summer and fall.

The impact of air-water exchange on dissolved phase phenanthrene concentrations in Raritan Bay was quantified by dividing the calculated fluxes by the depth of Raritan Bay, which represents the phenanthrene mass transfer rate per unit volume ( $\text{ng m}^{-3} \text{d}^{-1}$ ). Given the average depth of 6 m in Raritan Bay, net volatilization removes up to 300  $\text{ng phenanthrene m}^{-3} \text{d}^{-1}$ , and net absorption contributes up to 160  $\text{ng phenanthrene m}^{-3} \text{d}^{-1}$ . This indicates that air-water exchange could influence

phenanthrene concentrations in Raritan Bay over a few days, because dissolved phase phenanthrene concentrations ranged from 500 to 9550 ng m<sup>-3</sup>.

### **Instantaneous phytoplankton bioaccumulation fluxes**

To estimate instantaneous water-phytoplankton exchange fluxes, average phenanthrene concentrations in phytoplankton are needed. Phenanthrene concentrations in phytoplankton were estimated using the laboratory determined phenanthrene kinetic parameters because suspended particulate phase phenanthrene concentrations measured in Raritan Bay overestimated those in phytoplankton phase (chapter 3). Given the assumptions that phytoplankton surface sorption is at equilibrium with dissolved phase phenanthrene concentrations resulting in a surface sorption flux of zero, and that the phenanthrene concentration in the internal compartment,  $C_{p,i}$ , is at 50% of steady-state with respect to the dissolved phase, water-phytoplankton exchange flux can be calculated as:

$$F_{p-w} = -\frac{k_{ad}}{k_{des}} \cdot C_w \cdot POC \cdot k_G \cdot h_{mix} + h_{mix} \cdot k_u \cdot POC \cdot (C_{p,i,50\%} \frac{k_d + k_G}{k_u} - C_w) \quad (4-9)$$

where  $C_{p,i,50\%}$  represents 50% saturated phenanthrene concentration in the phytoplankton internal compartment. The first term in equation 4-9 is the phenanthrene flux from water into the cell surface of new biomass (the product of POC and phytoplankton growth rate). Parameters used and water-phytoplankton exchange fluxes estimated in the instantaneous calculations are listed in Table 4.4. Water-phytoplankton phenanthrene bioaccumulation fluxes ranged from 16 ng m<sup>-2</sup>d<sup>-1</sup> (Oct/2000) to 527 ng m<sup>-2</sup>d<sup>-1</sup> (Apr/2000), and increased in proportion to the product of POC and dissolved phase phenanthrene concentration. Given the range of water-phytoplankton phenanthrene mass transfer rate of 3 to 90 ng m<sup>-3</sup>d<sup>-1</sup>,



phenanthrene bioaccumulation in phytoplankton has a smaller impact on dissolved phenanthrene concentrations in Raritan Bay than air-water exchange does. For example, the average air-water mass transfer rate in Aug/2000 which is much higher than the average water-phytoplankton mass transfer rate of  $3 \text{ ng m}^{-3} \text{ d}^{-1}$ .

Phenanthrene accumulated by phytoplankton can be carried to bottom sediment with settling cells. Given the same phenanthrene concentrations in phytoplankton used for instantaneous phytoplankton bioaccumulation fluxes, and an average particle sedimentation rate of  $3.6 \text{ g m}^{-2} \text{ d}^{-1}$  in Raritan Bay<sup>18</sup>, the sedimentation fluxes of phenanthrene can be estimated using equation 3 in Table 4.5. The estimated sedimentation fluxes of phenanthrene ranged from  $4 \text{ ng m}^{-2} \text{ d}^{-1}$  (Oct/2000) to  $44 \text{ ng m}^{-2} \text{ d}^{-1}$  (Apr/2000), indicating about 10 ~ 20% of accumulated phenanthrene in phytoplankton was carried to bottom sediment by sinking cells, since the instantaneous phytoplankton bioaccumulation fluxes ranged from  $16 \text{ ng m}^{-2} \text{ d}^{-1}$  (Oct/2000) to  $527 \text{ ng m}^{-2} \text{ d}^{-1}$  (Apr/2000).

#### **Application of a dynamic air-water-phytoplankton model to Raritan Bay**

A dynamic mass balance model of coupled air-water exchange, phytoplankton bioaccumulation, and sedimentation processes in Raritan Bay was constructed based on the model of Dachs et al<sup>10</sup> using the modeling framework Stella (High Performance System Inc., Hanover, NH). Figure 4.2 and Table 4.5 show the processes considered and the equations used in this dynamic simulation. The simulations were performed using the time-varying measured gas phase phenanthrene concentrations as input. Measured dissolved phase phenanthrene and estimated phytoplankton phenanthrene concentrations

were used as initial conditions, the model then predicted the time-dependent dissolved and phytoplankton phase concentrations. Other variables used to perform the simulations included total suspended matter, *POC*, growth rate, sinking flux, air temperature, wind speed, and mixing depth (Table 4.6). Measured dissolved phase concentrations of phenanthrene were used to validate the model.

### **Short-term simulations of dissolved phenanthrene**

Short-term simulations of dissolved phenanthrene concentrations were performed for each sampling cruise. Gas phase concentrations and other variables used in the simulations are listed in Table 4.3. The results are shown in Figure 4.3. All the dissolved phase phenanthrene simulation lines show a stable increase or decrease over 3 days and the modeled results always overestimated dissolved phenanthrene.

### **Annual simulations of dissolved and suspended particle phenanthrene concentrations**

Long-term simulations were performed using seasonal average gas phase concentrations of phenanthrene measured over Raritan Bay, and monthly average concentrations measured at nearby Sandy Hook, New Jersey. In the case of using seasonal average concentrations, the measured gas phase concentrations in Apr/2000 and Apr/2001 were used for the spring season, and summer and fall seasons were represented by Aug/2000 and Oct/2000 data. The result measured from a pilot cruise on December 3, 1999 was used for the winter season. Values of phenanthrene gas phase concentrations, and other parameters used in the year-long simulation are listed in Table 4.7. Figures 4.4

and 4.5 show the simulation results and the measured average dissolved and particle phase concentrations of phenanthrene. The results obtained from seasonal average gas phase concentrations indicate that dissolved phase concentrations are relatively invariant in spring season, since using seasonal average concentration would minimize the daily variation of gas phase concentrations and subsequently decrease the fluctuation of fluxes (instantaneous fluxes of  $-1850$  to  $1600 \text{ ng m}^{-2} \text{ d}^{-1}$  in Apr/2000). Predicted water concentrations increased in summer and fall as a result of the gas sorption deriving from elevated gas phase concentrations inputs of Aug/2000 and Oct/2000, and peaked in winter, then decreased in early spring. Compared with the measured water concentrations, dynamic simulations overestimated water concentrations by a factor of 6 in summer and 16 in fall. No measured data is available to validate the predicted peak dissolved phase concentrations in winter.

Using monthly average gas phase phenanthrene concentrations from Sandy Hook, the model predicted dissolved phenanthrene concentrations were closer to measured values in the summer and fall (Figure 4.4).

The predicted phytoplankton phase concentrations of phenanthrene are shown in Figure 4.5, indicating that predicted phytoplankton phase concentrations is a function of predicted dissolved phase concentrations. This result suggests that air-water exchange supports dissolved phase concentrations of phenanthrene and subsequently supports the bioaccumulation of phenanthrene in phytoplankton.

## **4.4 Discussion**

### **Short-term simulations of dissolved phenanthrene**

It is observed that gas phase phenanthrene concentrations vary both temporally and spatially around Raritan Bay. However, the daily variation in gas phase phenanthrene is not linked to dissolved phase variability by simple instantaneous air-water exchange (Figure 4.3). The daily disequilibrium between air and water suggests that other sources and sinks control dissolved phenanthrene or that air-water movement complicates the air-water linkage.

### **Predicted dissolved phase concentrations**

The annual simulation using the gas phase concentrations measured from four seasonal sampling cruises overestimated the measured dissolved phase concentrations. The daily variation in gas phase measurements from such four cruises could affect the performance of the simulation. For comparison, a long-term monthly collected database of phenanthrene concentrations measured in a over-land sampling site in Sandy Hook (Figure 3.1 in chapter 3) obtained by NJADN<sup>19</sup> were used to perform the simulation. The average gas phase concentrations in Sandy Hook were 2 times greater than those over Raritan Bay in 1998<sup>9</sup>. However, it is believed that the Sandy Hook database can reasonably represent Raritan Bay because of its close proximity to Raritan Bay and the greater sampling frequency of the long-term monitoring site. The gas phase concentrations of phenanthrene and variables used in the simulations are listed in Table 4.8. Gas phase concentrations of phenanthrene at Sandy Hook ranged from 2800 to 6810  $\text{pg m}^{-3}$ . The predicted results are shown in Figures 4.4 and 4.5. The results are in good agreement with the present measured data indicating a decreasing dissolved phase

concentration in summer and fall. The results also agreed with the field measurement in July 1998 (averaged  $1740 \text{ ng m}^{-3}$ )<sup>9</sup>.

The results are also consistent with the increasing dissolved phase concentrations of phenanthrene in winter. The low temperature in winter, resulting in a low Henry's law constant, can affect the flux direction and the magnitude of HOCs. Bamford et al (1999)<sup>7</sup> suggested that high wind driven resuspension effect contributed to an elevated dissolved phase concentration of phenanthrene measured in February 18–20, 1997 of Chesapeake Bay. However, such elevated dissolved phase concentrations of phenanthrene in the late winter could be a result of the winter absorption scenario (low temperature), and it may reach equilibrium with gas phase concentrations in Chesapeake Bay judging by the low fluxes calculated<sup>7</sup>. It is expected that this elevated water concentration would decrease in early spring as temperature increases. Such results raise questions about the validity of the intensive sampling cruises in predicting long-term air-water exchange. It is believed that over-water measurements are more representative than over-land data in monitoring air-water fluxes. However, due to the spatial and temporal variation in field sampling, a long-term high temporal resolution monitoring network is likely to better represent environmental variability.

### **Predicted phenanthrene concentrations in phytoplankton**

Predicted phenanthrene concentrations in phytoplankton using either the over water or Sandy Hook data as input are similar, and show a dependence on dissolved phase concentrations of phenanthrene and *POC* concentrations (Figure 4.5). In the instantaneous evaluations, the dissolved phase concentrations are controlled by the physical process of air-water exchange, and the contribution from phytoplankton is

minor. However, it is expected that phytoplankton would have a greater effect on the dissolved phase concentration for high bioconcentration factors and high uptake rate constant PAHs ( high molecular weight PAHs). Further investigation is needed to determine the bioaccumulation kinetic parameters for other PAHs.

Due to major soot-like particulate partitioning of phenanthrene, the phenanthrene concentrations in suspended particulate in Raritan Bay can not be used for validating the simulation performance on the phenanthrene concentrations in phytoplankton. Applying a soot carbon-partitioning model<sup>20</sup> and monitoring the soot carbon abundance in Raritan Bay, the phenanthrene concentrations in particulate organic carbon, assumable as representing phytoplankton, can be estimated and used for validation in the dynamic simulations.

### **Variables affecting air-water-phytoplankton exchange simulations**

In the simulations, bioaccumulation and air-water exchange are the two major processes controlling the air-water-phytoplankton exchange. In addition to the concentration gradient between gas and dissolved phases, variables such as wind speed, temperature, mixing depth, phytoplankton biomass (*POC*), and growth rate, control the direction and magnitude of fluxes (equations 4-2 and 4-3). Physical variables such as wind speed and temperature have nonlinear influences on air-water exchange. Wind speed determines the mass transfer coefficients and temperature affects the magnitude of Henry's law constant, *H*. *POC* and mixing depth,  $h_{mix}$ , exert a linear influence on the phytoplankton bioaccumulation fluxes. In this study, a well-mixed water column was assumed. However, shallower mixing depths that would occur as a result of stratification

would decrease water to phytoplankton SOC fluxes. During the spring and summer when *POC* levels are highest, it is expected that the accumulation of SOC<sub>s</sub> by phytoplankton and their sedimentation fluxes will be greatest.

The mixing depth and biological variables such as *POC* and the kinetic parameters were identical in both simulations. Among the other variables, gas phase concentration of phenanthrene was found to be the most important controlling factor. It was observed that the different gas phase concentrations in the two database sets affected the magnitude and directions of air-water exchange fluxes. Using the seasonal cruise database resulted in higher dissolved phase phenanthrene concentrations as a result of gas absorption in summer and fall. On the other hand, using Sandy Hook database resulted in lower dissolved phase concentrations due to volatilization. These results indicate that the variability of gas phase concentrations of phenanthrene plays an important role in the simulations. However, other variables do not have very significant impacts on the simulations in this study. The physical variables such as temperature and wind speed resulted in similar mass transfer coefficients and Henry's law constants.

### **Mass balance budgets**

In this study, the mass balance budget for the simulations uses air-water-phytoplankton exchange and sedimentation as the major inputs and outputs in the water column. These processes have been considered most important in biogeochemical cycles<sup>11</sup>. However, in an estuary, potential inputs for phenanthrene should include advection from rivers and as a result of wind driven flow and tidal action, and outputs should include reactions such as transformation and degradation. To improve the

simulation performance, parameters related to these processes should be further investigated and verified.

#### **4.5 Conclusions**

A dynamic simulation of coupled air-water exchange, phytoplankton bioaccumulation, and sedimentation was applied to phenanthrene in Raritan Bay from four intensive sampling cruises during April 2000 to April 2001. Using the seasonal average gas phase concentrations of phenanthrene over the four cruises, the simulation results overestimated the dissolved phase concentrations in summer and fall, resulting from the elevated gas phase concentrations measured in Aug/2000 and Oct/2000. Using a shore-base but monthly average phenanthrene concentration database of Sandy Hook, better agreement with field measurements was obtained, suggesting the need for high temporal resolution sampling data (no greater than one month) to represent the environmental variability associated with atmosphere concentrations. The predicted suspended particle phase concentrations of phenanthrene depend on dissolved phase concentrations and *POC* concentrations. The predicted suspended particle phase concentrations of phenanthrene, which are needed to assess possible trophic transfer, needs to be further verified in the field.

#### **References**

- (1). Sijm, D.T.H.M.; Broersen, K.W.; de Roode, D.F.; Mayer, P. Bioconcentration kinetics of hydrophobic chemicals in different densities of *Chlorella pyrenoidosa*. *Environ Toxicol Chem.* **1998**, *17*, 1695 -1704.



- (2). Koelmans, A.A.; van der Woude, H.; Hattink, J.; Niesten, D.J.M. Long-term bioconcentration kinetics of hydrophobic chemicals in *Selenastrum capricornutum* and *Microcystis aeruginosa*. *Environ Toxicol Chem.* **1999**, 18, 1164 -1172.
- (3). Swackhamer, D.L.; Skoglund, R.S. Bioaccumulation of PCBs by algae: kinetics versus equilibrium. *Environ Toxicol Chem.* **1993**, 12, 831 -838.
- (4). Halling-Sorenson, B.; Nyholm, N.; Kusk, K.O.; Jacobsson, E. Influence of Nitrogen Status on the Bioconcentration of Hydrophobic Organic Compounds to *Selenastrum carcornutum*. *Ecotoxicol Environ Saf.* **2000**, 45, 33 -42.
- (5). Achman, D.R.; Hornbuckle, K.C.; Eisenreich, S.J. Volatilization of polychlorinated biphenyls from Green Bay, Lake Michigian. *Environ Sci Technol.* **1993**, 27, 75 -87.
- (6). Nelson, E.D.; Macconnell, L.L.; Baker, J.E. Diffusive exchange of gaseous polycyclic aromatic hydrocarbons and polychlorinated biphenyls across the air-water interface of the Chesapeake bay. *Environ Sci Technol.* **1998**, 32, 912 -919.
- (7). Bamford, H.A.; Offenber, J.H.; Larsen, R.K.; Ko, F.; Baker, J.E. Diffusive exchange of polycyclic aromatic hydrocarbons across the air-water interface of the Patapsco River, an urbanized subestuary of the Chesapeake Bay. *Environ Sci Technol.* **1999**, 33, 2138 -2144.
- (8). Swackhamer, D.L.; Schottler, S.; Pearson, R.F. Air-water exchange and mass balance of toxaphene in the Greak Lakes. *Environ Sci Technol.* **1999**, 33, 3864 -3872.
- (9). Gigliotti, C.L.; Brunciak, P.A.; Dachs, J.; Glenn IV, T.R.; Nelson, E.D.; Totten, L.A.; Eisenreich, S.J. Air-water exchange of polycyclic aromatic hydrocarbons in the NY-NJ harbor estuary. *Environ Toxicol Chem.* **2002**, 21, 235 -244.
- (10). Dachs, J.; Eisenreich, S.J.; Baker, J.E.; Ko, F.; Jeremiason, J.D. Coupling of phytoplankton uptake and air-water exchange of persistent organic pollutants. *Environ Sci Technol.* **1999**, 33, 3653 -3660.
- (11). Dachs, J.; Eisenreich, S.J.; Hoff, R.M. Influence of eutrophication on air-water exchange, vertical fluxes, and phytoplankton concentrations of persistent organic pollutants. *Environ Sci Technol.* **2000**, 34, 1095 -1102.
- (12). Gigliotti, C.L.; Dachs, J.; Nelson, E.D.; Brunciak, P.A.; Eisenreich, S.J. Polycyclic aromatic hydrocarbons in the New Jersey coastal atmosphere. *Environ Sci Technol.* **2000**, 34, 3547 -3554.
- (13). Broman, D.; Naf, C.; Roiff, C.; Zebuhr, Y. Occurrence and dynamics of polychlorinated dibenzo-p-dioxins and dibenzofurans and polycyclic aromatic hydrocarbons in the mixed surface layer of remote coastal and offshore waters of the Baltic. *Environ Sci Technol.* **1991**, 25, 1850 -1864.

- (14). Schwarzenbach, R.P., Gschwend, P.M., Imboden, D.M. Environmental Organic Chemistry. Wiley-Interscience:New York, 1993.
- (15). ; Reid RC, Prausnitz JM, and Poling BE, editors. The Properties of Gases and Liquids. 4th ed. McGraw-Hill:Boston, 1987.
- (16). Wanninkhof, R. Relationship between wind speed and gas exchange over the ocean. *J Geophys Res.* **1992**, 97, 7373 -7382.
- (17). Zhang, H.; Eisenreich, S.J.; Franz, T.R.; Baker, J.E.; Offenberg, J.H. Evidence for increased gaseous PCB fluxes to lake Michigan from Chicago. *Environ Sci Technol.* **1999**, 33, 2129 -2137.
- (18). Van Ry, D.A.; Dachs, J.; Gigliotti, C.L.; Brunciak, P.A.; Nelson, E.D.; Eisenreich, S.J. Atmospheric seasonal trends and environmental fate of alkylphenols in the lower Hudson river estuary. *Environ Sci Technol.* **2000**, 34, 2410 -2417.
- (19). Eisenreich, S.J. and Reinfelder, J.R. New Jersey Atmospheric Deposition Network, NJADN. 2002;
- (20). Gustafsson, O.; Haghseta, F.; Chan, C.; Macfarlane, J.; Gschwend, P.M. Quantification of the dilute sedimentary soot phase: implication for PAH speciation and bioavailability. *Environ Sci Technol.* **1997**, 31, 203 -209.

Table 4.1 Physical-chemical properties of phenanthrene.

PAH	$\Delta H$ kJ mol <sup>-1</sup>	$H_{298}$ atm m <sup>-3</sup> mol <sup>-1</sup>	$MW$	$V_m$ cm <sup>3</sup> mol <sup>-1</sup>	log $K_{ow}$
Phenanthrene	47.3	4.24×10 <sup>-5</sup>	178.2	199	4.57

Table 4.2 Kinetic parameters for bioaccumulation of phenanthrene by phytoplankton.

PAH	$BCF_{oc}$ $m^3 kgC^{-1}$	$k_{ad}$ $m^3 kgC^{-1} d^{-1}$	$k_{des}$ $d^{-1}$	$k_u$ $m^3 kgC^{-1} d^{-1}$	$k_d$ $d^{-1}$
Phenanthrene	36.3	5445	600	16.34	0.6

Table 4.3 Gas and dissolved concentrations of phenanthrene, environmental parameters used for instantaneous and dynamic simulations.

Apr/2000		Apr/19/00		Apr/20/00		Apr/21/00	
		AM	PM	AM	PM	AM	PM
$C_a$	pg m <sup>-3</sup>	7094	7094	1945	2744	709	709
$C_w$	ng m <sup>-3</sup>	9551	3397	4442	3465	4165	4165
$u_{10}$	m s <sup>-1</sup>	7.3	6.2	4.4	5.7	10	10
air temp	°C	9	10	14.5	14.5	8.2	8.2
salinity		23	23	23	23	23	23
$TSM$	mg L <sup>-1</sup>	10	19	10	10	13	13
$POC$	µg L <sup>-1</sup>	1500	3000	1100	1900	1500	1200
$k_G$	d <sup>-1</sup>	0.25	0.25	0.25	0.25	0.25	0.25
$F_{settling}$	g m <sup>-2</sup> d <sup>-1</sup>	3.6	3.6	3.6	3.6	3.6	3.6
Aug/2000		Aug/21/00		Aug/22/00		Aug/23/00	
$C_a$	pg m <sup>-3</sup>	15325	18977	20984	7986	3344	4739
$C_w$	ng m <sup>-3</sup>	2024	1350	869	1126	843	900
$u_{10}$	m s <sup>-1</sup>	2.1	1.8	1.5	2.6	5.5	6.4
air temp	°C	20	22	22	24	22	23
salinity		23	23	23	23	23	23
$TSM$	mg L <sup>-1</sup>	2.9	2.7	2.8	3.0	7.3	6.0
$POC$	µgC L <sup>-1</sup>	551	513	756	720	1971	1560
$k_G$	d <sup>-1</sup>	0.75	0.75	0.75	0.75	0.75	0.75
$F_{settling}$	g m <sup>-2</sup> d <sup>-1</sup>	3.6	3.6	3.6	3.6	3.6	3.6
Oct/2000		Oct/25/00		Oct/26/00		Oct/27/00	
$C_a$	pg m <sup>-3</sup>	14171	9487	5621	3985	46303	43454
$C_w$	ng m <sup>-3</sup>	649	509	480	538	670	467
$u_{10}$	m s <sup>-1</sup>	0.8	2.1	0.4	1.1	0.7	0.2
air temp	°C	18	21	13	15	16	20
salinity		26	26	26	26	26	26
$TSM$	mg L <sup>-1</sup>	2.2	2.2	2.1	2.7	2.2	2.2
$POC$	µgC L <sup>-1</sup>	440	405	315	432	295	350
$k_G$	d <sup>-1</sup>	0.5	0.5	0.5	0.5	0.5	0.5
$F_{settling}$	g m <sup>-2</sup> d <sup>-1</sup>	3.6	3.6	3.6	3.6	3.6	3.6
Apr/2001		Apr/24/01		Apr/25/01		Apr/26/01	
$C_a$	pg m <sup>-3</sup>	6202	3941	4312	4312	2823	2803
$C_w$	ng m <sup>-3</sup>	3961	2864	2385	2385	2445	2117
$u_{10}$	m s <sup>-1</sup>	1.9	3.8	3.8	3.8	2.2	1.8
air temp	°C	23	25	9	9	14	17
salinity		25	25	25	25	25	25
$TSM$	mg L <sup>-1</sup>	8.7	11	3.7	3.7	3.8	5
$POC$	µgC L <sup>-1</sup>	1305	2640	555	555	684	850
$k_G$	d <sup>-1</sup>	0.25	0.25	0.25	0.25	0.25	0.25
$F_{settling}$	g m <sup>-2</sup> d <sup>-1</sup>	3.6	3.6	3.6	3.6	3.6	3.6

Table 4.4 Average surface water parameters and instantaneous water-phytoplankton fluxes in Raritan Bay.

		<b>Apr/2000</b>	<b>Aug/2000</b>	<b>Oct/2000</b>	<b>Apr/2000</b>
$C_w$	$\text{ng m}^{-3}$	4864	1186	555	2755
POC	$\mu\text{gC L}^{-1}$	1730	980	380	1100
$h_{mix}$	m	6	6	6	6
$k_G$	$\text{d}^{-1}$	0.25	0.75	0.5	0.25
$C_{p,i.50\%}$	$\text{ng kgC}^{-1}$	46750	7200	4100	26480
$F_{p-w}$	$\text{ng m}^{-2}\text{d}^{-1}$	527	104	16	190

Table 4.5 Equations used in the coupled model.

- Concentration =  $\Sigma(\text{Flux}_{\text{in}} - \text{Flux}_{\text{out}}) / h_{\text{mix}}$

- $\text{Flux}_t = \text{flux}_{(t-dt)} + (\text{input} - \text{output}) \cdot dt$ ,

where  $dt = 1.5$  min intervals for simulation.

1. Air-water exchange (net) =  $F_{A-W} = k_{ol} \cdot (C_w - \frac{C_A}{H'})$

Volatilization =  $k_{ol} \cdot C_w$

Absorption =  $k_{ol} \cdot \frac{C_A}{H'}$

2. Bioaccumulation (net) =

$$F_{P-W} = h_{\text{mix}} \cdot k_{ad} \cdot POC \cdot (C_{p,s} \frac{k_{des}}{k_{ad}} - C_w) + h_{\text{mix}} \cdot k_u \cdot POC \cdot (C_{p,d} \frac{k_d + k_G}{k_u} - C_w)$$

Uptake =  $h_{\text{mix}} \cdot (k_{ad} + k_u) \cdot POC \cdot C_w$

Depuration =  $h_{\text{mix}} \cdot POC \cdot C_{p,s} \cdot (k_{des}) + h_{\text{mix}} \cdot POC \cdot C_{p,d} \cdot (k_d + k_G)$

3. Sedimentation (net) =  $F_{S-W} = F_{\text{settling}} \cdot \frac{POC}{TSM} \cdot (C_{p,s} + C_{p,d})$

Table 4.6 Variables used in dynamic simulations.

Definition	Symbol	Data source	unit
Particulate organic matter	<i>POC</i>	measured	$\mu\text{g C L}^{-1}$
Total suspended matter	<i>TSM</i>	measured	$\mu\text{g L}^{-1}$
Air temp	<i>T</i>	measured	$^{\circ}\text{C}$
Wind speed	$u_{10}$	measured	$\text{m s}^{-1}$
phytoplankton growth rate	$k_G$	measured	$\text{d}^{-1}$
Depth of Raritan Bay	$h_{\text{mix}}$	6	m
Salinity	—	measured	—
Particulate sinking flux	$F_{\text{settling}}$	3.6	$\text{g m}^{-2}\text{d}^{-1}$



Table 4.7 Parameters used in dynamic simulations for phenanthrene in Raritan Bay. Simulation were conducted using cruises data.

Simulated season	Cruise	$C_a$ pg m <sup>-3</sup>	$u_{10}$ m s <sup>-1</sup>	Air Temp °C	$k_G$ d <sup>-1</sup>	POC µg L <sup>-1</sup>	TSM µg L <sup>-1</sup>
Spring	Apr/2000	3140	7	11	0.25	1730	13000
Summer	Aug/2000	11900	3.5	22	0.75	980	4050
Fall	Oct/2000	20500	1	17	0.5	380	2300
Winter	Dec/1999	9000	9	9	0.1	420	2500
Spring	Apr/2001	4020	3	16	0.25	1100	6000

**Table 4.8** Parameters used in dynamic simulations for phenanthrene in Raritan Bay. Simulation were conducted using Sandy Hook database.

Date	$C_a$ pg m <sup>-3</sup>	$u_{10}$ m s <sup>-1</sup>	Air Temp °C	$k_G$ d <sup>-1</sup>	POC µg L <sup>-1</sup>	TSM µg L <sup>-1</sup>
Apr/1998	5290	5.8	11	0.25	1730	13000
May/1998	4780	5.4	17	0.25	1730	13000
June/1998	2810	4.7	19	0.75	980	4050
July/1998	6810	4.8	24	0.75	980	4050
Aug/1998	3200	3.9	24	0.75	980	4050
Sep/1998	4840	4.9	21	0.5	380	2300
Oct/1998	2920	6.4	15	0.5	380	2300
Nov/1998	3330	5.5	8	0.5	380	2300
Dec/1998	8200	6.6	10	0.1	420	2500
Jan/1999	5600	5.1	3.4	0.1	420	2500
Feb/1999	3260	7.9	0	0.1	420	2500

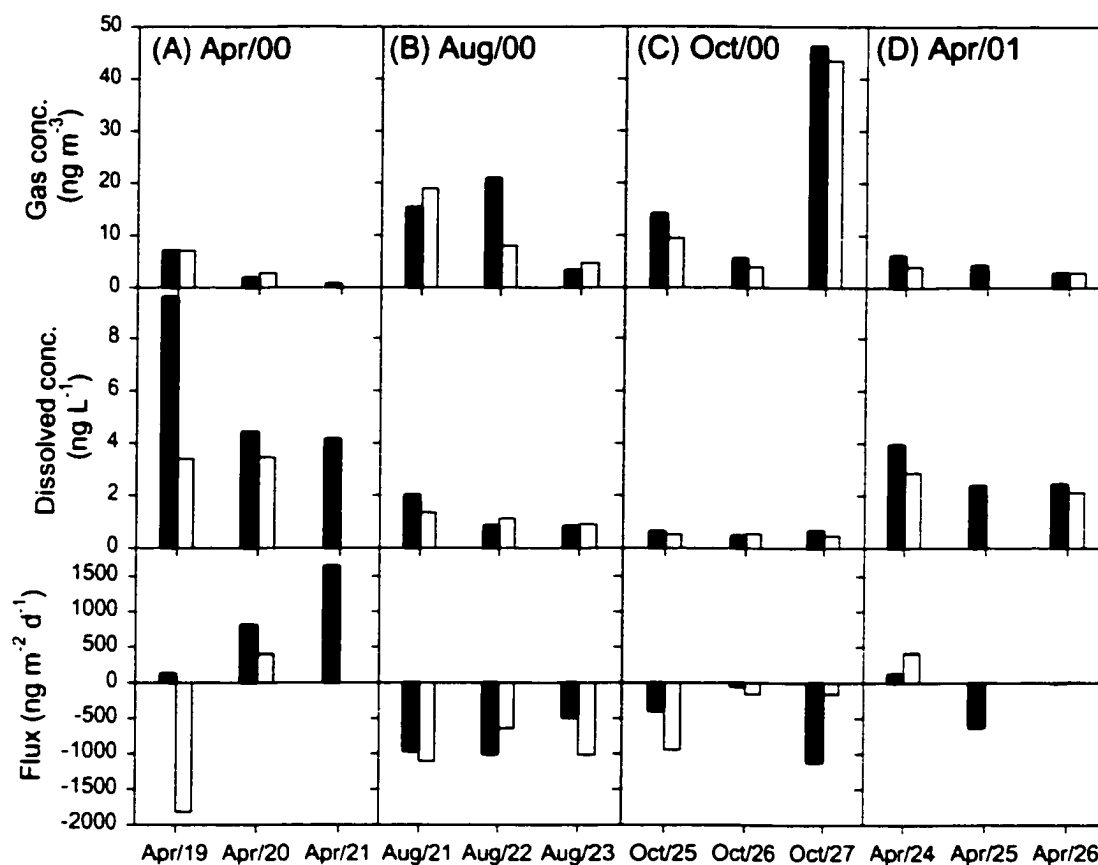


Figure 4.1 Phenanthrene concentrations in gas and dissolved phases and instantaneous air-water exchange fluxes in the morning (■), and afternoon (□) in Raritan Bay. Negative fluxes denote gas absorption into surface water, and positive fluxes denote volatilization to atmosphere.

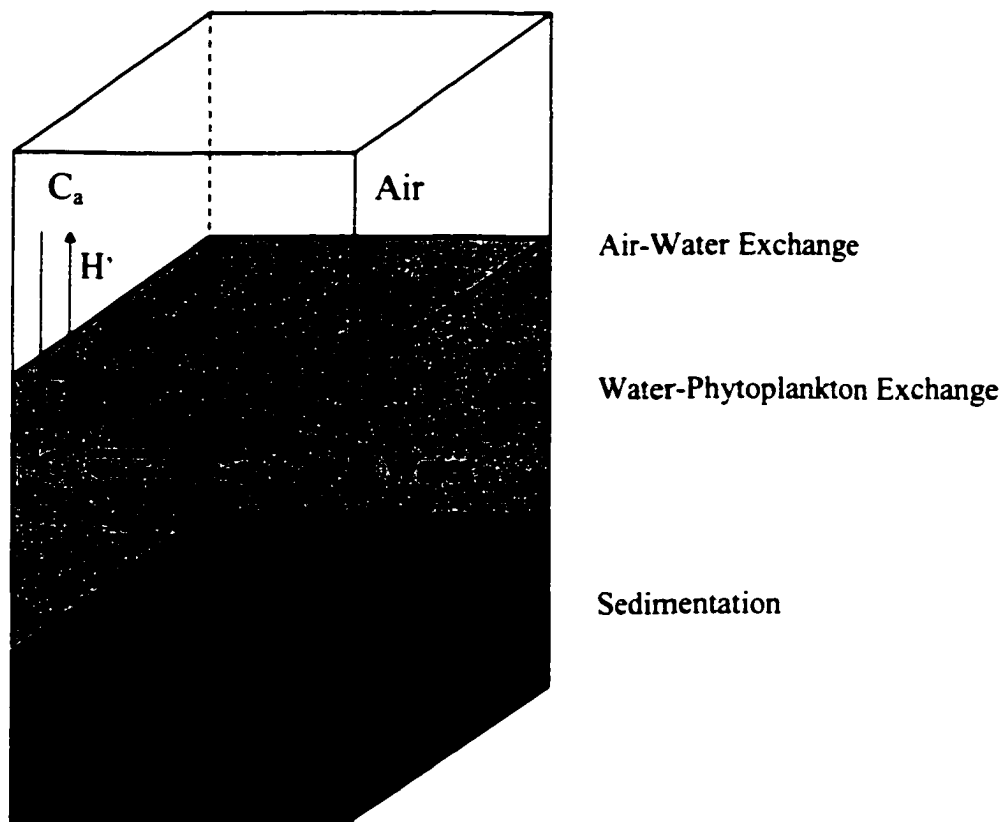


Figure 4.2 Schematic of the air-water-phytoplankton exchange of phenanthrene in Raritan Bay.

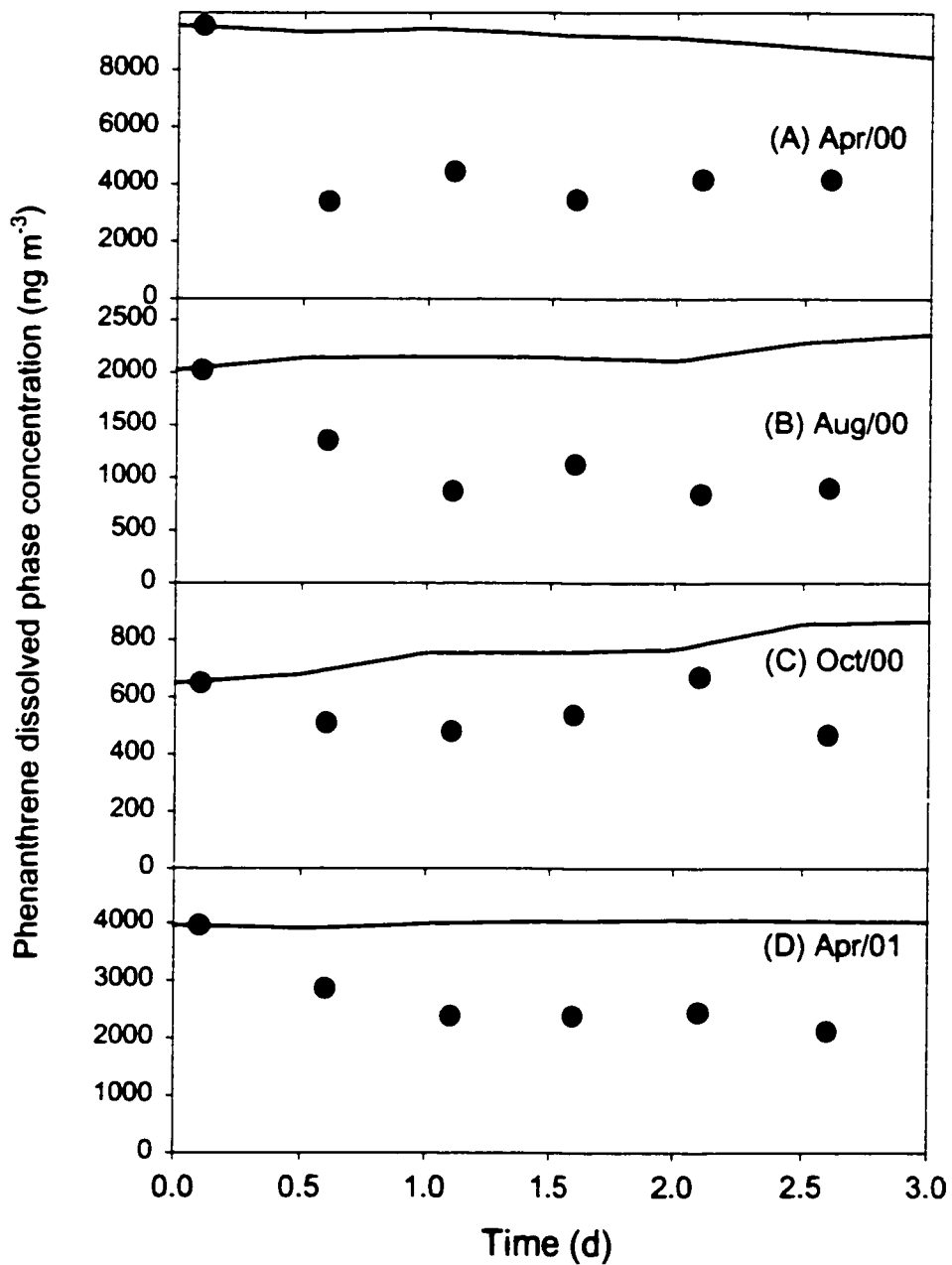


Figure 4.3 Predicted and measured dissolved phase concentrations of phenanthrene in Raritan Bay. Lines represent the predicted results and dots represent measured results.

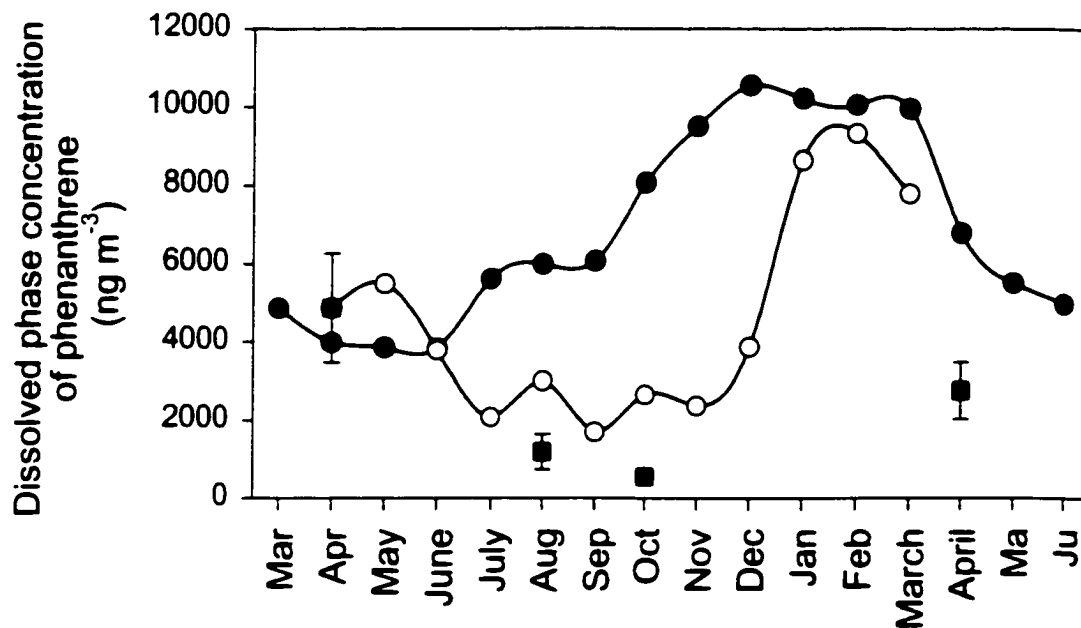


Figure 4.4 Predicted and measured dissolved phase concentrations of phenanthrene in Raritan Bay. Simulations were based on gas phase concentrations of phenanthrene from (●) sampling cruises in Raritan Bay or (○) Sandy Hook, New Jersey. Solid squares (■) represent the measured data in Raritan Bay.

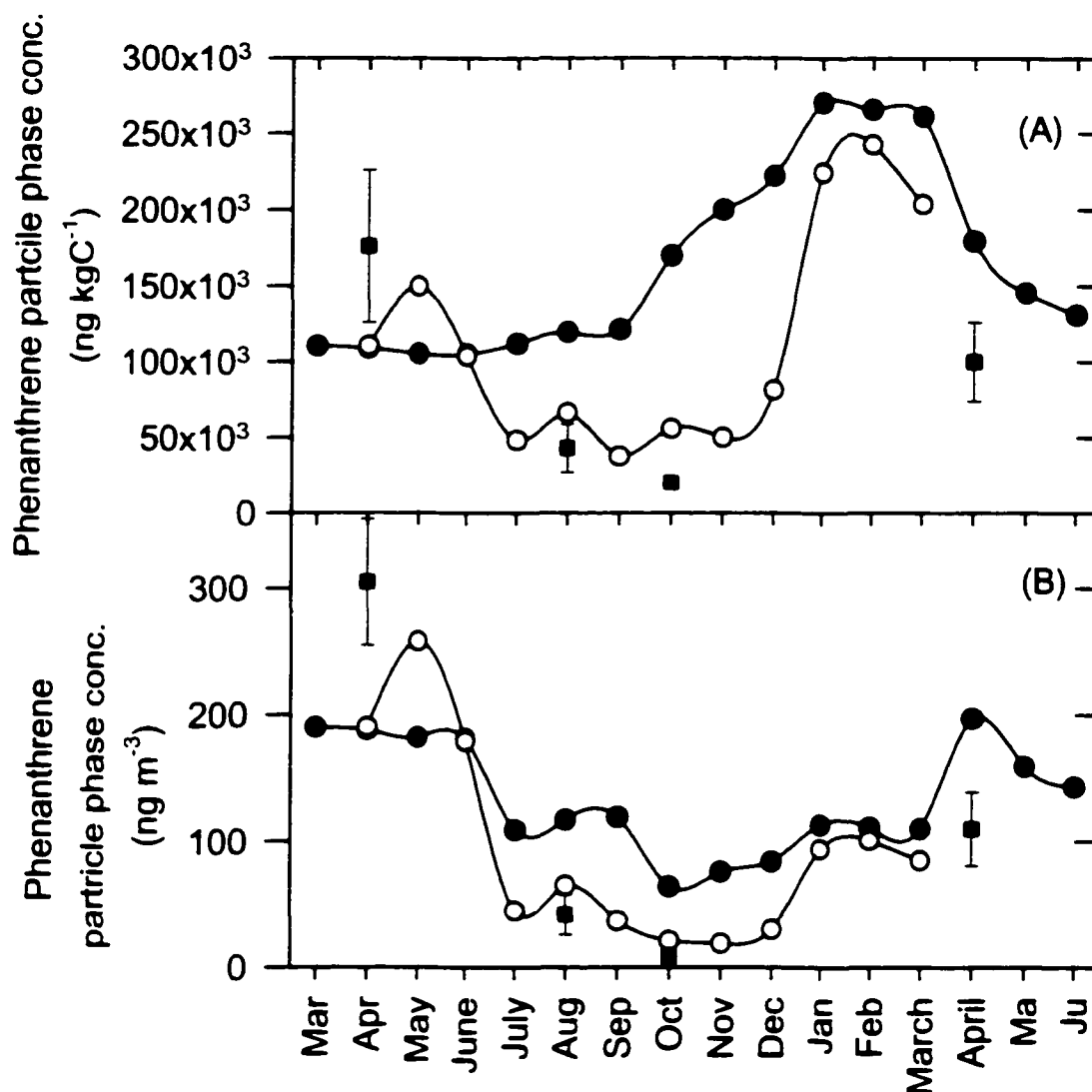


Figure 4.5 Predicted phenanthrene concentrations in particulate organic carbon (POC). Phenanthrene concentrations are presented in the unit of (A)  $\text{ng kgC}^{-1}$  and (B)  $\text{ng m}^{-3}$ . Simulations were based on gas phase concentrations of phenanthrene from (●) sampling cruises in Raritan Bay or (○) Sandy Hook database. Solid squares (■) represent the estimated phenanthrene concentrations in suspended particles corrected for soot fraction (Chapter 3).

## **Chapter 5. Conclusions and Future Work**

### **5.1 Conclusions**

The results of the present kinetic studies demonstrate that phenanthrene bioaccumulation in two marine diatoms follows a two-compartment mechanism in which the compound first partitions in the cell surface and subsequently diffuses into the cell's interior consistent with earlier studies of other HOCs<sup>1,2,3,4</sup>. Surface sorption was faster than accumulation in the cell interior. In this two-compartment model, cell size (the ratio of cell surface area to cell volume,  $A/V$ ) is an important factor controlling phenanthrene accumulation kinetics in the cell surface compartment, the relative contribution of cell surface sorption to overall bioaccumulation, and possibly phenanthrene trophic transfer. The long-term loss rate constants of phenanthrene in diatoms are similar to those obtained for other HOCs with a range of hydrophobicities and chemical structures in various algal species<sup>2,4</sup>. This observation may help simplify the modeling of organic contaminant bioaccumulation. Organic carbon-normalization resulted in very similar bioconcentration factors for the two algal species studied, suggesting that organic carbon is the sorbing matrix for phenanthrene in these cells.

The organic carbon-normalized bioconcentration factors determined in the present work and a previously reported organic carbon-partitioning model<sup>5</sup> underestimated the measured partition coefficients for phenanthrene, methylphenanthrenes and pyrene in Raritan Bay by 2-3 orders of magnitude, suggesting that : (1) PAH partitioning is affected by the presence of an additional strongly sorbing particulate phase such as soot<sup>6</sup>; (2) organic carbon-normalized bioconcentration factors are insufficient to predict PAH partition coefficients in Raritan Bay.



A dynamic simulation of coupled air-water exchange, phytoplankton bioaccumulation, and sedimentation was applied to phenanthrene field data in Raritan Bay collected during four intensive sampling cruises between April 2000 to April 2001. Using the average gas phase concentrations of phenanthrene measured during the four cruises, the simulation results overestimated the dissolved phase concentrations in summer and fall. Using a shore-based, but monthly collected phenanthrene concentration database from nearby Sandy Hook, the predicted results are in closer agreement with field measurements, suggesting the need for high temporal resolution input (gas phase concentration) data. Predicted phytoplankton phase concentrations of phenanthrene, which may affect trophic transfer, need to be further verified with field measurements of PAHs in different compartments (soot, phytoplankton, and other) of the total suspended particulate matter.

## **5.2 Future work**

Future research should focus on addressing the following issues:

1. Before phenanthrene sorption kinetics data for marine diatoms can be applied to other microalgae and other compounds, accumulation kinetics for various classes of phytoplankton and a range of HOCs with different hydrophobicities should be investigated further.
2. To evaluate the extent to which kinetically determined  $x_1$  values represent the cell fractionation controlling phenanthrene assimilation in suspension feeders and thus trophic transfer, the subcellular fractionation of phenanthrene in diatoms need to be determined. A preliminary study of

subcellular fractionation of phenanthrene in *T. weissflogii* ( $x_1 = 0.23$ ) was conducted using sonification to break cells, and centrifugation to separate the cytoplasmic (supernatant) and membrane fractions (pellet). An alternative method involving the measurement of evaporation loss in concentrated cells was also used. The results are shown in Appendix I. Cell fractionation (sonification) showed that the membrane fractions contained 10-50% of cellular phenanthrene in *T. weissflogii* exposed for 3 to 6 d. However, this method<sup>7</sup> suffered from heavy loss of phenanthrene radiotracer during sonification. The evaporation loss method indicated that about 30% of accumulated phenanthrene was in the membrane fraction.

3. The bioaccumulation of phenanthrene in zooplankton should include both dissolved and trophic accumulation. In the study of bioaccumulation of copper in marine copepods, Chang and Reinfelder (2002)<sup>8</sup> suggested that dissolved uptake of copper could be important in contaminated waters. Quantification of both pathways is needed to predict aquatic food web accumulation. Dissolved uptake of phenanthrene in copepods was measured in animals exposed to phenanthrene for 1-3 h. The results are shown in Appendix II and suggest a dissolved phase concentration dependent bioaccumulation of phenanthrene in copepods.
4. It is suggested that elevated PAH partition coefficients from field surveys primarily resulted from the presence of soot-like particles in estuarine waters<sup>9</sup>. In order to account for the elevated partition coefficients of phenanthrene, methylphenanthrenes, and pyrene measured in Raritan Bay,

the soot carbon abundance in suspended particulate matter needs to be quantified, and further studies are required to understand the environmental behavior and effects of soot particles.

5. To improve the performance of coupled air-water-phytoplankton exchange dynamic models, parameters related to inputs/outputs processes such as advection and transformation should be further investigated and verified.

## Reference

- (1). Koelmans, A.A.; Jimenez, C.S.; Lijklema, L. Sorption of chlorobenzenes to mineralizing phytoplankton. *Environ Toxicol Chem.* **1993**, 12, 1425 -1439.
- (2). Koelmans, A.A.; Anzion, S.F.; Lijklema, L. Dynamics of organic micropollutant biosorption to cyanobacteria and detritus. *Environ Sci Technol.* **1995**, 29, 933 -940.
- (3). Skoglund, R.S.; Stange, K.; Swackhamer, D.L. A kinetics model for predicting the accumulation of PCBs in phytoplankton. *Environ Sci Technol.* **1996**, 30, 2113 -2120.
- (4). Dachs, J.; Eisenreich, S.J.; Baker, J.E.; Ko, F.; Jeremiason, J.D. Coupling of phytoplankton uptake and air-water exchange of persistent organic pollutants. *Environ Sci Technol.* **1999**, 33, 3653 -3660.
- (5). Karickhoff, S.W. Semi-empirical estimation of sorption of hydrophobic pollutants on natural sediments and soils. *Chemosphere.* **1981**, 10, 833 -846.
- (6). Gustafsson, O.; Haghseta, F.; Chan, C.; Macfarlane, J.; Gschwend, P.M. Quantification of the dilute sedimentary soot phase: implication for PAH speciation and bioavailability. *Environ Sci Technol.* **1997**, 31, 203 -209.
- (7). Chang, S.I.; Reinfelder, J.R. Bioaccumulation, Subcellular Distribution, and Trophic Transfer of Copper in a Coastal Marine Diatom. *Environ Sci Technol.* **2000**, 34, 4931 -4935.
- (8). Chang, S.I.; Reinfelder, J.R. Relative importance of dissolved versus trophic bioaccumulation of copper in marine copepods. *Mar Ecol Prog Ser.* **2002**, 231, 179 -186.

(9). Zhou, J.L.; Fileman, T.W.; Evans, S.; Donkin, P.; Readman, J.W.; Mantoura, R.F.C.; Rowland, S. The partition of fluoranthrene and pyrene between suspended particles and dissolved phase in the Humber estuary: a study of the controlling factors. *The Science of the Total Environment*. **1999**, 243/244, 305 -321.

## **Appendix I. Subcellular fractionation of phenanthrene radiotracer in *T. weissflogii***

**Cultures.** *Thalassiosira weissflogii* (clone ACTIN)

**Chemicals.** Radiolabeled PAH (9-<sup>14</sup>C– Phenanthrene)

### **1. Fractionation method**

*T. weissflogii* cells exposed to <sup>14</sup>C– Phenanthrene were homogenized in an ice bath by sonification and centrifuged at 10 000 g for 5 min at room temperature, as described by Chang and Reinfelder (2000)<sup>1</sup>.

#### **1.1 Results**

The results are presented in Table A.1.1 and show that phenanthrene membrane fractions ranged from 10% to 50% in *T. weissflogii* for cells exposed for 3 to 6 d. However, this method suffered from heavy loss of phenanthrene radiotracer during sonification.

### **2. Evaporation method**

*T. weissflogii* cells exposed to <sup>14</sup>C– Phenanthrene were collected in 10 ml aliquots on GF/F filters and placed in an exhaust hood for 10 – 500 min.

#### **2.1 Results**

The dpm measured at each time point were divided by the value at time zero, and plotted in Figure A.1.1 to show the percentage drop. The results show that dpm decreased with the evaporation time in two steps, a slow decrease followed by a rapid drop, possibly representing two different mechanisms. By extrapolating the dpm after 200 min, the slowly exchanging pool accounted for about 30% of the total accumulated phenanthrene (Figure A.1.1).

### Reference

- (1). Chang, S.I.; Reinfelder, J.R. Bioaccumulation, Subcellular Distribution, and Trophic Transfer of Copper in a Coastal Marine Diatom. *Environ Sci Technol.* **2000**, *34*, 4931 -4935.

Table A.1.1 Subcellular fractionation of phenanthrene radiotracer in *T. weissflogii*. The fractions of membrane bound phenanthrene were calculated by dividing the radioactivity in the pellet fraction by the radioactivity of intact cells.

	Exposure time (d)	Membrane %	Mass loss %
Experiment I	5	30±16	23±10
	7	30±8	19±5
Experiment II	3	12±6	60±4
	5	28±8	37±5
	6	49±3	17±2

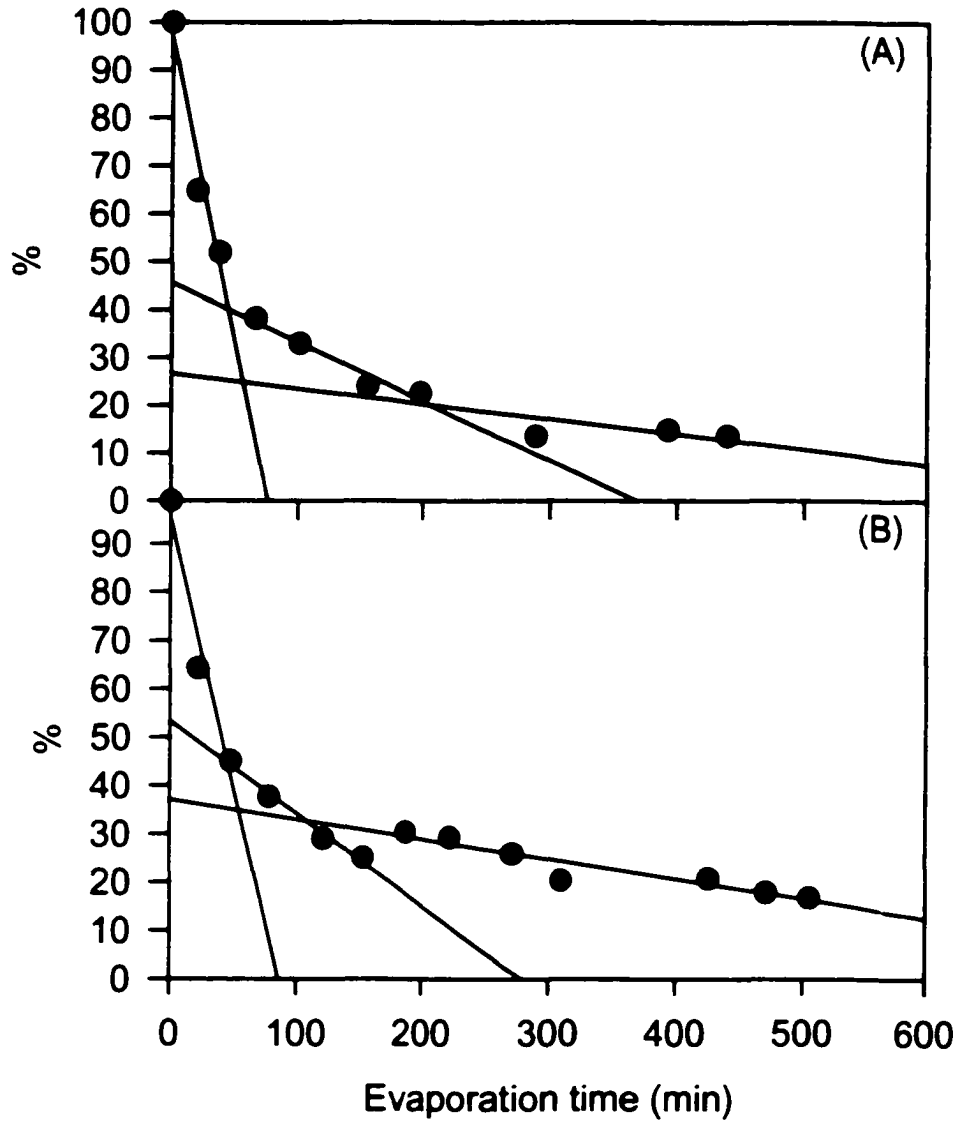


Figure A.1.1 Evaporation results over (A) 5 d and (B) 7 d exposure time.



## **Appendix II. Zooplankton bioaccumulation of phenanthrene**

**Chemicals.** Radiolabeled PAH (9-<sup>14</sup>C– Phenanthrene)

**Copepods.** Copepods were collected with a plankton net (63 µm Nylon mesh) from Cheesequake Creek near Raritan Bay in August 2000, and were a mixture of 80% *Acartia* and 20% *Temora*. Average dry weight and body length were  $5.0 \pm 0.7$  µg/individual and  $680 \pm 10$  µm/individual, as shown in Figure A.2.1.

### **Methods**

Dissolved uptake of phenanthrene in copepods was measured over 1-3 h exposure times with concentrations ranging from  $1.36 \times 10^{-8}$  to  $8.26 \times 10^{-8}$  M. 20 individuals were exposed to the phenanthrene in 30-ml vials with 20 ml media.

### **Results**

The results indicate a dissolved phase concentration dependent bioaccumulation (Figure A.2.2).

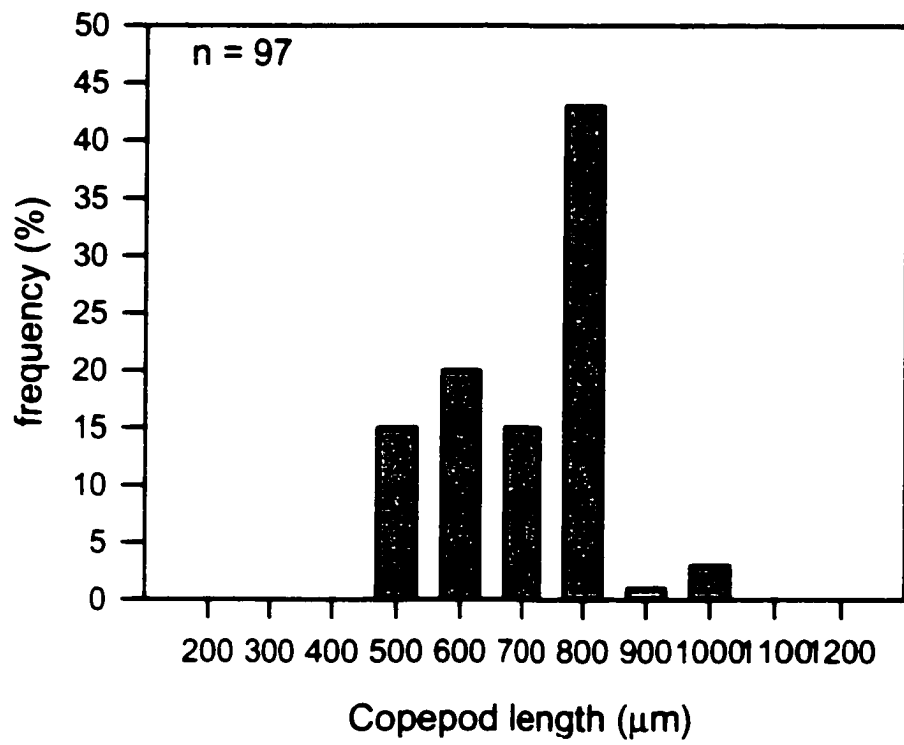


Figure A.2.1. Frequency of the body length in 97 copepod individuals.

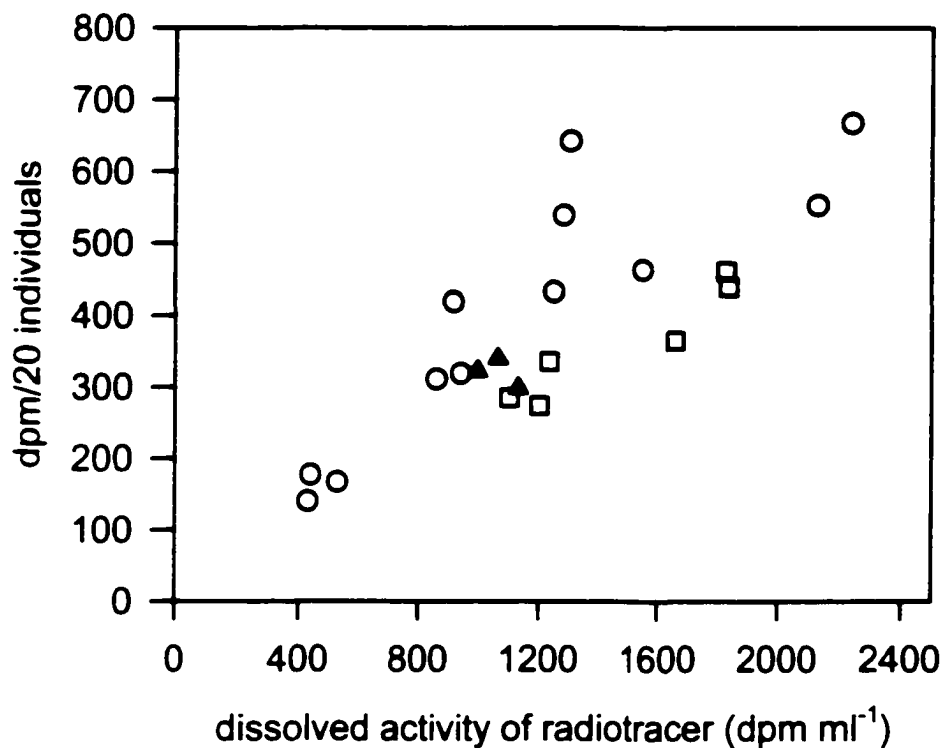


Figure A.2.2 Accumulation of dissolved phenanthrene in copepods with concentrations ranged from  $1.36 \times 10^{-8}$  to  $8.26 \times 10^{-8}$  M over (○) 1h, (□) 2 h, and (▲) 3 h exposure time.

## Appendix III. Organic carbon and elemental carbon measurements

### Methods

Plankton net samples in April/2001 were analyzed for relative fraction of organic carbon and elemental carbon by thermal-optical method<sup>1</sup>.

### Results

The results showed the EC/OC ratios averaged 3% for plankton net samples. Given  $f_{oc}$  measurements of 0.27 – 0.34,  $f_{sc}$  values are estimated to be 0.008 – 0.010 (Table A.3.1).

Using the measures of  $f_{sc}$  and soot carbon-partitioning model, the measured  $K_d$  values in situ can be explained by the presence of soot particles. However, the predicted  $K_d$  values including soot phase are higher than the measured  $K_d$  (Table A.3.2), possibly because the activated carbon partition coefficients ( $K_{sc}$ ) are higher than the in situ soot carbon partition coefficients<sup>2</sup>.

### References

- (1). Birth, M.E.; Cary, R.A. Elemental carbon-based method for monitoring occupational exposures to particulate diesel exhaust. *Aerosol Sci Technol.* **1996**, *25*, 221 -241.
- (2). Gustafsson, O.; Haghseta, F.; Chan, C.; Macfarlane, J.; Gschwend, P.M. Quantification of the dilute sedimentary soot phase: implication for PAH speciation and bioavailability. *Environ Sci Technol.* **1997**, *31*, 203 -209.

Table A.3.1 Elemental and organic carbon measurements of plankton net samples in Raritan Bay

Samples	EC/OC ratio	$f_{oc}$	$f_{ec}$
04/24 AM	0.031	0.269	0.008
04/24 AM	0.040		
04/24 PM	0.035	0.338	0.010
04/24 PM	0.017		

Table A.3.2 Organic carbon-partitioning and soot carbon-partitioning models applied to plankton net samples in Raritan Bay.

	log $K_d$	
	AM	PM
Actual measured in situ	4.7	4.6
$K_d = K_{oc} f_{oc}$	3.6	3.8
$K_d = K_{oc} f_{oc} + K_{sc} f_{sc}$	5.0	5.1

Log  $K_{oc}$  and log  $K_{sc}$  for phenanthrene are 4.2 and 7.1 (Gustafsson et al, 1997)

## CURRICULUM VITA CHENG-WEI FAN

### Education:

<u>Date</u>	<u>Department</u>	<u>Degree</u>
September 1994 – July 2002	Department of Environmental Sciences Rutgers, The State University of New Jersey USA	Ph.D.
September 1986 – June 1988	Department of Botany National Chung-Hsing University Taiwan	M.S.
October 1982 – June 1986	Department of Forestry National Taiwan University Taiwan	B.S.

### Professional Experiences:

1999-2002	Graduate Assistant	Department of Environmental Sciences Rutgers University USA
1998-1999	Teaching Assistant	Department of Environmental Sciences Rutgers University USA
1996-1998	Research Assistant	Environmental and Occupational Health Sciences Institute University of Medicine & Dentistry of New Jersey USA
1993-1994	Research Assistant	Institute of Botany Academia Sinica Taiwan
1991-1992	Assistant Manager	R&D department Y.S.W. Corp. Taiwan
1990-1991	Research Assistant	National Chung-Hsing University Taiwan

**Publications:**

1. Fan, Cheng-Wei and Zhang, Junefeng (2001) Characterization of emissions from portable household combustion devices: particle size distributions, emission rates and factors, and potential exposures, *Atmos. Environ.*, 35(7):1281-1290.
2. Pennise, David M., Smith, Kirk R., Kithinji, Jacob P., Rezende, Maria Emilia, Raad, Tulio Jardim, Zhang, Junefeng, and Fan, Cheng-Wei (2001) Emissions of greenhouse gases and other airborne pollutants from charcoal making in Kenya and Brazil. *J. Geophys. Res.*, 106(D20):24143-24155.
3. Fan, Z.H., Zhang, J.F., Fan, C.W. and Pennise, D.M. (2001) The MMT bag for emission source sampling: Design and evaluation. *J. Air Waste Management Ass.*, 51:60-68.
4. Hwang, Y.H., Fan, C.W. and Yin, M.H. (1996) Primary production and chemical composition of emergent aquatic macrophytes, *Schoenoplectus mucronatus ssp robustus* and *Sparganium fallax*, in Lake Yuan-Yang, Taiwan", *Botanical Bulletin of Academia Sinica*, 37: 265-273.
5. Chen, Pei-Chung and Fan, Cheng-Wei (1993) The algal removal efficiency in Fung-Yuang water treatment plant. *J. of Chinese Ins. of Environ. Eng.*, V3, 4:279-283. (in Chinese)
6. Chen, Pei-Chung and Fan, Cheng-Wei (1992) Studies of water quality and algal flora of Ta-Chia river. *J. of Chinese Ins. of Environ. Eng.* V2, 4:245-253. (in Chinese)
7. Fan, Cheng-Wei and Chen, Pei-Chung (1991) The algal flora of water treatment procedure in Fung-Yuang water treatment plant. *Yushania*, 8:61-85 (in Chinese)
8. Fan, Cheng-Wei and Chen, Pei-Chung (1990) The algal study of water treatment procedure in Fung-Yuang water treatment plant. *Proc. of VII water supply problem, Taiwan*, 27-37 (in Chinese)